MINERAL
RESOURCES

J5 and Bungalbin East Iron Ore Proposal
Response to Submissions – Appendix D
Flora Species Distribution Modelling Report

Topographic determinants of habitat suitability for rare ironstone plants in semi-arid Western Australia

G. Di Virgilio[1], G. W. Wardell-Johnson[1], T. P. Robinson[2], D. Temple-Smith[3] and J. Hesford[3]

[1]School of Science, [2]School of Mines, Curtin University, GPO Box U1987, Perth, 6845 WA, Australia

[3]Mineral Resources, 1 Sleat Rd, Applecross, WA, Australia

Abstract

The banded ironstone formation (BIF) ranges of semi-arid Western Australia host a diverse and endemic flora. The ecological requirements of these plants are not well understood, a problem that is exacerbated by a lack of knowledge of the role of topography in shaping local-scale plant distributions in semi-arid settings. We built species distribution models to identify topographic and geochemical conditions defining range boundaries of eighteen conservation-significant plant species on the Helena and Aurora Range (HAR) and surrounds, and determine the locations where each species is likely to occur. Using maximum entropy modelling, we performed species-specific tuning of model settings by varying model complexity and a penalty term to minimise over-fitting. The spatial variation in predicted habitat suitability differed between species, though high-suitability habitat for several taxa was generally concentrated on the topographically complex HAR. Threatened species were restricted near the ridgelines of ironstone summits. In contrast, suitable habitat for species of lower conservation significance is further from the ridgeline and more widespread across mid and low-elevation hillslopes and at specific locations on the surrounding plains. The primary mechanism involved in topographic control of these patterns was attenuation of incident solar radiation, whereby heat stress experienced by plants is reduced, presumably creating local differences in evaporation and evapotranspiration. Plant species of lower conservation significance are tolerant of a broader spectrum of topographic and geochemical conditions than threatened taxa which are restricted to the well-drained, high elevation zone. The mapped variation in predicted habitat suitability for species can contribute to time and cost-effective biological surveys by targeting survey effort at habitats most likely to be important for species of interest. Our findings provide a preliminary insight into environmental tolerances of rare ironstone plant species, indicating the potential topographic and geochemical conditions necessary for their establishment and persistence.

Key words: Banded ironstone formations; conservation planning; ecological rehabilitation; endemism; environmental niche modelling; maximum entropy; model complexity; species distribution modelling; true skill statistic

Introduction

Relatively little is known about the role of micro-topographic factors in determining vegetation patterns at the local scale of individual hillslopes in arid and semi-arid environments (Moeslund et al., 2013). In particular, few studies have specifically investigated the topographic determinants of multiple, conservation-significant plants in a semi-arid, rocky environment. The banded ironstone formation (BIFs) ranges of semi-arid Western Australia are ancient, sedimentary rock formations that exhibit high micro-topographic complexity (Gibson *et al.*, 2012; Nistelberger *et al.*, 2014). These distinctive formations host a diverse and endemic flora (Hopper & Gioia, 2004; Gibson *et al.*, 2010) and are the dominant features in an otherwise subdued and predominantly flat landscape (Fig. 1).

Topography moderates heat and moisture, creating a range of micro-climates (Anderson & Ferree, 2010), potentially at small geographic scales (O'Brien *et al.*, 2000). The high topographic complexity of ironstone formations may have a greater influence on structuring vegetation communities in arid areas where moisture is a limiting factor, than in environments with fewer constraints on plant growth. In environments where rock substrates experience intense solar radiation, rapid moisture loss and shallow soil cover (Coates & Kirkpatrick, 1992), topographic features such as slopes of varying aspect, fissures and depressions offer protection from insolation (Bennie et al., 2008), causing differences in evaporation and evapotranspiration. Topography controls surface hydrology, influencing drainage, and sediment transport and deposition. Depressions and fissures are also important for trapping moisture and for the deposition of dispersed seeds (Larson et al., 2000). Micro-topographic variation facilitates the availability of nutrients (Bruland &

Richardson, 2005; Araya et al., 2011; Simmons et al., 2011) and soil accumulation (Kuntz & Larson, 2006).

Species distribution models (SDMs) correlate environmental conditions with species occurrences to determine their ecological requirements (Vetaas, 2002; Guisan & Thuiller, 2005; Robinson *et al.*, 2010). They can also be used to predict variation in the relative suitability of habitat across geographic space. SDMs have been applied to identify sites of high potential occurrence of rare species (Engler et al., 2004) and suitable locations for species reintroduction (Pearce & Lindenmayer, 1998). Here, we build SDMs for eighteen conservation-significant plant species on the Helena and Aurora Range (HAR) in semi-arid Western Australia, which exhibits high plant diversity and endemism at comparatively small spatial scales (Gibson *et al.*, 2012). Understanding the specific microhabitat requirements of individual ironstone taxa is potentially important both to conservation and rehabilitation ecology.

We address three main aims: 1) what are the topographic and geochemical conditions that define the ranges of conservation-significant plant species on the HAR and surrounding plains? This will determine the relative importance of geophysical conditions to influencing the distribution of species; 2) where is each species most likely to occur at fine spatial scale? This can potentially identify locations where new populations of species of interest are likely to be found; 3) do plant species at higher risk of extinction have similar topographic determinants, and how might these differ for plants of lesser conservation significance? Furthermore, the output from these models can be used to create spatially explicit predictions of varying habitat suitability for each species. This will help to determine likely current distributions, including areas not previously targeted for sampling.

Method

Study area

The study area comprises the HAR and the surrounding BIFs and plains, a total area of 1605 km^2. The HAR is located in the south-western Australian Floristic Region (SWAFR) 400 km north-east of Perth, the main metropolitan centre of Western Australia (Fig. 2). This area experiences a semi-arid Mediterranean climate with annual rainfall ranging from 250 to 300 mm, and high inter-annual variation (BOM, 2015). Surface temperatures are typically high, frequently reaching 40˚C during summer. The approximate surface area of the HAR is 52 km^2. The HAR comprises BIF outcrop, duricrust and talus slopes surrounded by outwash and sand plains (Hocking et al., 2007). BIFs are Archean sedimentary rocks comprising repeated bands of iron oxides, alternating with layers of shale and chert. The highest point of the range is 702 m above sea level (asl), approximately 200 m above the predominately flat surrounding plains.

Plant data

The plant data consist of 25,077 species occurrences, comprising eighteen conservation-significant plant species in 11 families and 14 genera (Table 1). Targeted surveys of conservation significant taxa covered the topographical, geographical and floristic variation of the region, with survey transects covering all habitat types. Sampling was conducted between 2006 and 2014. Records with uncertain taxonomic status or that were spatially inaccurate were excluded from analyses. The most intensive survey effort was focused on the BIF summits (for GPS-logged transects see Supplementary Materials Figure S1; S2 for locations of species occurrences). As of January 2016, three species are designated as threatened (T), i.e. specially protected under Schedule 1 of the *Wildlife Conservation Act 1950* (Western Australia) and listed under the *Environment Protection and Biodiversity Conservation Act 1999* (Commonwealth) – ‘the EPBC Act’. *Tetratheca aphylla subsp. aphylla* and *Tetratheca harperi* are listed as *vulnerable* (VU) under both pieces of legislation because they face a high risk of extinction in the wild and meet IUCN criteria C2a; D1+2 and D2, respectively (see IUCN (2001) for an explanation of these criteria). *Leucopogon spectabilis* is critically endangered (CR - facing an extremely high risk of extinction in the wild under the *Wildlife Conservation Act 1950*; listed as CE – critically endangered under the EPBC Act) and meets IUCN criteria B1ab(iii; v) and 2ab(iii; v). Plant species potentially under threat, but either not meeting survey criteria, or data are deficient to enable listing under the *Wildlife Conservation Act 1950* are added to Priority Flora Lists (Priorities 1 to 3) by the Western Australian Department of Parks and Wildlife (DPaW) in order of precedence for survey and evaluation of conservation status. Priority 4 species are adequately surveyed, are rare but not threatened, or meet criteria for near threatened, or have been removed from threatened species or protected flora lists for other than taxonomic reasons (DPaW, 2015).

Table 1. The threatened and priority plant species analysed. See main text for explanation of Western Australian Government conservation status and ranking codes; IUCN criteria are listed at: http://www.iucnredlist.org/technical-documents/categories-and-criteria/2001-categories-criteria.

Family	**Species**	**Observations**	**Conservation Status (Ranking)**
Fabaceae	*Acacia adinophylla*	2061	P1
Fabaceae	*Acacia shapelleae Maslin*	84	P1
Myrtaceae	*Baeckea sp. Bungalbin Hill (B.J. Lepschi & L.A. Craven 4586)*	66	P3
Proteaceae	*Banksia arborea*	3945	P4
Euphorbiaceae	*Beyeria rostellata*	47	P1
Myrtaceae	*Eucalyptus formanii*	108	P4
Proteaceae	*Grevillea erectiloba*	324	P4
Proteaceae	*Grevillea georgeana*	1407	P3
Dilleniaceae	*Hibbertia lepidocalyx subsp. tuberculata*	2813	P3
Cyperaceae	*Lepidosperma bungalbin*	751	P1
Cyperaceae	*Lepidosperma ferricola*	250	P3
Ericaceae	*Leucopogon spectabilis*	232	T (CR) / T (CE)
Fabaceae	*Mirbelia ferricola*	1014	P3
Poaceae	*Neurachne annularis*	3924	P3
Lamiaceae	*Spartothamnella sp. Helena & Aurora Range (P.G. Armstrong 155-109)*	120	P3
Rhamnaceae	*Stenanthemum newbeyi*	5974	P3
Elaeocarpaceae	*Tetratheca aphylla subsp. aphylla*	1884	T (VU)
Elaeocarpaceae	*Tetratheca harperi*	72	T (VU)
		25076	

Environmental variables

Elevation data sources

We used three sources of elevation data to generate 2 m digital elevation models (DEM), subsequently mosaicked into a composite DEM from which all topographic predictors were derived (Fig. 2):

1) LiDAR data was acquired for the vast majority of the study area (~1524 km^2 delineated by red in Fig. 2) from five fixed wing aircraft sorties. The LiDAR point data have vertical and horizontal accuracies of 0.2 m and 0.4 m respectively. A 2 m resolution DEM was interpolated using a natural neighbour interpolation algorithm applied to ca 75 million last return spot heights.

2) A separate aerial survey flown over the north-west of the study area (~69 km^2 delineated by blue in Fig. 2) measured spot heights at 0.1 m resolution using a radar altimeter with vertical accuracy of 0.3 m. Ground heights were calculated by subtracting these spot heights from differential global positioning system (GPS) height readings. We used a 2 m resolution DEM previously interpolated from these data using a bicubic spline algorithm in analyses.

3) A 5 m DEM covering the remaining 12 km^2 (0.75%) of the study area without either LiDAR or radar coverage was derived by photogrammetry sourced from digital aerial photography that was flown for coverage of 1:100,000 map sheets. Vertical accuracy for 90% of these data is within +/- 1.5 m. However, we observed considerable noise in this DEM that could not be rectified. This DEM was resampled to 2 m resolution.

Predictive variables

Initially fifteen predictive topographic variables were derived from the DEM. Curvature represents the degree to which the slope deviates from a plane. Natural slopes are generally concave and limit the loss of sediment from the slope (as opposed to linear slope profiles). Slope influences surface water flow and is therefore related to soil moisture and development, with gentler surfaces having higher soil moisture. We used the ArcGIS software (ESRI, 2014) to calculate the solar radiation incident on the surface for 2014 (in watt hours per m^2) using monthly intervals for calculations. Topographic wetness indices (TWI) describe the geographic distribution of saturation for runoff generation as a function of upslope catchment area and slope angle. Essentially, TWI characterises how micro-topography controls hydrological processes and affects local patterns of moisture and surface saturation. TWI was calculated as per equation 1 (Moore et al., 1993):

$$TWI = ln\left(\frac{a}{tan\,\beta}\right) \qquad \text{(Eq. 1)}$$

Where *a* is a continuous flow accumulation surface (catchment area) in m^2. This is the upslope contributing area per unit contour length, indicating the area flowing to a specific location and β is the local slope angle in radians, measuring the potential drainage. Choice of algorithm to calculate catchment area (*a*) can affect performance of the TWI in different geographic settings (Sorensen et al., 2006; Kopecky & Cizkova, 2010). We thus tested the performance of three TWIs, where each was generated from an input catchment area calculated using either the D-infinity (Tarboton, 1997), Multiple Flow Direction (MFD)

(Freeman, 1991) or Multiple Triangular Flow Direction (MTFD) algorithms (Seibert & McGlynn, 2007).

Soil geochemical data were obtained from version 1 of the Australian soil pH, total phosphorus and total nitrogen products of the Soil and Landscape Grid of Australia (Viscarra Rossel et al., 2014). These surfaces express the estimated percentage content of N and P and variation in pH per ~90 m × 90 m grid cell and have a temporal coverage from ~1950-2013. These rasters were generated using decision trees with piecewise linear models and kriging of residuals developed from soil site data (Viscarra Rossel et al., In preparation). We used only pH, N and P values at a depth of 0 to 5 cm and resampled these to 2 m resolution.

We removed TWIs derived from the MTFD and DInfinity layers *a priori* because initial correlation analyses revealed they were less effective predictors of species distributions than the MFD-derived TWI. We tested for global multicollinearity between the remaining predictors using correlation analyses and removed the minimum subset necessary to ensure that all variables had $r^2 < 0.60$. The highest, pairwise correlation between the remaining variables was between the DEM and slope ($r^2 = 0.45$). This left eight environmental predictors used in all models: curvature, elevation (m), slope (radians), solar radiation (watt hours per m^2), topographic wetness index (TWI), nitrogen (%), phosphorous (%) and pH. Climatic variables were not considered, because at the scale that these surfaces are generated (e.g. Worldclim), each layer shows negligible change across this study area. We noted that slope and all measures of elevation heterogeneity were strongly correlated (r^2 = 0.94 to 0.98).

Modelling approach

We treated the plant species occurrence records as presence-only data. We used maximum entropy modelling 'maxent' (Phillips *et al.*, 2006; Phillips & Dudik, 2008) version 3.3.3k to relate occurrences for individual priority and threatened plant species to the environmental variables. Maxent performs consistently well with presence-only data in comparison to other contemporary modelling methods (Elith *et al.*, 2006; Hernandez *et al.*, 2006; Wisz *et al.*, 2008; Tittensor *et al.*, 2009). It estimates the potential geographic distribution of a species by finding the probability distribution of maximum entropy, which is the distribution closest to uniform, subject to the environmental constraints derived from the species occurrence data. These constraints require the mean of each environmental variable under the predicted distribution to be close to the empirical average over the observed sample. A sample of the cells comprising the study area, 'background points', represents the space over which the maximum entropy probability distribution is defined (Phillips et al., 2006).

During model generation, background points are compared with species occurrence data to differentiate environmental conditions under which a species can potentially occur. By default, the maxent model applies a prior expectation that a species is equally likely to occur anywhere within the study area. Consequently, each location within the complete study area extent has an equal chance of being selected as a background point (Merow *et al.*, 2013). However, the specification of this background selection can also be manipulated. One approach is that the background sample should be selected so as to best characterise the environmental conditions that one wishes to differentiate (Merow *et al.*, 2013). Thus, we built two different classes of model, where each class uses a different background selection method. Background points were sampled from the entire study area, ‘unconstrained background selection’, to investigate how habitat favourable to each species (based on topographic and geochemical predictive variables) differs from non-favourable habitat (aim 1). Background selection was also enforced using ‘bias files’ to model locations where each species is presently likely to occur (aim 2). This is ‘constrained background selection’. This was done to restrict selection of background points to occupied locations, thus capturing a narrower range of environmental conditions to the above model class. This avoids sampling background points from habitat greatly outside of a species geographic range (Yates *et al.*, 2010; Elith *et al.*, 2011; Merow *et al.*, 2013). Hence, when building models for each species, we restricted the selection of background data to observed point occurrences of the relevant species, plus a radius of 300 m around each of these points. We assume that dispersal is not a limiting factor within this study area.

Species-specific calibration of model settings

Maxent creates different mathematical transformations of each environmental variable and then uses these functions to model the environmental requirements of the target species. A linear transformation is the mean of the variable (thus the mean of an environmental condition where a species is predicted to occur is an approximate match to the mean value where it is observed to occur). A quadratic function is the square of a predictive variable. When a quadratic transformation is used together with a linear feature, this models a species’ tolerance for variation from optimal conditions (Anderson & Gonzalez Jr, 2011). A hinge feature has a value of zero below a given threshold, but this value increases according to a continuous linear function once the threshold is exceeded. Using both linear and hinge features together is redundant (Elith *et al.*, 2011).

For each species, we varied model complexity by calibrating models either with linear features only, both linear and quadratic features, hinge features only, and both hinge and quadratic features. Then for each level of model complexity, we varied the degree to which the models are penalised to reduce over-fitting by changing the regularisation parameter (a penalty term applied equally to all feature classes). For each feature type setting, the following regularisation parameters were tested: 0.5, 0.75, 1 (the default setting), 2, 3, 5, 7 and 9. Thus, 32 separate models were built and evaluated for each of the eighteen species, for each class of model.

We assessed model performance by calculating the true skill statistic (TSS) for each model configuration (Allouche *et al.*, 2006). TSS is a threshold-dependent measure of model accuracy. It is similar to the Kappa statistic, a commonly used threshold-dependent measure of model accuracy (Fielding & Bell, 1997), except TSS is not sensitive to species prevalence. We used the 10 percentile training presence threshold calculated by maxent as the threshold criterion (Tinoco *et al.*, 2009; Jarnevich & Reynolds, 2011). The test area under the receiver operating characteristic curve (AUC) score is often used to evaluate the performance of models generated by maxent, but AUC scores have the limitation that they are correlated with area size as well as species prevalence (Lobo *et al.*, 2008). Consequently, we used TSS scores generated by each model configuration to select the feature and regularisation settings for a definitive model for each species.

For all maxent models, logistic output was generated and the following parameters altered from their default settings: 5000 maximum iterations (the number of iterations of the optimisation algorithm before training is stopped), with a 25% random test percentage. All variables are continuous. The default values were used for the remaining parameters. We performed five-fold cross-validation to estimate model performance.

Results

Model type 1: unconstrained 'default' background selection

TSS scores were high (mean = 0.848; SD = 0.090), indicating accurate model predictions (Landis & Koch, 1977) (Table 2). In the majority of cases, regularisation values higher than the default setting of one produced superior model performance. A combination of quadratic and hinge feature classes also tended produced better performing models. AUC scores against the test data were also high (> 0.85 in all cases).

Table 2. Highest true skill statistic (TSS) scores for each plant species model, and the corresponding feature classes and regularisation parameters. QH = quadratic and hinge features; L = linear feature; LQ = linear quadratic features.

Species	Highest TSS	Feature Class(es)	Regularisation Parameter
Acacia adinophylla	0.843	QH	0.50
Acacia shapelleae Maslin	0.944	L	9.00
Baeckea sp. Bungalbin Hill BJ Lepschi	0.768	QH	1.00
Banksia arborea	0.888	QH	1.00
Beyeria rostellata	0.724	QH	2.00
Eucalyptus formanii	0.859	QH	2.00
Grevillea erectiloba	0.868	QH	2.00
Grevillea georgeana	0.877	LQ	1.00
Hibbertia lepidocalyx subsp tuberculata	0.900	QH	5.00
Lepidosperma bungalbin	0.918	LQ	5.00
Lepidosperma ferricola	0.837	QH	2.00
Leucopogon spectabilis	0.875	L	5.00
Mirbelia ferricola	0.892	H	3.00
Neurachne annularis	0.800	H	0.75
Spartothamnella sp. Helena Aurora Range	0.563	QH	1.00
Stenanthemum newbeyi	0.879	QH	5.00
Tetratheca aphylla subsp aphylla	0.901	QH	5.00
Tetratheca harperi	0.932	QH	3.00

The relative contribution of each environmental predictor to increasing goodness-of-fit of the models generated varies for each species (Table 3). However, in all cases (except *S. sp. Helena Aurora Range*) either elevation or slope are the predictors with the largest influence.

Curvature has a negligible effect on any model, surprising, given that this variable identifies rapid changes in slope and aspect. Splitting curvature into its constituent parts (plan and profile) did not alter this outcome. Solar radiation and TWI make a substantial contribution to model gain only for *Beyeria rostellata* and *Grevillea georgeana* respectively.

Model type 2: limited background selection

The TSS scores generated for models employing restricted/constrained background selection are lower (mean = 0.541; SD = 0.099). A TSS of > 0.6 is considered good, 0.2–0.6 fair to moderate; <0.2 poor (Landis & Koch, 1977). TSS scores were low for four species only (*A. adinophylla, A. shapelleae Maslin, B. sp. Bungalbin Hill* and *S. sp. Helena and Aurora Range*) (mean = 0.159; SD = 0.129). Hence we revert to the default, unconstrained models for these four taxa only and disregard the background constrained versions.

Generally, elevation and slope again make the largest overall contributions to model gain (Table 3), though in several instances the contribution of slope is reduced relative to the unconstrained models. Solar radiation makes a considerably larger relative contribution for many species (e.g. *L. bungalbin* and *L. ferricola*) than was the case for the corresponding unconstrained models.

Table 3. The estimated relative contribution of each environmental predictor to increasing the gain (goodness-of-fit) for both model types (background selection unconstrained versus selection constrained) generated for each species, where the default background selection was used. NA = constrained model not generated for this species, because the true skill statistic score was too low; hence we revert to the unconstrained model for these species.

Species	**Variable % Relative Contribution (unconstrained background model / *constrained model*)**															
	Elevation		Slope		Solar Radiation		TWI		Curvature		N		P		pH	
A. adinophylla	17.6	*NA*	75.1	*NA*	0.3	*NA*	0.2	*NA*	0.0	*NA*	1.5	*NA*	1.0	*NA*	4.1	*NA*
A. shapelleae Maslin	63.9	*NA*	21.4	*NA*	1.2	*NA*	0.9	*NA*	0.0	*NA*	12.3	*NA*	0.0	*NA*	0.2	*NA*
B. sp. Bungalbin Hill	49.5	*NA*	2.9	*NA*	0.0	*NA*	0.1	*NA*	0.1	*NA*	9.2	*NA*	28.0	*NA*	10.3	*NA*
B. arborea	3.0	*16.5*	95.6	*64.4*	0.0	*3.2*	0.3	*0.2*	0.0	*0.0*	0.2	*5.0*	0.4	*1.7*	0.5	*9.1*
B. rostellata	23.0	*10.5*	63.4	*0.0*	9.5	*16.5*	0.5	*1.6*	0.0	*0.0*	0.7	*1.0*	0.8	*8.2*	2.1	*62.2*
E. formanii	83.1	*50.3*	0.0	*3.3*	3.8	*5.2*	0.1	*0.3*	0.1	*0.0*	0.6	*3.2*	1.9	*27.3*	10.3	*10.3*
G. erectiloba	48.3	*71.2*	39.3	*2.2*	0.4	*2.2*	0.0	*0.3*	0.0	*0.0*	1.6	*13.2*	3.7	*6.8*	6.6	*4.1*
G. georgeana	61.1	*41.4*	24.5	*46.8*	0.2	*6.7*	10.6	*0.0*	0.1	*0.0*	0.0	*3.3*	0.6	*0.2*	2.8	*1.7*
H. lepidocalyx subsp tuberculata	4.4	*16.3*	91.9	*54.3*	0.0	*2.2*	0.0	*0.7*	0.0	*0.0*	0.5	*1.2*	0.2	*7.4*	3.0	*18.0*
L. bungalbin	72.8	*22.6*	14.0	*4.8*	1.3	*36.9*	3.8	*0.1*	0.0	*0.1*	3.0	*2.7*	3.0	*14.5*	2.2	*18.4*
L. ferricola	5.5	*15.1*	76.5	*0.8*	0.1	*45.0*	0.0	*1.0*	0.0	*0.0*	0.7	*1.7*	17.2	*33.9*	0.0	*2.4*
L. spectabilis	16.1	*6.2*	60.2	*30.4*	1.6	*14.3*	0.0	*1.6*	0.2	*1.2*	1.5	*6.7*	20.2	*29.8*	0.4	*9.7*
M. ferricola	4.9	*27.6*	90.2	*19.7*	0.1	*26.8*	0.0	*0.0*	0.0	*0.0*	0.0	*0.0*	1.0	*10.5*	3.7	*15.4*
N. annularis	3.6	*10.4*	89.7	*66.0*	0.0	*0.9*	0.0	*0.1*	0.0	*0.1*	0.7	*1.5*	5.3	*19.2*	0.8	*1.8*
S. sp. Helena Aurora Range	32.4	*NA*	3.2	*NA*	4.3	*NA*	1.0	*NA*	0.0	*NA*	3.6	*NA*	14.4	*NA*	41.2	*NA*
S. newbeyi	8.2	*12.1*	85.4	*31.1*	0.0	*5.7*	0.0	*0.4*	0.0	*0.0*	0.0	*0.6*	1.5	*4.3*	4.9	*45.8*
T. aphylla subsp aphylla	22.7	*69.5*	74.4	*12.0*	0.0	*4.5*	0.0	*0.3*	0.0	*0.3*	0.0	*1.3*	2.4	*2.8*	0.5	*9.4*
T. harperi	93.8	*6.5*	1.4	*12.4*	2.7	*5.7*	0.4	*5.3*	0.0	*7.3*	0.3	*1.0*	0.4	*57.9*	1.1	*3.8*

Maps of model predictions for constrained and unconstrained models

Model prediction maps express habitat suitability of each location in the study area (i.e. each 2 × 2 m grid cell) as a function of environmental variables at each location. A high value of the function at a particular location indicates that it is predicted to provide suitable topographic/geochemical conditions for a given species. The computed model is a probability distribution over all grid cells. The maps use colours to show the predicted probability that environmental conditions are suitable, with warmer colours (red, orange and yellow) indicating a higher probability of suitable environmental conditions for a given species, green indicating conditions typical of those where the species is found, and blue shades indicating low predicted probability of suitable conditions.

The maps of model predicted habitat suitability show substantial variation between species and also between the background constrained and unconstrained models. For brevity, we present the results only for selected species. Maps for species not discussed here are presented in the Supplementary Materials (Fig. S3-S54). We also assess the ways in which topographic determinants are similar for 'rarer' species, i.e. all threatened and priority one taxa and how this differs to the topographic influence on all priority three and four taxa.

For *T. aphylla* subsp. *aphylla*, the model employing unconstrained background selection (i.e. model type 1) predicts that habitat conditions are suitable across the mid-to-high slopes of the HAR, with minimal variation in predicted suitability on the high-slopes (Fig. 3-4). In contrast, the model with restricted background selection produces predicted suitabilities that are considerably more spatially restricted and located closer to the HAR ridgeline (Fig. 6-7). Also, whilst habitat suitability is identified as favourable on the mid-slopes, the predicted magnitude is lower than for the Type 1 model. For both model types, predicted suitability is low across the plains surrounding the HAR. Note that both model types predict minimal differences in the favourability of habitat on north and south-facing slopes.

In contrast to *T. aphylla subsp. aphylla*, models for *L. bungalbin* produced mapped predictions that are slightly higher on south-facing as opposed to north-facing slopes, and also surfaces providing shade irrespective of their aspect (Fig. 9-10). This pattern was more pronounced for the restricted-background sample model (Fig. 11-12), where suitable habitat is more restricted to the south-facing slopes than the default model. Incident solar radiation is comparatively lower at these same locations, whereas its intensity is higher at the locations predicted as unsuitable for this species. Both elevation and incident solar radiation were estimated as having the greatest contribution to the constrained model for *L. bungalbin* (22.6% and 36.9% respectively, Table 3). The partial dependence plots show the marginal response of *L. bungalbin* to elevation and solar radiation, as values of remaining variables are fixed at their average sample values (Fig. 13). The predicted suitability in terms of elevation is positively correlated up until a threshold of approximately 660 m. Thus, beyond this threshold, the marginal effect of increasing elevation is a decrease in predicted suitability for *L. bungalbin*. In terms of solar radiation, the response is high and uniform for radiation values in the range of approximately 200,000 WH/m^2 to 400,000 WH/m^2. The response shows a steep decrease at values > 1.1M WH/m^2. Consequently, the marginal effect of increasing solar radiation beyond this point (once the effect of all the other variables has already been accounted for) is a decrease in predicted suitability for this species.

The likely geographic distributions of *Baeckea sp. Bungalbin Hill* are very different to the two species discussed above (Figure 14). This species is more likely to occur on the plains to the south, west and north-east of the HAR. This landscape is low elevation and gently undulating, and solar radiation intensity is lower at the locations of high predicted suitability. Several other plant species show high predicted habitat suitability on the plains (one example is *Neurachne annularis* see Supplementary Materials Fig. S41-44).

As for *T. aphylla subsp. aphylla* and *L. bungalbin*, the default (unconstrained) model for *L. ferricola* predicts that favourable habitat is almost exclusively located on the HAR summits (Fig. 16-17). In contrast, the background-constrained model predicts likely occurrences in multiple locations across the plains (Fig. 18). Furthermore, relative to the unconstrained model predictions, habitat suitability on the HAR itself is substantially more restricted to the south-facing slopes (Fig. 19). This predicted range across the ironstone surfaces is more constrained than for *L. bungalbin* and again closely resembles areas where incident solar radiation is comparatively lower.

Topographic determinants of rare plant species

Rarer plant species (i.e. the seven threatened and priority one species, Table 1) are restricted to the narrower, higher elevation zone near to the HAR ridgeline (Fig. 20-21). There is a tendency for these taxa to prefer the south-facing slopes and shaded areas. In general, the surrounding plains are not predicted as suitable for this group of particularly sensitive species, though the series of hillocks in the south-east have moderate to low predicted suitability. In contrast, locations predicted as suitable for all priority three and priority four taxa occur over a much broader range of elevations extending from the ridgeline to lower positions on the hillslope (Fig. 22-23). Again, the most suitable habitats are on south facing slopes or areas where incident radiation is lower. Notably, a much larger proportion of the surrounding plains are predicted to have medium suitability for this group of plants.

Model cross-validation

There was only minimal variation in cross-validated AUC scores between models for the target taxa. The average SD of the test AUC for the replicate runs was 0.009. The responses of most taxa to the predictive variables also showed minimal variation between models, though there were some exceptions. For instance, the response of *B. sp. Bungalbin Hill* showed a greater degree of variability to N and solar radiation.

Discussion

We built SDMs for eighteen priority and threatened flora growing on or near the HAR and assessed how topographic and geochemical predictors shape their distributions. Elevation, slope and topographic mediation of solar radiation were the principal variables that determined the degree of habitat suitability for most of the plant species assessed. We now consider the underlying mechanisms by which topography influences the distribution of threatened and conservation priority plants in the HAR and potentially on similar landscapes.

Topographic mechanisms shaping rare plant distributions

The habitat suitability maps highlighted that rare ironstone plants are most likely to occur on the surface of the HAR than on the surrounding, flatter landscape. In particular, the rarer plant species (e.g. *T. aphylla subsp. aphylla, L. bungalbin*) are more likely to occur nearer to the BIF ridgeline, relative to downslope locations. Anderson and Ferree (2010) also observed that rare plant species in the north-eastern US were largely restricted to a single elevational zone. The higher elevation areas nearer the HAR ridge are better drained than the lower hillslopes. This result may suggest that the very arid conditions higher on the BIF slopes lead to intense competition between plants for the fissures, pits and depressions that trap moisture. Rainfall in semi-arid ecosystems such as the HAR is variable. Consequently, the shallow soils of BIFs will experience prolonged periods of drying with only occasional pulses of moistening (Austin *et al.*, 2004). The threatened and priority one ironstone taxa must be well-adapted to survival on these well-drained, dry surfaces and they may have a competitive advantage over other plants species in such areas.

Another general pattern is that favourable habitat is predicted to occur across a much larger spatial extent and a broader range of ecological gradients for the priority three and priority four species which are at lower levels of conservation risk than the comparatively rarer, threatened and priority one taxa. These species appear to be more tolerant of a broader spectrum of topographic and geochemical conditions than the rarer taxa predominantly restricted to high elevation zones.

Slope had an important influence on determining habitat suitability for most plant species (irrespective of their conservation status). During model selection, we found a strong correlation between slope and different measures of elevation heterogeneity, such as the standard deviation of local elevation, which is a measure of the variability of local relief (Crisp *et al.*, 2001). High variance of local relief represents high variation in aspect, slope and gaps over small distances. High surface complexity is a characteristic feature of the HAR and also of other BIFs in Australia and elsewhere in the world (Klein, 2005; Jacobi *et al.*, 2007; Nistelberger *et al.*, 2014). We excluded local elevation heterogeneity from the models because of its strong correlation with slope. However, high variation in the latter is clearly representative of high habitat heterogeneity. Thus a high level of micro-topographic heterogeneity seems to be favourable for endemic plants on the HAR. This could be because the high surface complexity of the HAR broadens niche width; in short there are a greater variety of micro-habitats, all with varying environmental conditions. These confer a greater capacity for more species and individual plants to find a niche space (VivianSmith, 1997). High topographic heterogeneity is probably relevant to a variety of processes. For instance, it may be important to seed dispersal, because the high surface complexity affords cracks, fissures and gaps into which seeds can settle. Such features may also help gather available soil, nutrients and runoff.

In many cases (e.g. *L. bungalbin*, *L. ferricola* and *B. sp. Bungalbin Hill*) there was a strong habitat preference for locations on the HAR and plains where the intensity of solar radiation was lower than at adjacent locations. Surfaces with south-facing aspects will experience lower temperatures than north-facing aspects and thus fewer drought events (Radcliffe & Lefever, 1981). This is a simple mechanism by which topography may mediate heat budgets, both across the undulating plains and on the surface of the HAR, and so facilitate higher plant biodiversity. The predicted habitat suitability map for *B. sp. Bungalbin Hill* is noteworthy because unlike many of the other taxa it occurs on the plains and not on the HAR. The terrain in this area does not resemble the high surface complexity of the BIF summits; however, neither is it flat and uniform. It exhibits a fine-scale variation in aspect, with much of this area receiving less solar radiation than elsewhere on the plains. Nonetheless, the high surface variability of the HAR will play an important role in protecting plants from heat. Optimum seed germination occurs in microhabitats in which evaporation is reduced, with irregular soil surface topographies providing the best conditions for minimising evaporation (Hamrick & Lee, 1987). High micro-topographic heterogeneity on the HAR is one factor that may contribute to the formation of an irregular surface profile.

More generally, our focus has been on how present-day topographic attributes constrain plant species ranges. However, historical geophysical factors may play an important role in that current species distributions might reflect processes that occurred on paleo-geological time-frames. For example, the OCBIL (Old Climatically Buffered Infertile Landscape) (Hopper, 2009) and Old Stable Landscape ideas (Mucina & Wardell-Johnson, 2011) have been proposed to explain the high species diversity and endemism on ancient landscapes in the SWAFR, such as the HAR.

Differences between background constrained and non-constrained models

Generally, the constrained model output predicted that suitable habitat was more geographically restricted than the corresponding predictions of the non-constrained model. A clear exception applied to *L. ferricola*. The unconstrained model for this species predicted broad habitat suitability across the HAR, but not on the surrounding plains. The constrained model showed habitat suitability was more restricted on the HAR, but conversely much higher levels of suitability on the plains. There is high local variation in elevation and slope aspect in these areas on the plains, possibly explaining why these locations are favourable to *L. ferricola*.

Methodological issues

There are additional variables that will be important determinants shaping plant communities on BIFs, but that could not presently be included in the models generated. Biotic interactions and direct climatic variables estimated at small spatial-scales are notable model externalities. The native resolution of the geochemical predictors was coarser than the topographic predictors, with the former requiring re-sampling as a result. Consequently, there will be significant smoothing/averaging of geochemical estimates at the scale of the local-scale topographic data.

The negligible influence of curvature on all model outputs was unexpected. This might be a consequence of the small size of the fixed neighbourhood of the algorithm used to generate the curvature surface. This calculates the curvature on a cell by cell basis by fitting a fourth order polynomial to a local neighbourhood gird of 3 × 3 cells. This local context might be too restricted for the comparatively fine resolution of our DEM, and high local-scale topographic variability. For instance, we obtained poor estimates of relief (variation in local elevation) by using a window less than 8 × 8 cells.

Applications to ecosystem rehabilitation

We built SDMs of threatened and priority plant species because their rarity means that they are likely to be at the forefront of considerations in the environmental impact assessment (EIA) process. Given that all of these species are narrow-range ‘endemic’ plants, they might be more vulnerable to environmental changes and disturbances (Brown, 1995; Thuiller *et al.*, 2005). For instance, in a drying, warming climate, even those specialised micro-habitats that currently confer suitable conditions for these plants may no longer be able to do so.

Mapping variation in predicted habitat suitability for sensitive plant species (Fig. 3 – 23; S3-S54) could be an effective contribution to the design of time and cost-effective biological surveys, for instance by directing survey effort at habitats most likely to be important for target species. The outputs from the maxent SDMs are also a preliminary insight into the environmental tolerances and niches of key plant species that occur on and around the HAR. These findings improve our understanding of the topographic and geochemical conditions favourable for the establishment and persistence of the plant species studied here. Similar principles may apply to endemic plant species in rocky, semi-arid settings elsewhere.

A pre-requisite for ecosystem rehabilitation is that the limitations to plant growth in a given area are understood. A key outcome of a rehabilitation project is to assemble the environmental conditions necessary for re-vegetation and to minimise and mitigate the environmental effects of any disturbance. The SDM approach used here has identified the relative importance of topographic and geochemical conditions influencing the distributions of different plant species. Understanding the specific microhabitat requirements of individual ironstone taxa targeted for rehabilitation increases the probability of success of conservation efforts. This information is pertinent to achieving a self-sustaining plant assemblage by replicating the ecological and landscape characteristics favourable to target species, such as the geomorphic features which minimise evaporation in semi-arid environments. The availability of a high number of microsites with varying physical profiles seems to be important for recruitment success in natural populations of ironstone taxa, and the same principal ought to apply to populations being established for rehabilitation projects. Differences in nutrient, moisture, soil and heat variables at the scale of pits, depressions and slopes of varying aspect result in differential colonisation preferences. A rehabilitation approach should aim to mimic this selective recruitment by recreating large numbers of differentiated microhabitats and thus maximising the number of specialised sites that can harbour endemic taxa with specialised habitat requirements.

Rehabilitation techniques have been applied in other environments to generate substantial degrees of surface complexity. An example is the Forestry Reclamation Approach

(FRA), used to restore coal-mined land to forest in Appalachia by recreating high fine-scale micro-topographic variation. This is achieved by dumping overburden into numerous mounds using the ‘end-dump’ method of minimising surface compaction (Zipper et al., 2011). It remains to be seen how well a similar method would work in an environment similar to the HAR. Given the high surface temperatures and low variable rainfall patterns at the HAR (and other BIFs in semi-arid zones) it seems this method would need modification to ensure that the re-constructed surfaces can provide adequate shelter from intense solar radiation.

The threshold relationship between species occurrences and solar radiation also shows that most species ‘prefer’ a habitat where micro-topography limits incident radiation and so probably reduces the rate of evaporation and evapotranspiration. This must confer an advantage to many species in semi-arid environments such as the HAR. Desiccation and water stress can compromise reintroduction of plants or rehabilitation of disturbed habitats (Ackerly et al., 2010), which is a particular risk for seed germination on the HAR where high seedling mortality rates have been observed (Yates et al., 2011). Similarly, 90% of newly emerged tree species seedlings on cliff-faces perished (Matthes & Larson, 2006). Consequently, basing a rehabilitation project around the use of seedlings may have limited success. A more fruitful strategy might be to relocate juvenile plants to an artificial landscape of high local-scale heterogeneity and in particular, locating plants on south-facing or sheltered aspects of this landscape to help attenuate heat budgets.

References

Ackerly, D.D., Loarie, S.R., Cornwell, W.K., Weiss, S.B., Hamilton, H., Branciforte, R. & Kraft, N.J.B. (2010) The geography of climate change: implications for conservation biogeography. *Diversity and Distributions*, **16**, 476-487.

Allouche, O., Tsoar, A. & Kadmon, R. (2006) Assessing the accuracy of species distribution models: prevalence, kappa and the true skill statistic (TSS). *Journal of Applied Ecology*, **43**, 1223-1232.

Anderson, M.G. & Ferree, C.E. (2010) Conserving the Stage: Climate Change and the Geophysical Underpinnings of Species Diversity. *Plos One*, **5**, 10.

Anderson, R.P. & Gonzalez Jr, I. (2011) Species-specific tuning increases robustness to sampling bias in models of species distributions: An implementation with Maxent. *Ecological Modelling*, **222**, 2796-2811.

Araya, Y.N., Silvertown, J., Gowing, D.J., McConway, K.J., Linder, H.P. & Midgley, G. (2011) A fundamental, eco-hydrological basis for niche segregation in plant communities. *New Phytologist*, **189**, 253-258.

Austin, A., Yahdjian, L., Stark, J., Belnap, J., Porporato, A., Norton, U., Ravetta, D. & Schaeffer, S. (2004) Water pulses and biogeochemical cycles in arid and semiarid ecosystems. *Oecologia*, **141**, 221-235.

Bennie, J., Huntley, B., Wiltshire, A., Hill, M.O. & Baxter, R. (2008) Slope, aspect and climate: Spatially explicit and implicit models of topographic microclimate in chalk grassland. *Ecological Modelling*, **216**, 47-59.

BOM (2015) *Climate data online*. Bureau of Meteorology, Commonwealth of Australia.

Brown, J.H. (1995) *Macroecology*. University of Chicago Press.

Bruland, G.L. & Richardson, C.J. (2005) Hydrologic, Edaphic, and Vegetative Responses to Microtopographic Reestablishment in a Restored Wetland. *Restoration Ecology*, **13**, 515-523.

Coates, F. & Kirkpatrick, J.B. (1992) Environmental relations and ecological responses of some higher plant species on rock cliffs in northern Tasmania. *Australian Journal of Ecology*, **17**, 441-449.

Crisp, M.D., Laffan, S., Linder, H.P. & Monro, A. (2001) Endemism in the Australian flora. *Journal of Biogeography*, **28**, 183-198.

DPaW (2015) *Threatened species and communities*. Available at: http://www.dpaw.wa.gov.au/plants-and-animals/threatened-species-and-communities (accessed January 20 2015).

Elith, J., Phillips, S.J., Hastie, T., Dudik, M., Chee, Y.E. & Yates, C.J. (2011) A statistical explanation of MaxEnt for ecologists. *Diversity and Distributions*, **17**, 43-57.

Elith, J., Graham, C.H., Anderson, R.P., Dudik, M., Ferrier, S., Guisan, A., Hijmans, R.J., Huettmann, F., Leathwick, J.R., Lehmann, A., Li, J., Lohmann, L.G., Loiselle, B.A., Manion, G., Moritz, C., Nakamura, M., Nakazawa, Y., Overton, J.M., Peterson, A.T., Phillips, S.J., Richardson, K., Scachetti-Pereira, R., Schapire, R.E., Soberon, J., Williams, S., Wisz, M.S. & Zimmermann, N.E. (2006) Novel methods improve prediction of species' distributions from occurrence data. *Ecography*, **29**, 129-151.

Engler, R., Guisan, A. & Rechsteiner, L. (2004) An improved approach for predicting the distribution of rare and endangered species from occurrence and pseudo-absence data. *Journal of Applied Ecology*, **41**, 263-274.

Environment (1999) An Act relating to the protection of the environment and the conservation of biodiversity, and for related purposes, Parliament of Australia. In:

ESRI (2014) ArcGIS Desktop: Release 10.3. In. Environmental Systems Research Institute, Redlands, CA.

Fielding, A.H. & Bell, J.F. (1997) A review of methods for the assessment of prediction errors in conservation presence/absence models. *Environmental Conservation*, **24**, 38-49.

Freeman, T.G. (1991) Calculating catchment-area with divergent flow based on a regular grid. *Computers & Geosciences*, **17**, 413-422.

Gibson, N., Yates, C. & Dillon, R. (2010) Plant communities of the ironstone ranges of South Western Australia: hotspots for plant diversity and mineral deposits. *Biodiversity and Conservation*, **19**, 3951-3962.

Gibson, N., Meissner, R., Markey, A.S. & Thompson, W.A. (2012) Patterns of plant diversity in ironstone ranges in arid south western Australia. *Journal of Arid Environments*, **77**, 25-31.

Guisan, A. & Thuiller, W. (2005) Predicting species distribution: offering more than simple habitat models. *Ecology Letters*, **8**, 993-1009.

Hamrick, J.L. & Lee, J.M. (1987) Effect of Soil Surface Topography and Litter Cover on the Germination, Survival, and Growth of Musk Thistle (Carduus nutans). *American Journal of Botany*, **74**, 451-457.

Hernandez, P.A., Graham, C.H., Master, L.L. & Albert, D.L. (2006) The effect of sample size and species characteristics on performance of different species distribution modeling methods. *Ecography*, **29**, 773-785.

Hocking, R.M., Australia, G.S.o.W., Industry, W.A.D.o. & Resources (2007) *A Classification System for Regolith in Western Australia: March 2007 Update*. Geological Survey of Western Australia.

Hopper, S.D. (2009) OCBIL theory: towards an integrated understanding of the evolution, ecology and conservation of biodiversity on old, climatically buffered, infertile landscapes. *Plant and Soil*, **322**, 49-86.

Hopper, S.D. & Gioia, P. (2004) The Southwest Australian Floristic Region: Evolution and conservation of a global hot spot of biodiversity. *Annual Review of Ecology Evolution and Systematics*, **35**, 623-650.

IUCN (2001) *IUCN Red List Categories. Version 3.1*. Available at: http://www.iucnredlist.org/technical-documents/categories-and-criteria/2001-categories-criteria. (accessed March 3 2015

Jacobi, C.M., do Carmo, F.F., Vincent, R.C. & Stehmann, J.R. (2007) Plant communities on ironstone outcrops: a diverse and endangered Brazilian ecosystem. *Biodiversity and Conservation*, **16**, 2185-2200.

Jarnevich, C.S. & Reynolds, L.V. (2011) Challenges of predicting the potential distribution of a slow-spreading invader: a habitat suitability map for an invasive riparian tree. *Biological Invasions*, **13**, 153-163.

Klein, C. (2005) Some Precambrian banded iron-formations (BIFs) from around the world: Their age, geologic setting, mineralogy, metamorphism, geochemistry, and origin. *American Mineralogist*, **90**, 1473-1499.

Kopecky, M. & Cizkova, S. (2010) Using topographic wetness index in vegetation ecology: does the algorithm matter? *Applied Vegetation Science*, **13**, 450-459.

Kuntz, K.L. & Larson, D.W. (2006) Microtopographic control of vascular plant, bryophyte and lichen communities on cliff faces. *Plant Ecology*, **185**, 239-253.

Landis, J.R. & Koch, G.G. (1977) The Measurement of Observer Agreement for Categorical Data. *Biometrics*, **33**, 159-174.

Larson, D.W., Matthes, U. & Kelly, P.E. (2000) *Cliff Ecology: Pattern and Process in Cliff Ecosystems*. Cambridge University Press.

Lobo, J.M., Jiménez-Valverde, A. & Real, R. (2008) AUC: a misleading measure of the performance of predictive distribution models. *Global Ecology and Biogeography*, **17**, 145-151.

Matthes, U.T.A. & Larson, D.W. (2006) Microsite and climatic controls of tree population dynamics: an 18-year study on cliffs. *Journal of Ecology*, **94**, 402-414.

Merow, C., Smith, M.J. & Silander, J.A. (2013) A practical guide to MaxEnt for modeling species' distributions: what it does, and why inputs and settings matter. *Ecography*, **36**, 1058-1069.

Moeslund, J.E., Arge, L., Bøcher, P.K., Dalgaard, T. & Svenning, J.C. (2013) Topography as a driver of local terrestrial vascular plant diversity patterns. *Nordic Journal of Botany*, **31**, 129-144.

Moore, I.D., Norton, T.W. & Williams, J.E. (1993) Modelling environmental heterogeneity in forested landscapes. *Journal of Hydrology*, **150**, 717-747.

Mucina, L. & Wardell-Johnson, G.W. (2011) Landscape age and soil fertility, climatic stability, and fire regime predictability: beyond the OCBIL framework. *Plant and Soil*, **341**, 1-23.

Nistelberger, H., Byrne, M., Coates, D. & Roberts, J.D. (2014) Strong Phylogeographic Structure in a Millipede Indicates Pleistocene Vicariance between Populations on Banded Iron Formations in Semi-Arid Australia. *PLoS ONE*, **9**, e93038.

O'Brien, E.M., Field, R. & Whittaker, R.J. (2000) Climatic gradients in woody plant (tree and shrub) diversity: water-energy dynamics, residual variation, and topography. *Oikos*, **89**, 588-600.

Pearce, J. & Lindenmayer, D. (1998) Bioclimatic analysis to enhance reintroduction biology of the endangered helmeted honeyeater (Lichenostomus melanops cassidix) in southeastern Australia. *Restoration Ecology*, **6**, 238-243.

Phillips, S.J. & Dudik, M. (2008) Modeling of species distributions with Maxent: new extensions and a comprehensive evaluation. *Ecography*, **31**, 161-175.

Phillips, S.J., Anderson, R.P. & Schapire, R.E. (2006) Maximum entropy modeling of species geographic distributions. *Ecological Modelling*, **190**, 231-259.

Radcliffe, J.E. & Lefever, K.R. (1981) Aspect influences on pasture microclimate at Coopers Creek, North Canterbury. *New Zealand Journal of Agricultural Research*, **24**, 55-56.

Robinson, T.P., van Klinken, R.D. & Metternicht, G. (2010) Comparison of alternative strategies for invasive species distribution modeling. *Ecological Modelling*, **221**, 2261-2269.

Seibert, J. & McGlynn, B.L. (2007) A new triangular multiple flow direction algorithm for computing upslope areas from gridded digital elevation models. *Water Resources Research*, **43**

Simmons, M.E., Wu, X.B. & Whisenant, S.G. (2011) Plant and Soil Responses to Created Microtopography and Soil Treatments in Bottom land Hardwood Forest Restoration. *Restoration Ecology*, **19**, 136-146.

Sorensen, R., Zinko, U. & Seibert, J. (2006) On the calculation of the topographic wetness index: evaluation of different methods based on field observations. *Hydrology and Earth System Sciences*, **10**, 101-112.

Tarboton, D.G. (1997) A new method for the determination of flow directions and upslope areas in grid digital elevation models. *Water Resources Research*, **33**, 309-319.

Thuiller, W., Lavorel, S. & Araujo, M.B. (2005) Niche properties and geographical extent as predictors of species sensitivity to climate change. *Global Ecology and Biogeography*, **14**, 347-357.

Tinoco, B.A., Asudillo, P.X., Latta, S.C. & Graham, C.H. (2009) Distribution, ecology and conservation of an endangered Andean hummingbird: the Violet-throated Metaltail (Metallura baroni). *Bird Conservation International*, **19**, 63-76.

Tittensor, D.P., Baco, A.R., Brewin, P.E., Clark, M.R., Consalvey, M., Hall-Spencer, J., Rowden, A.A., Schlacher, T., Stocks, K.I. & Rogers, A.D. (2009) Predicting global habitat suitability for stony corals on seamounts. *Journal of Biogeography*, **36**, 1111-1128.

Vetaas, O.R. (2002) Realized and potential climate niches: a comparison of four Rhododendron tree species. *Journal of Biogeography*, **29**, 545-554.

Viscarra Rossel, R., Chen, C., Grundy, M., Searle, R., Clifford, D. & Campbell, P. (In preparation) The Australian three-dimensional soil grid: Australia's contribution to the GlobalSoilMap project. *Soil Research*,

Viscarra Rossel, R., Chen, C., Grundy, M., Searle, R., Clifford, D., Odgers, N., Griffin, T., Liddicoat, C. & Kidd, D. (2014) Soil and Landscape Grid National Soil Attribute Maps - Total Nitrogen (3" resolution) - Version 1. In: (ed. Csiro), Australia.

VivianSmith, G. (1997) Microtopographic heterogeneity and floristic diversity in experimental wetland communities. *Journal of Ecology*, **85**, 71-82.

Wildlife (1950) An Act to provide for the conservation and protection of wildlife, Parliament of Western Australia. In:

Wisz, M.S., Hijmans, R.J., Li, J., Peterson, A.T., Graham, C.H., Guisan, A. & Group, N.P.S.D.W. (2008) Effects of sample size on the performance of species distribution models. *Diversity and Distributions*, **14**, 763-773.

Yates, C.J., McNeill, A., Elith, J. & Midgley, G.F. (2010) Assessing the impacts of climate change and land transformation on Banksia in the South West Australian Floristic Region. *Diversity and Distributions*, **16**, 187-201.

Yates, C.J., Gibson, N., Pettit, N.E., Dillon, R. & Palmer, R. (2011) The ecological relationships and demography of restricted ironstone endemic plant species: implications for conservation. *Australian Journal of Botany*, **59**, 691-699.

Zipper, C.E., Burger, J.A., Skousen, J.G., Angel, P.N., Barton, C.D., Davis, V. & Franklin, J.A. (2011) Restoring Forests and Associated Ecosystem Services on Appalachian Coal Surface Mines. *Environmental Management*, **47**, 751-765.

Figure 1. Banded ironstone formations (BIFs) in the study area (A). BIFs are topographically complex and comprise a mosaic of fractured rock surfaces with intricate variation in relief, slope and aspect (B). Many plant species grow on rocky surfaces with negligible soil cover, often in small gaps between rocks.

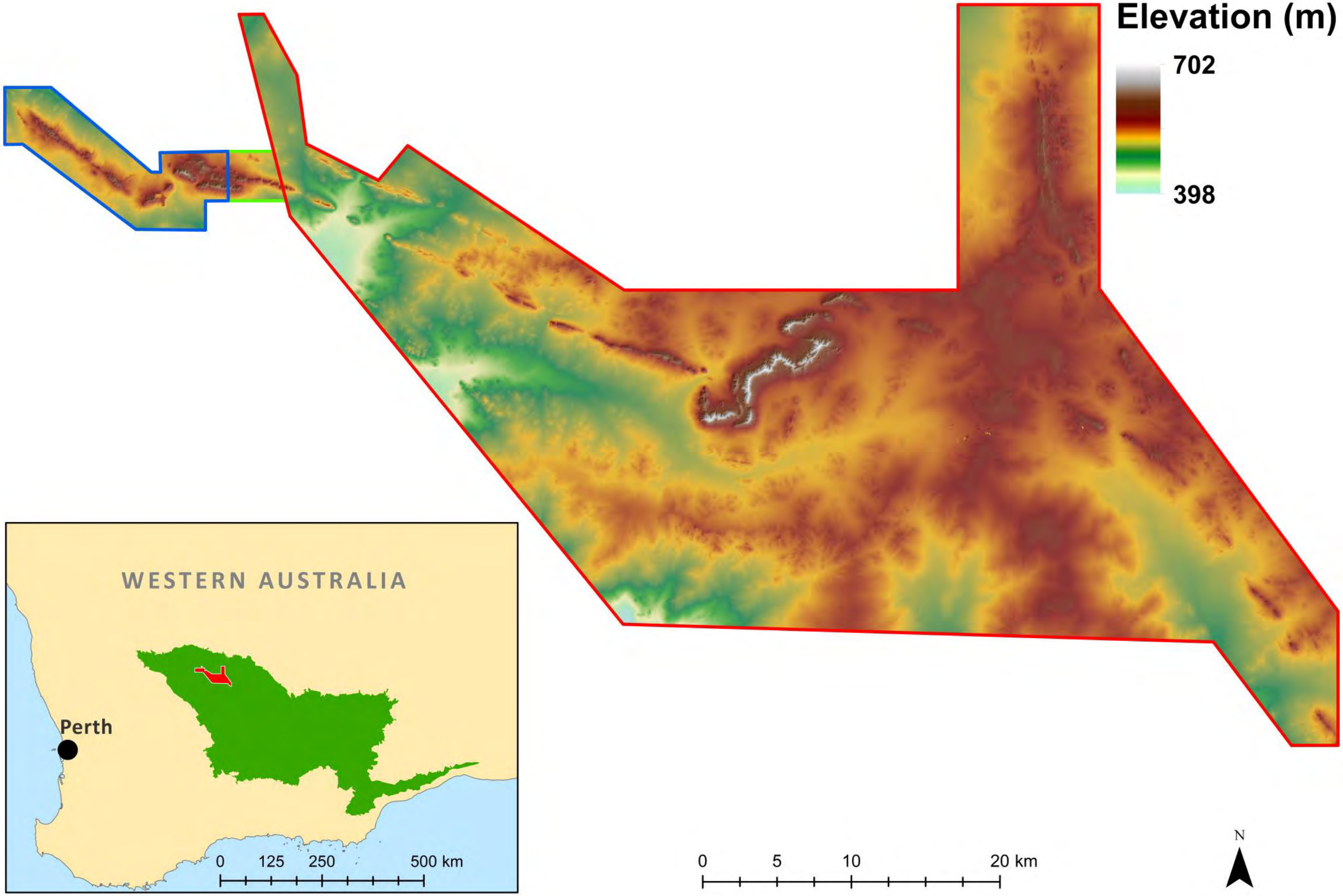

Figure 2. The study area comprises the Helena and Aurora Range banded ironstone formation (BIF) summits and surrounding BIFs and plains. The study area was scanned by three separate surveys: light detection and ranging (LiDAR, delineated in red, 1524 km^2), radar (delineated in blue, 69 km^2), aerial photography (delineated in green, 12 km^2). Inset: the location of the study area in the Coolgardie biogeographic region in south-western Australia.

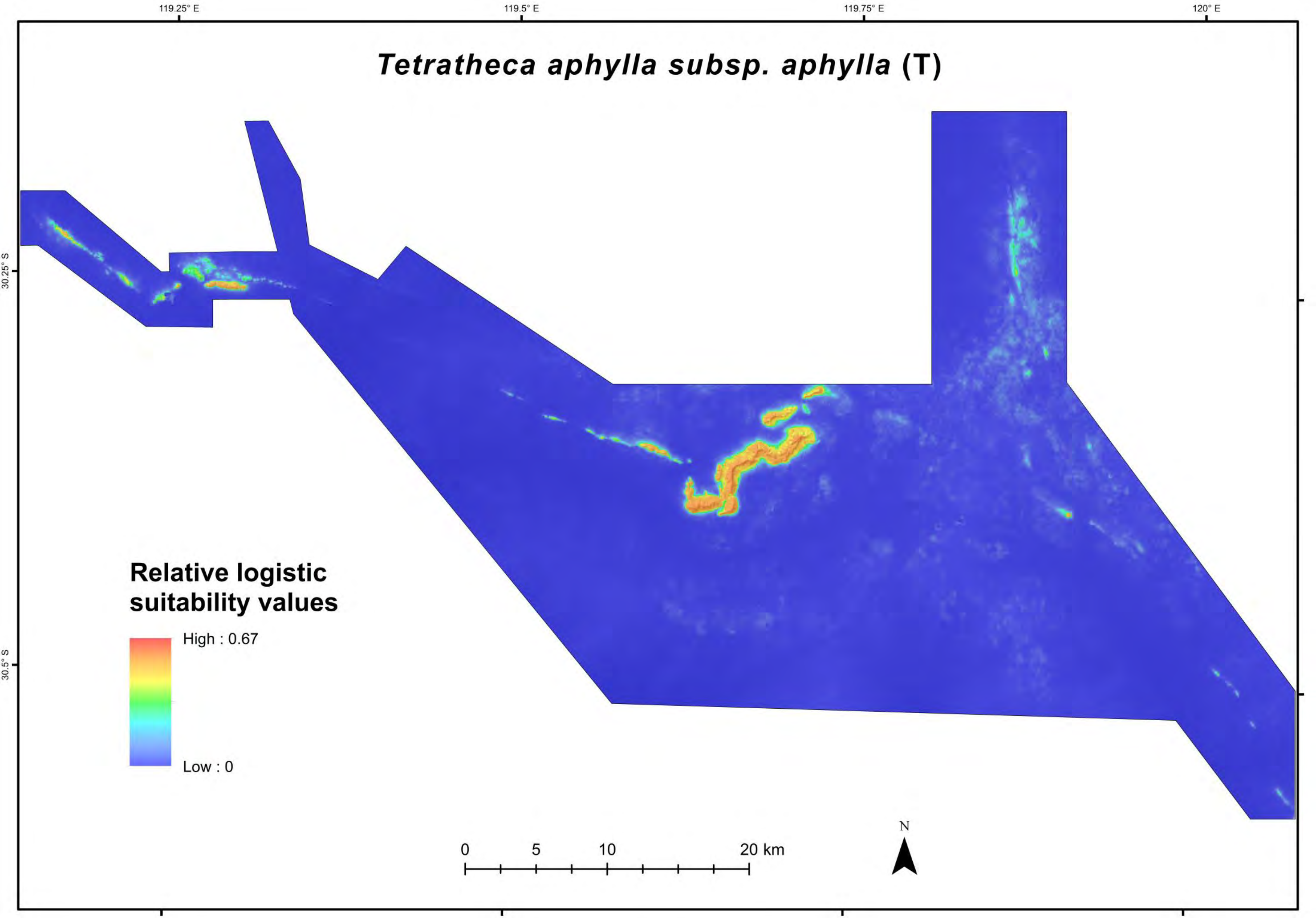

Figure 3. Predicted habitat suitability for *Tetratheca aphylla subsp. Aphylla* (default background sample selection).

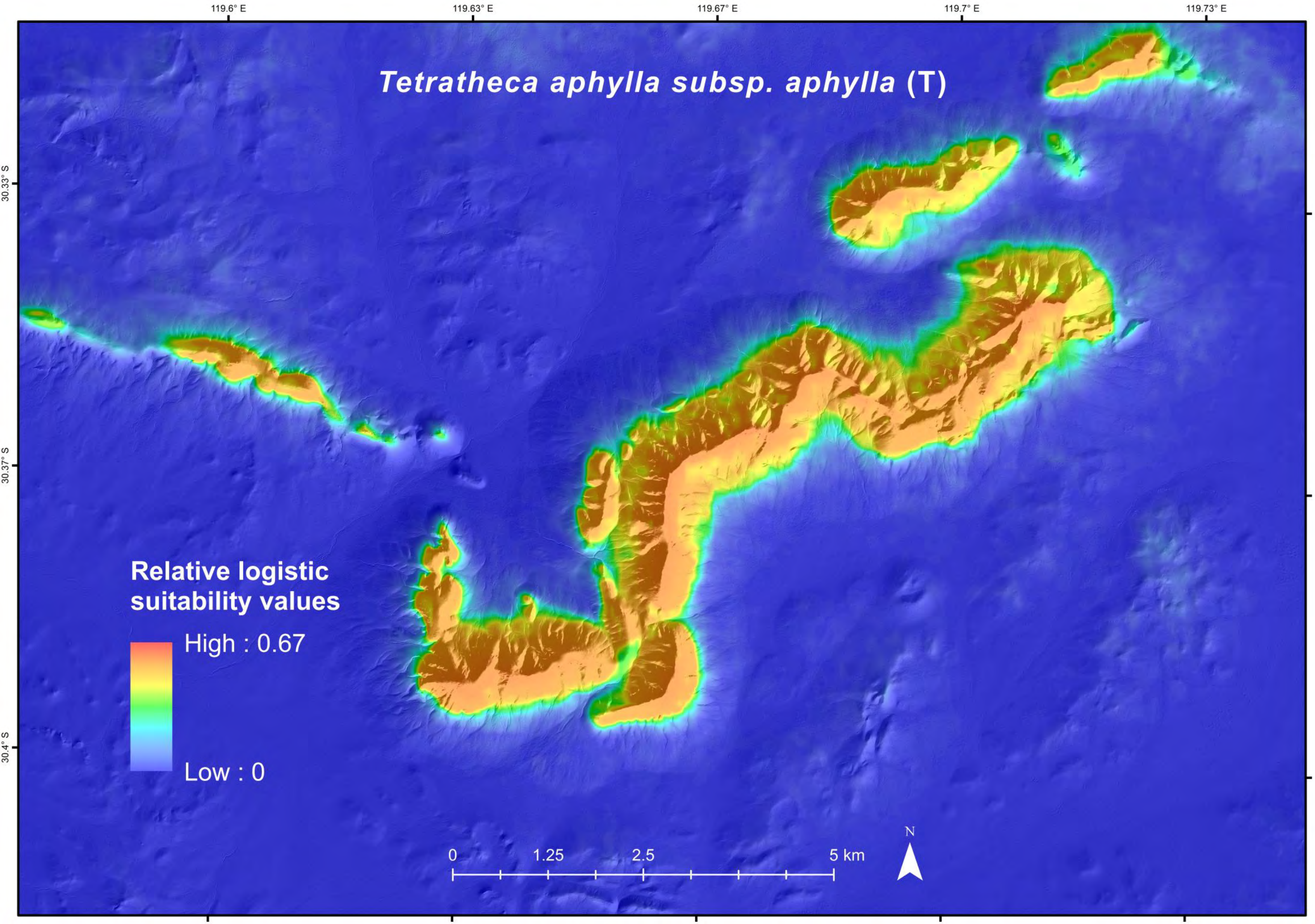

Figure 4. Predicted habitat suitability for *Tetratheca aphylla subsp. Aphylla* (default background sample selection).

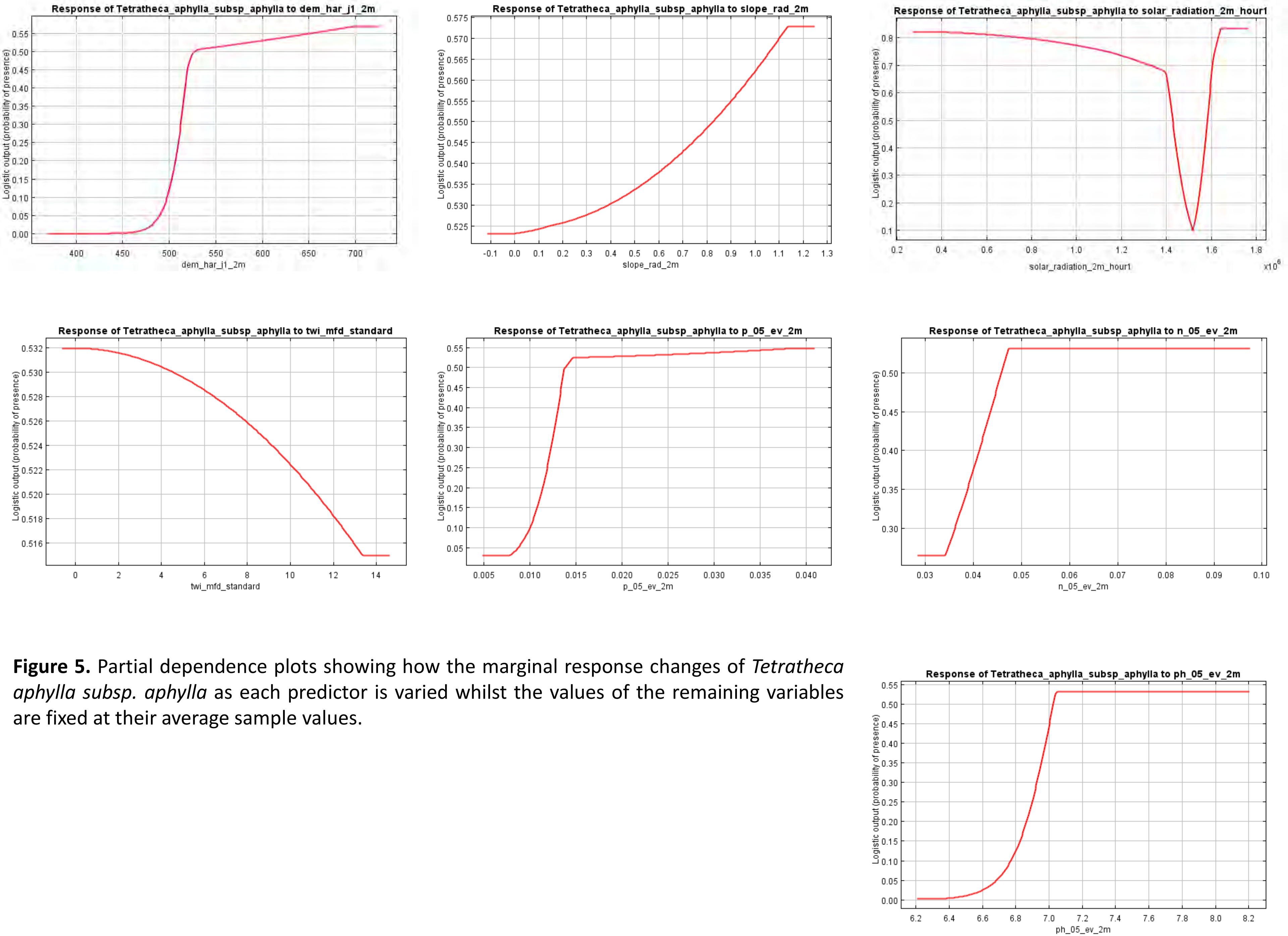

Figure 5. Partial dependence plots showing how the marginal response changes of *Tetratheca aphylla subsp. aphylla* as each predictor is varied whilst the values of the remaining variables are fixed at their average sample values.

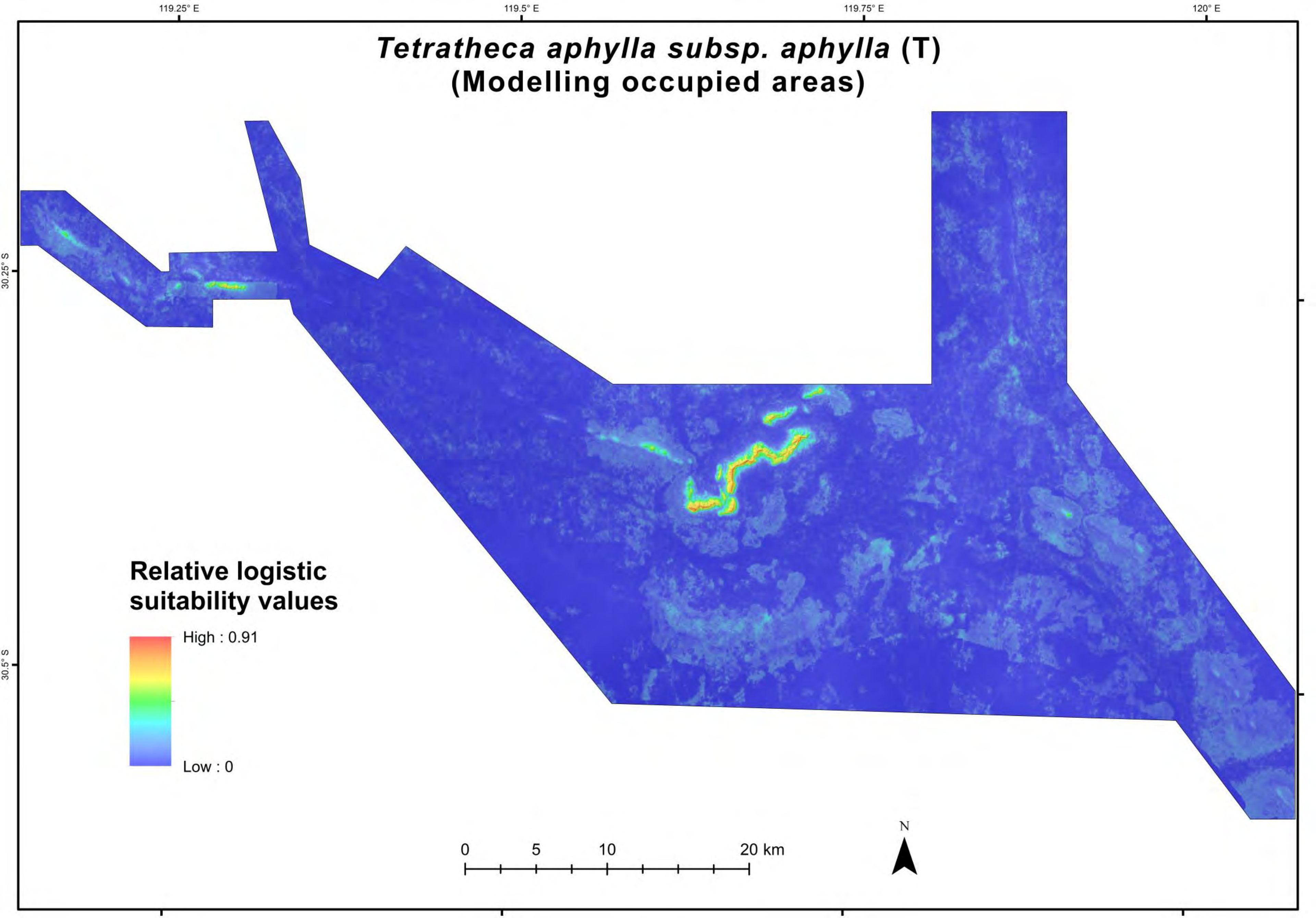

Figure 6. Predicted habitat suitability for *Tetratheca aphylla subsp. Aphylla* (restricted background sample selection).

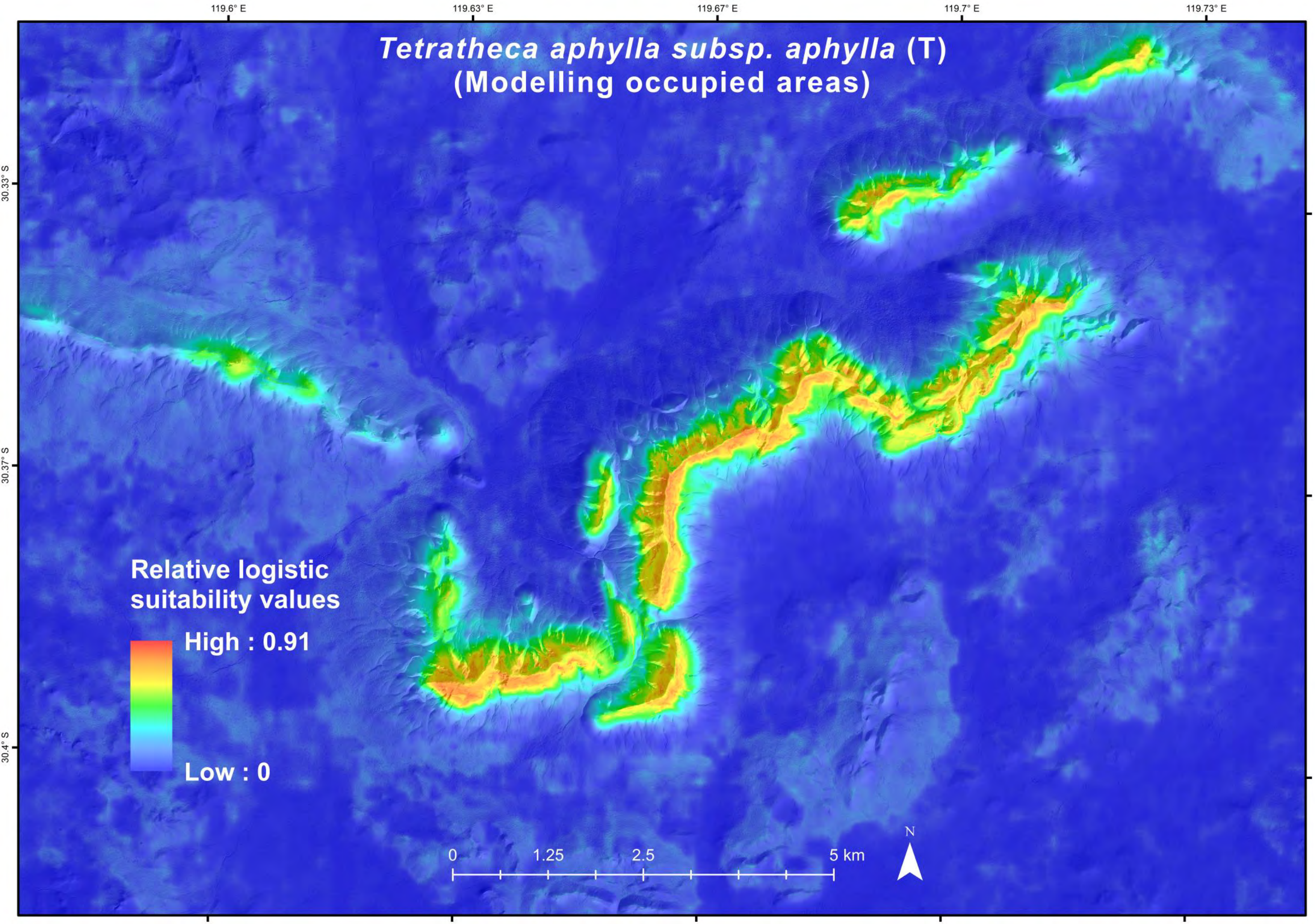

Figure 7. Predicted habitat suitability for *Tetratheca aphylla subsp. Aphylla* (restricted background sample selection).

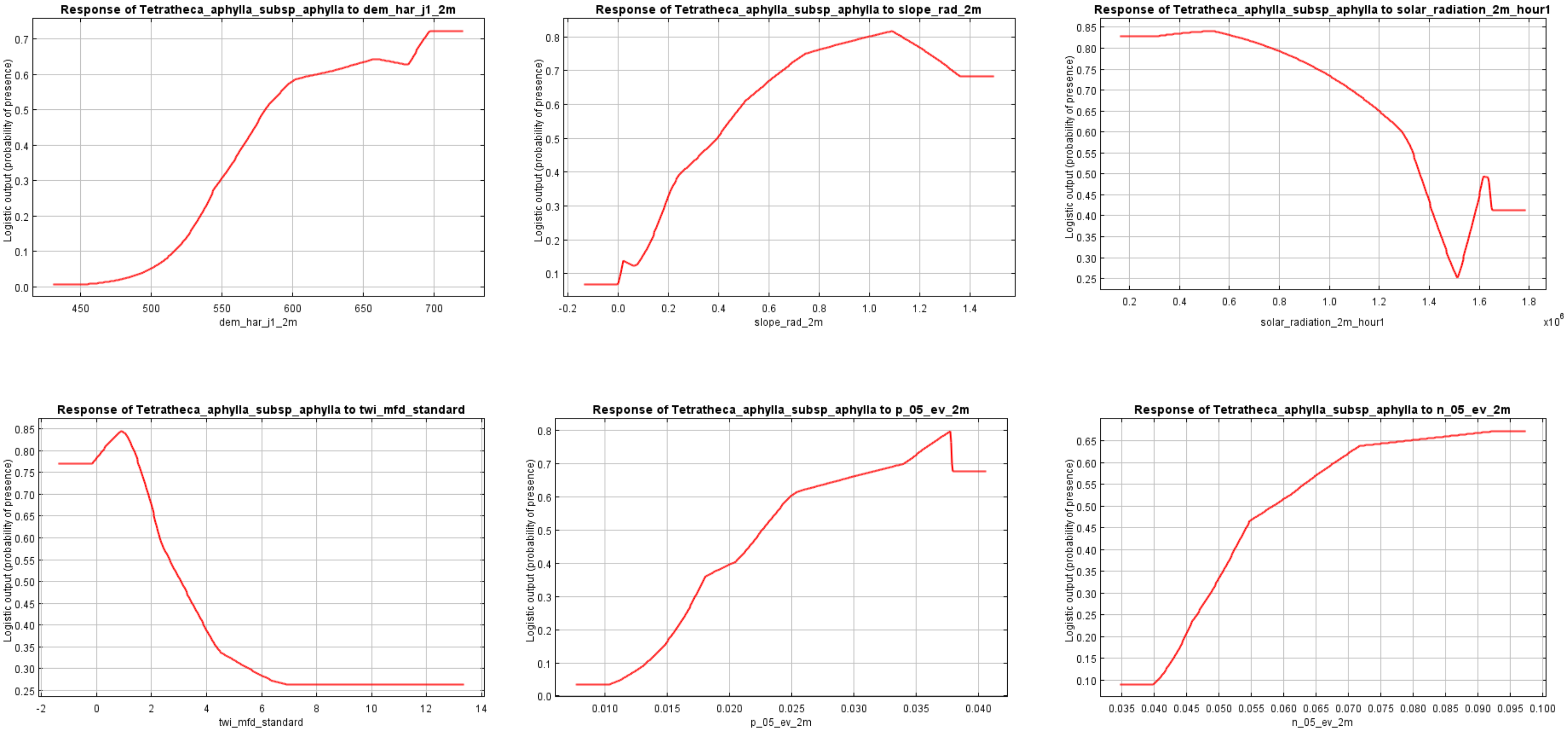
Response of Tetratheca_aphylla_subsp_aphylla to dem_har_j1_2m

Response of Tetratheca_aphylla_subsp_aphylla to slope_rad_2m

Response of Tetratheca_aphylla_subsp_aphylla to solar_radiation_2m_hour1

Response of Tetratheca_aphylla_subsp_aphylla to twi_mfd_standard

Response of Tetratheca_aphylla_subsp_aphylla to p_05_ev_2m

Response of Tetratheca_aphylla_subsp_aphylla to n_05_ev_2m

Figure 8. Partial dependence plots showing how the marginal response changes of *Tetratheca aphylla subsp. aphylla* as each predictor is varied whilst the values of the remaining variables are fixed at their average sample values.

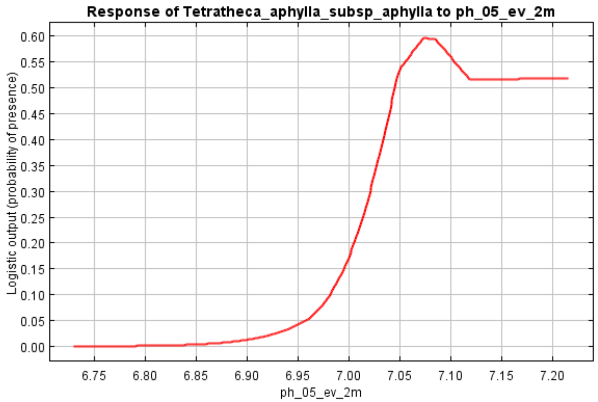
Response of Tetratheca_aphylla_subsp_aphylla to ph_05_ev_2m

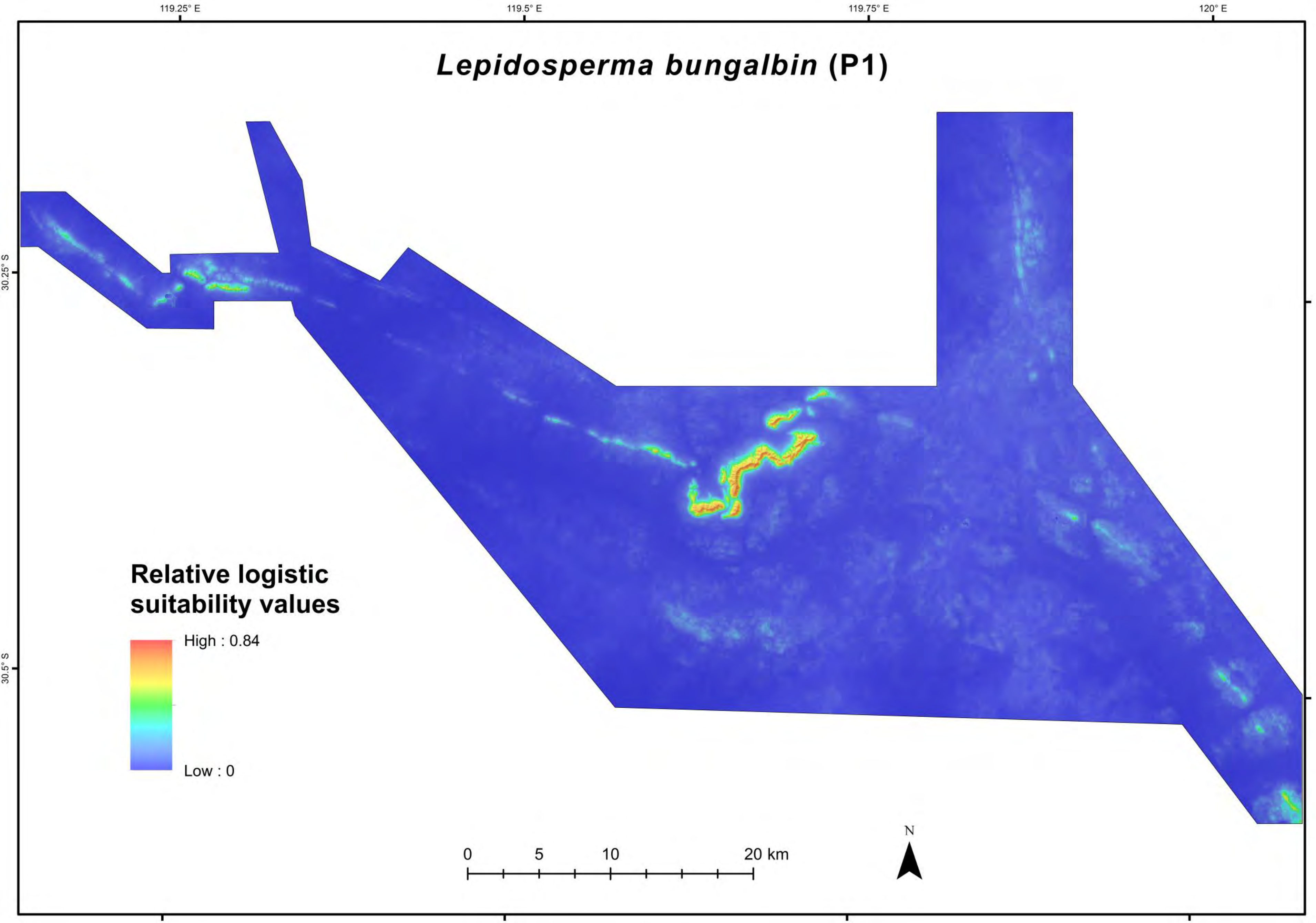

Figure 9. Predicted habitat suitability for *Lepidosperma bungalbin* (default background sample selection).

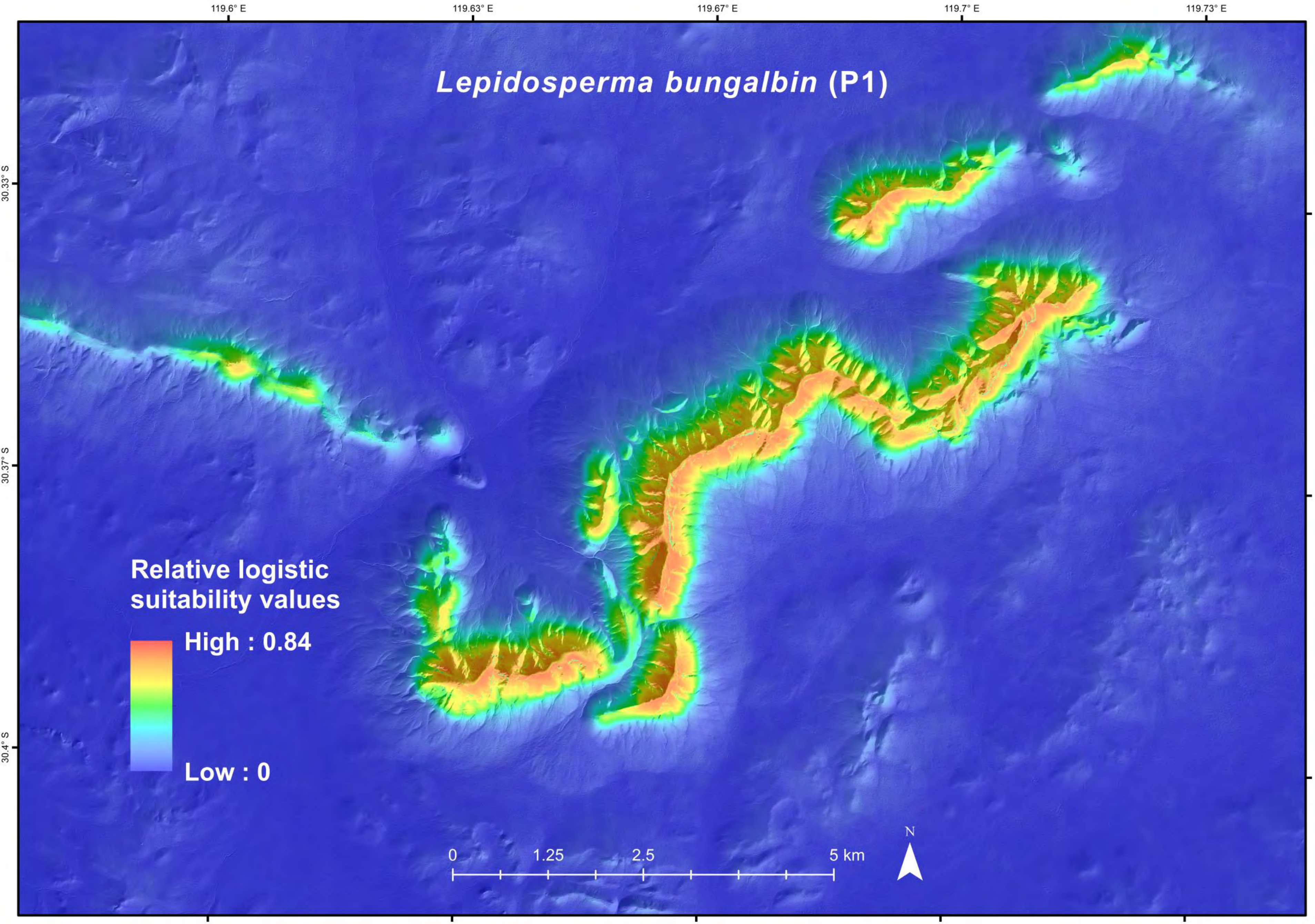

Figure 10. Predicted habitat suitability for *Lepidosperma bungalbin* (default background sample selection).

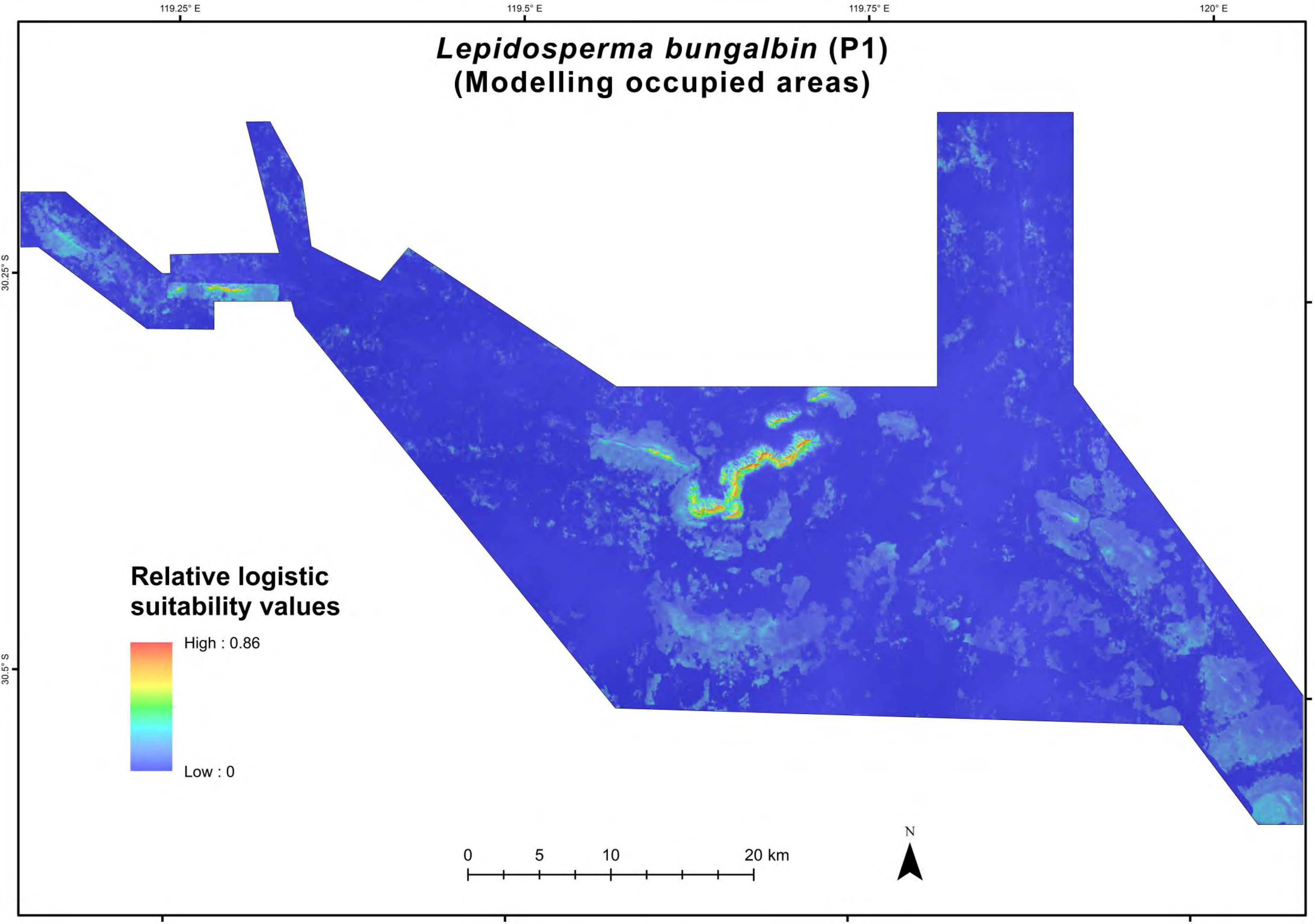

Figure 11. Predicted habitat suitability for *Lepidosperma bungalbin* (restricted background sample selection).

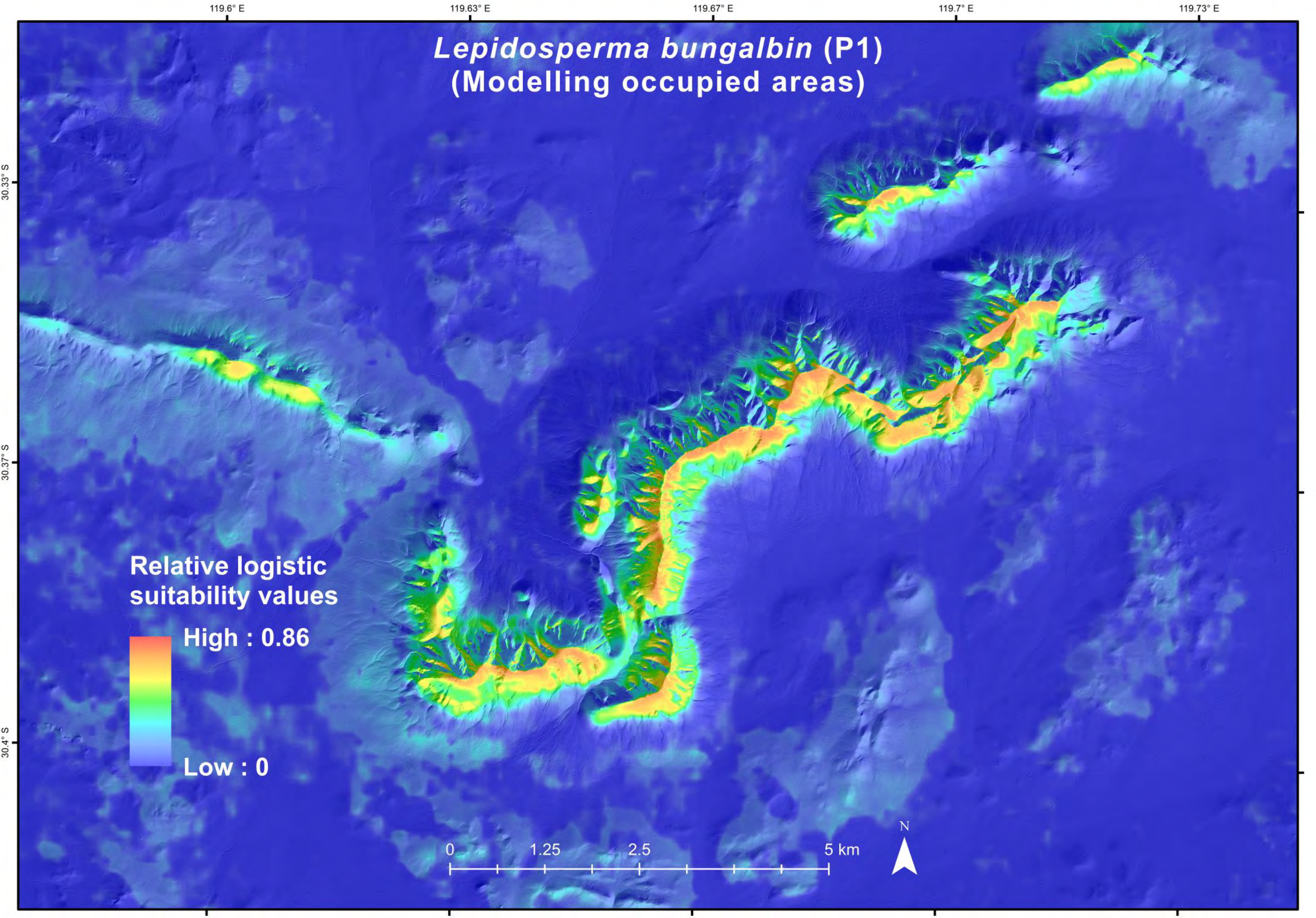

Figure 12. Predicted habitat suitability for *Lepidosperma bungalbin* (restricted background sample selection).

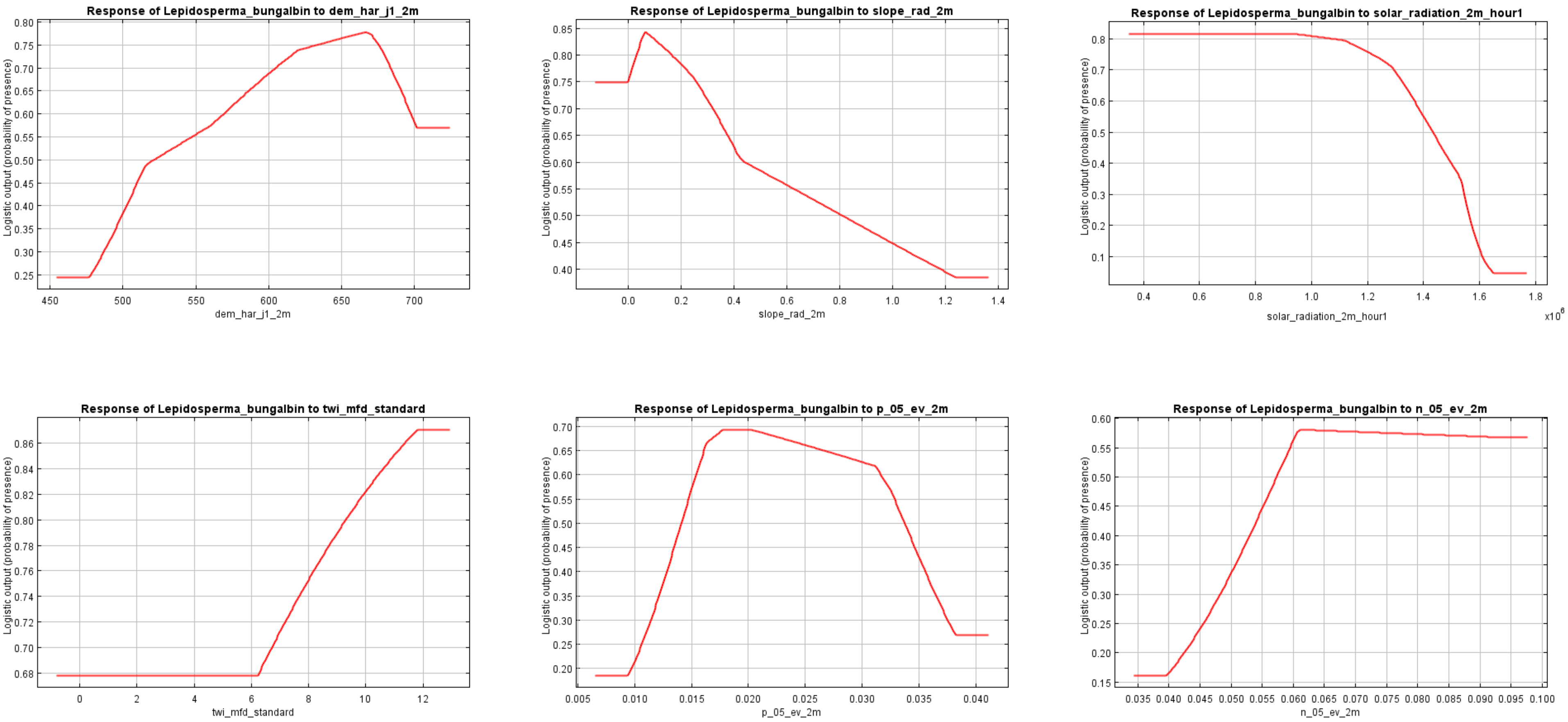

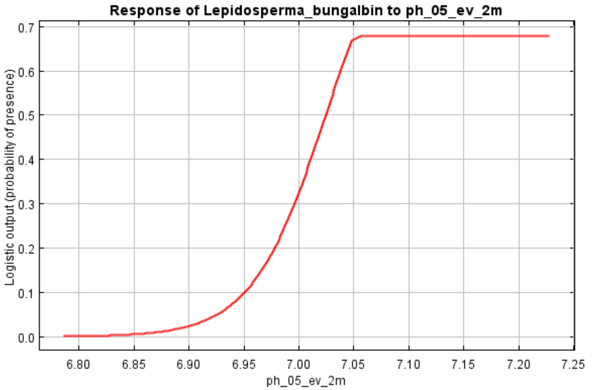

Figure 13. Partial dependence plots showing how the marginal response changes of *Lepidosperma bungalbin* as each predictor is varied whilst the values of the remaining variables are fixed at their average sample values.

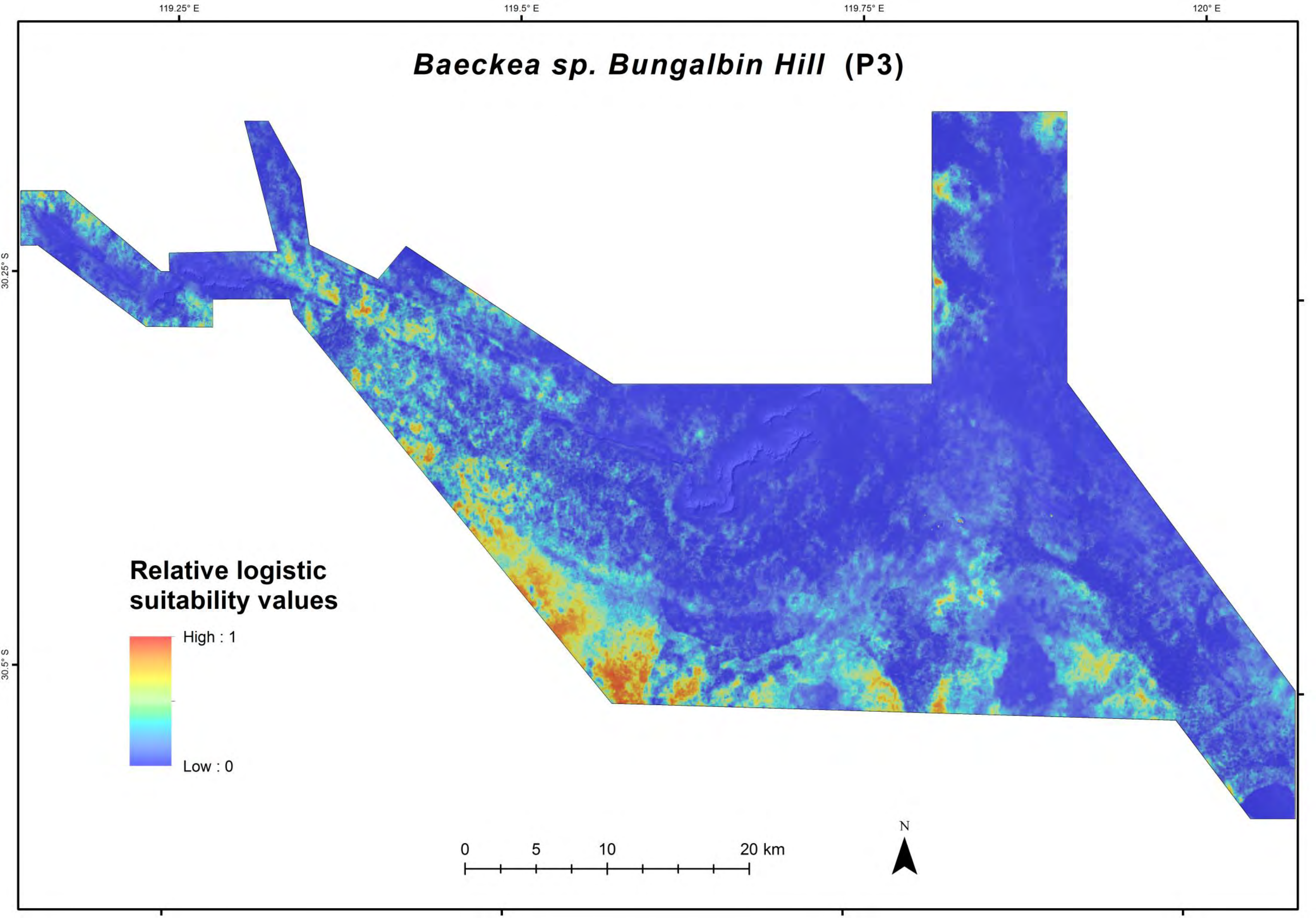

Figure 14. Predicted habitat suitability for *Baeckea sp. Bungalbin Hill* for each 2 × 2 m grid cell (default background sample selection).

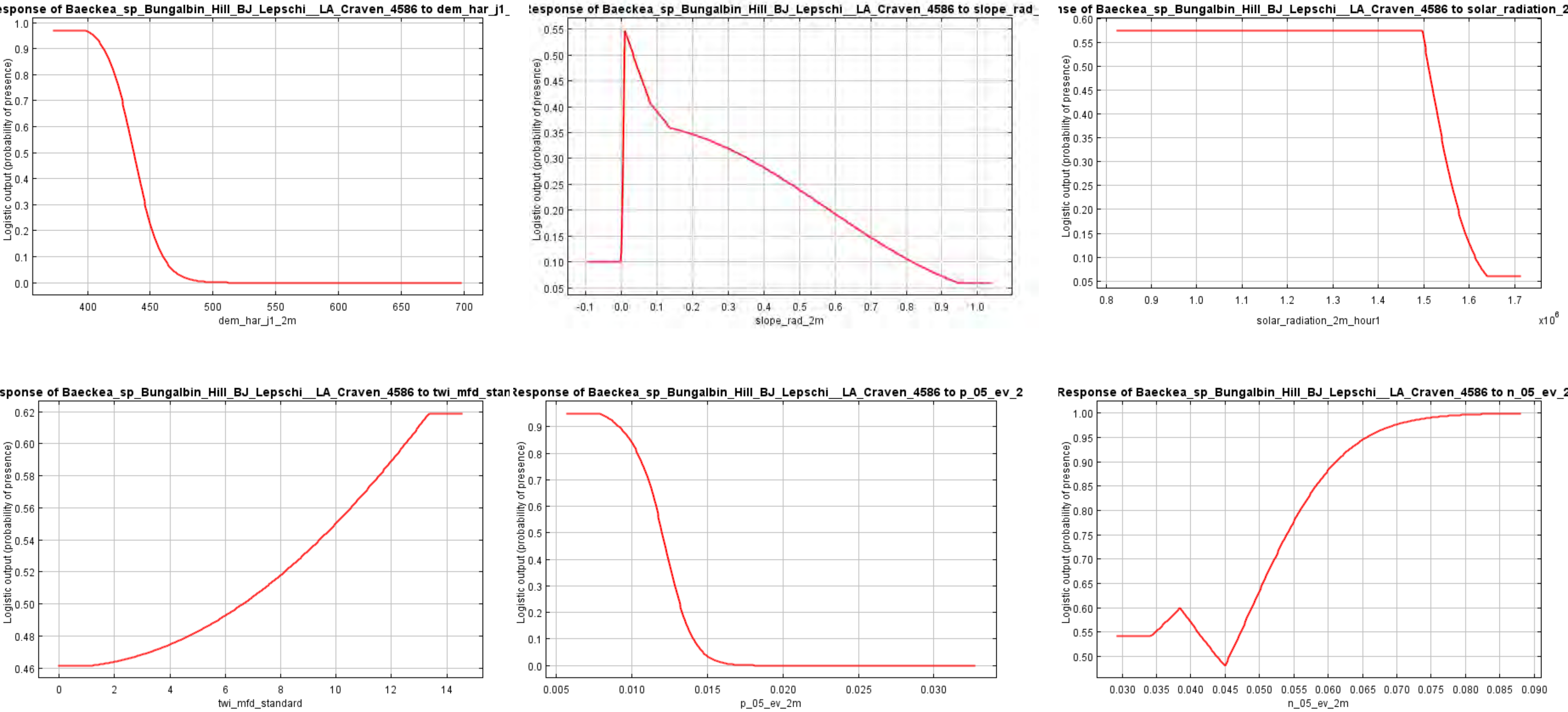

Figure 15. Partial dependence plots showing how the marginal response of *Baeckea sp. Bungalbin Hill* changes as each predictor is varied whilst the values of the remaining variables are fixed at their average sample values.

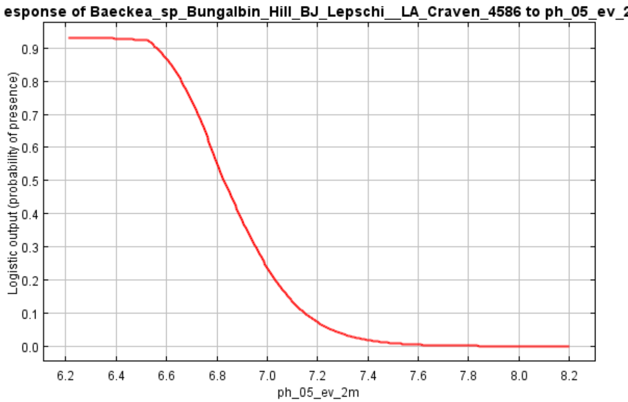

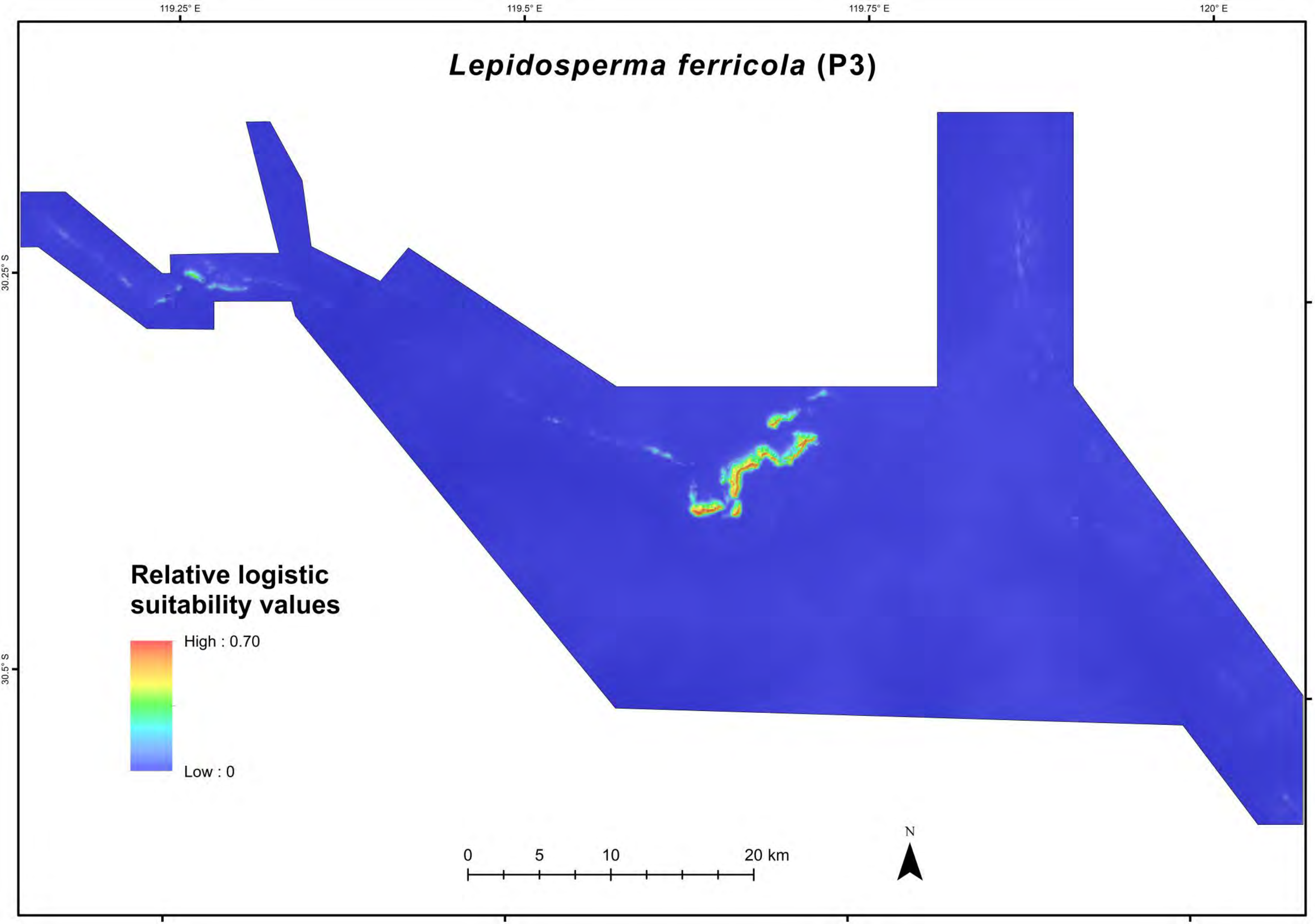

Figure 16. Predicted habitat suitability for *Lepidosperma ferricola* (default background sample selection).

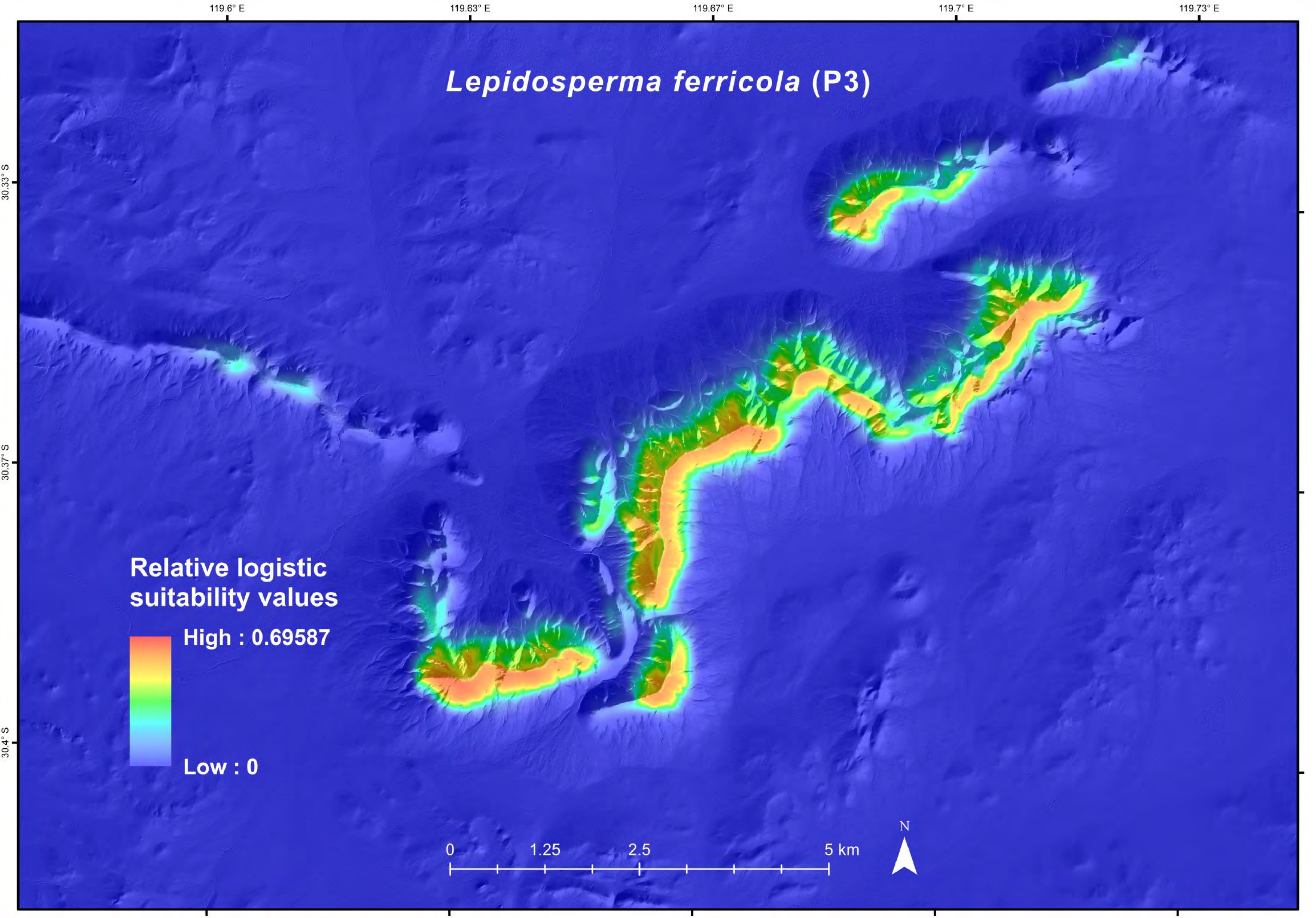

Figure 17. Predicted habitat suitability for *Lepidosperma ferricola* (default background sample selection).

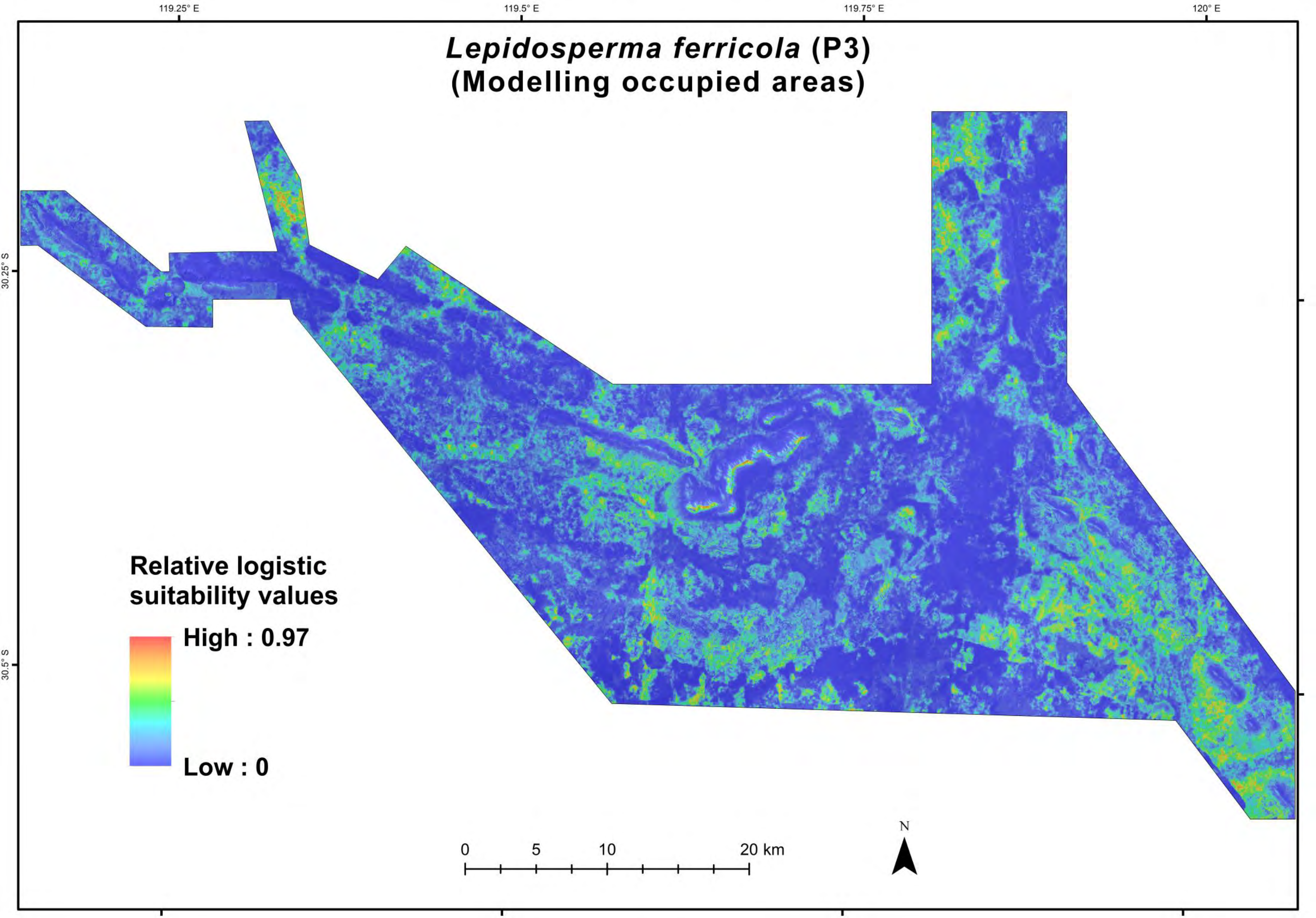

Figure 18. Predicted habitat suitability for *Lepidosperma ferricola* (default background sample selection).

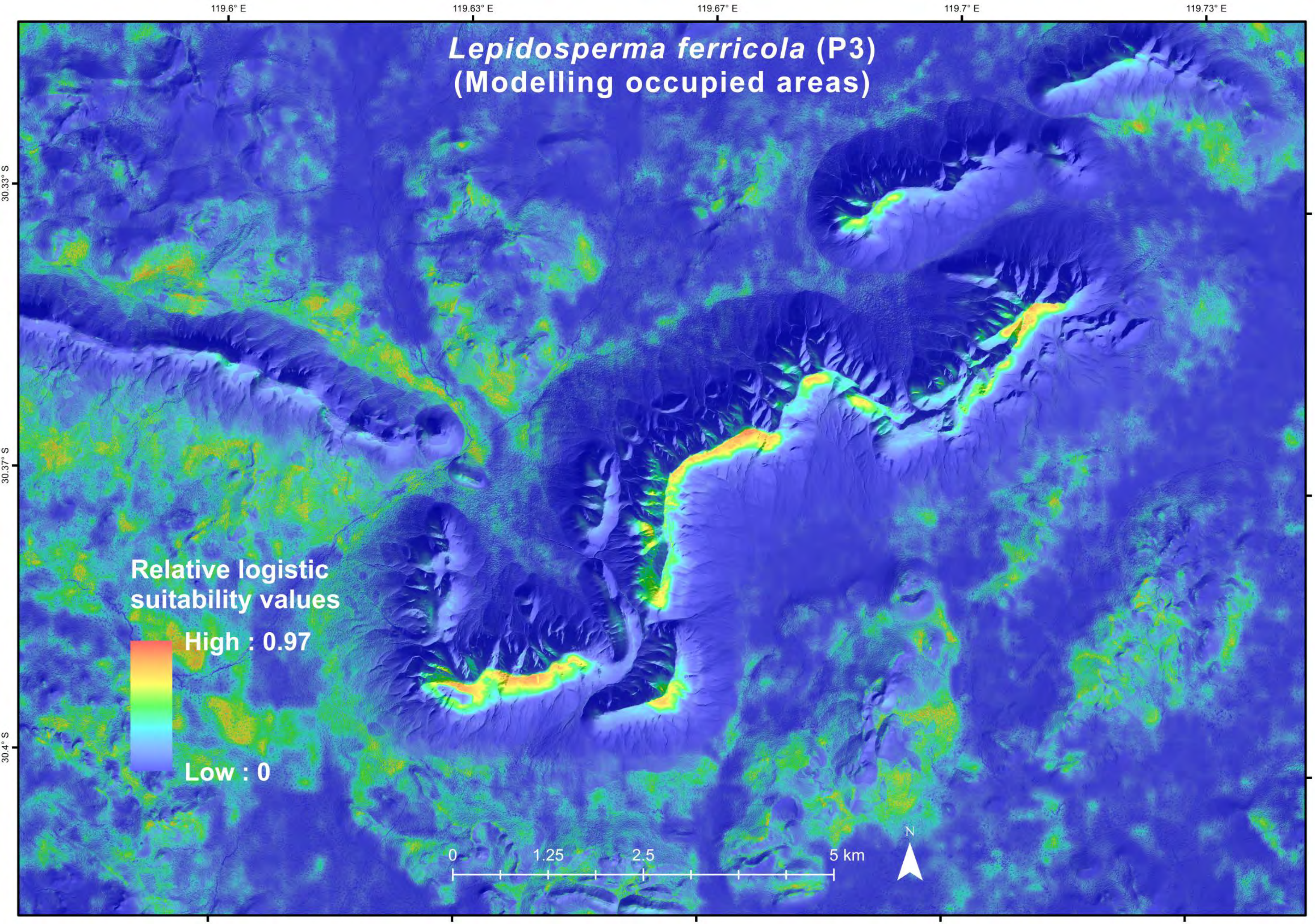

Figure 19. Predicted habitat suitability for *Lepidosperma ferricola* (restricted background sample selection).

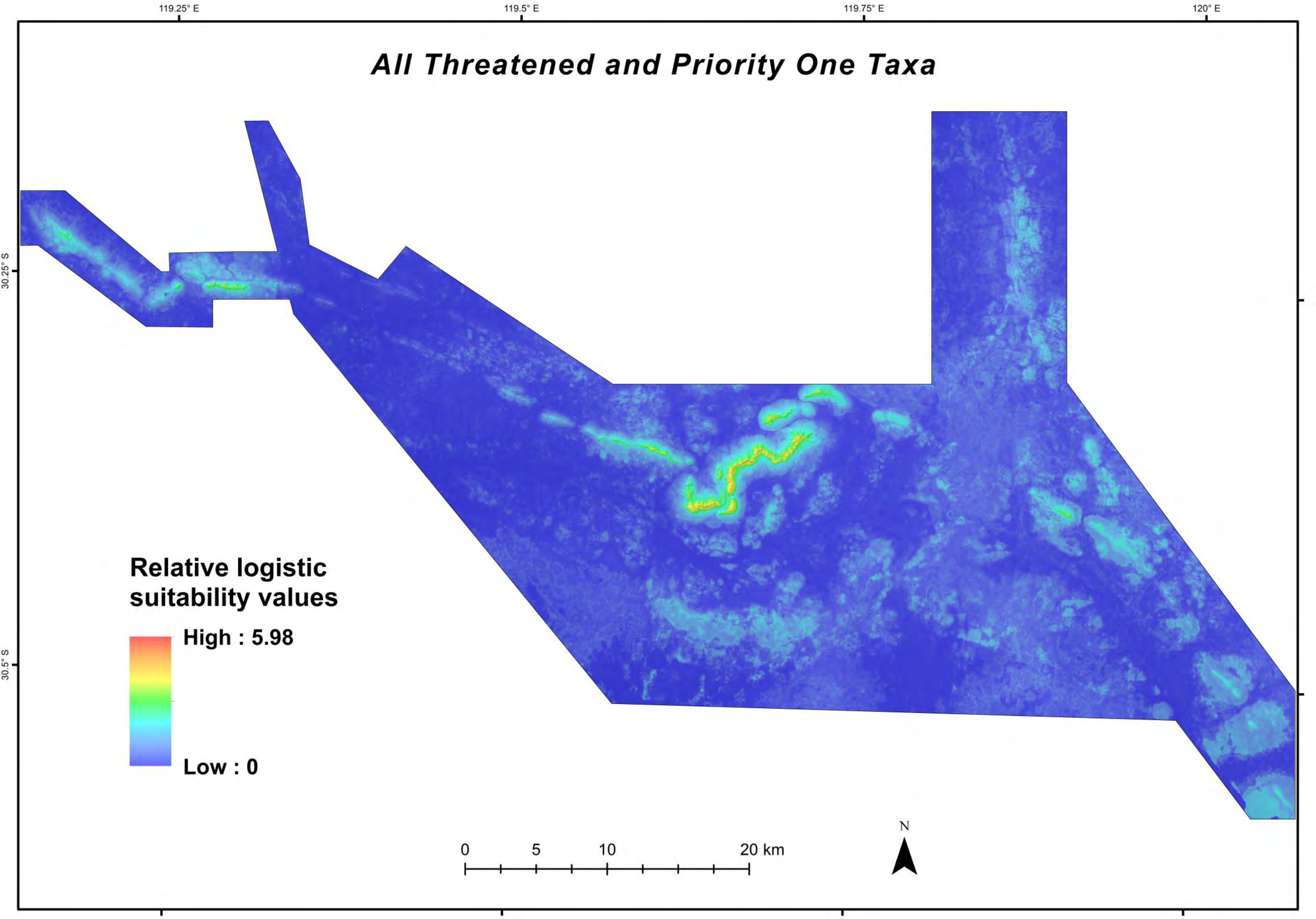

Figure 20. Predicted habitat suitability for all threatened and priority one taxa (restricted background sample selection).

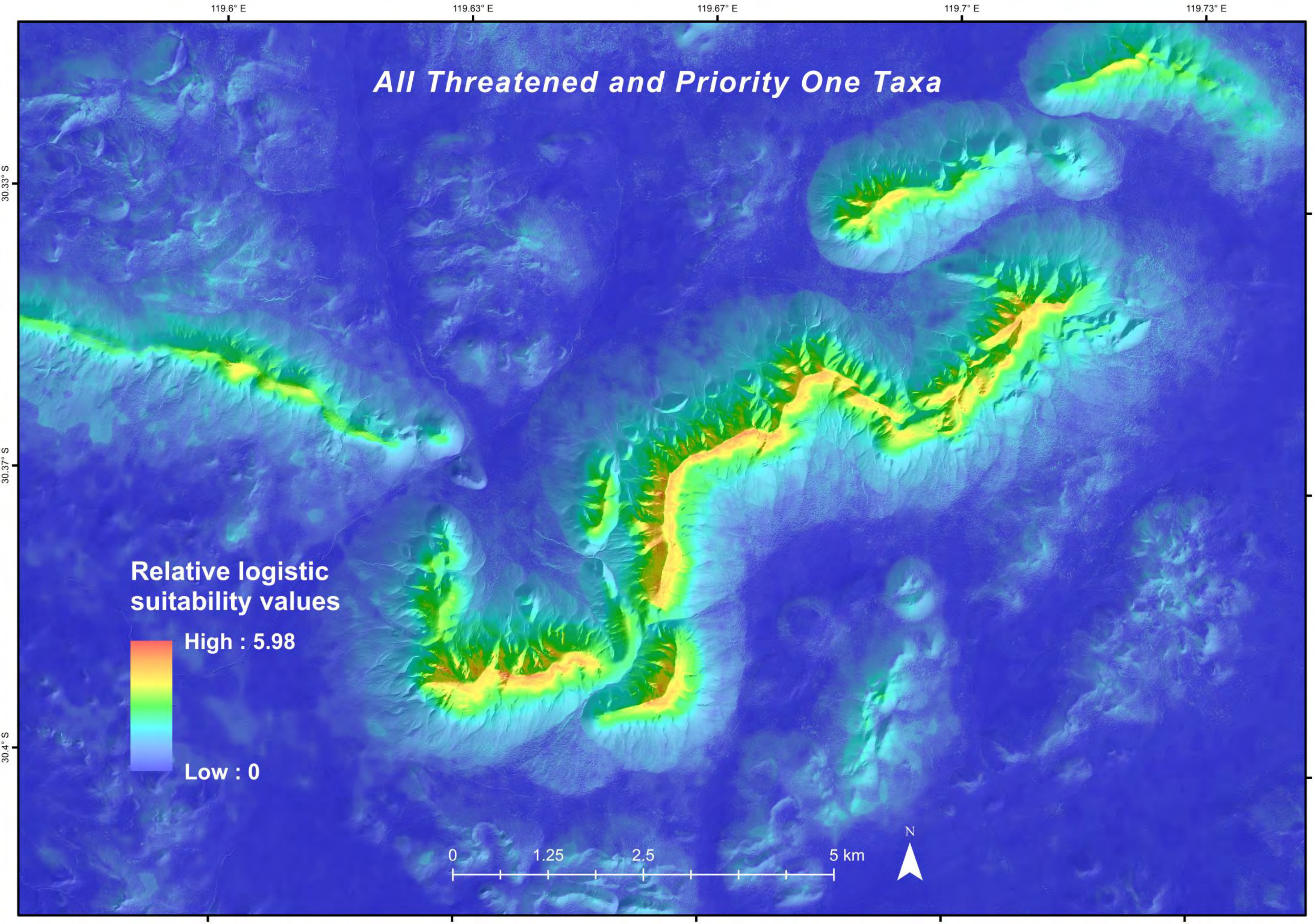

Figure 21. Predicted habitat suitability for all threatened and priority one taxa, focusing on the HAR (restricted background sample selection).

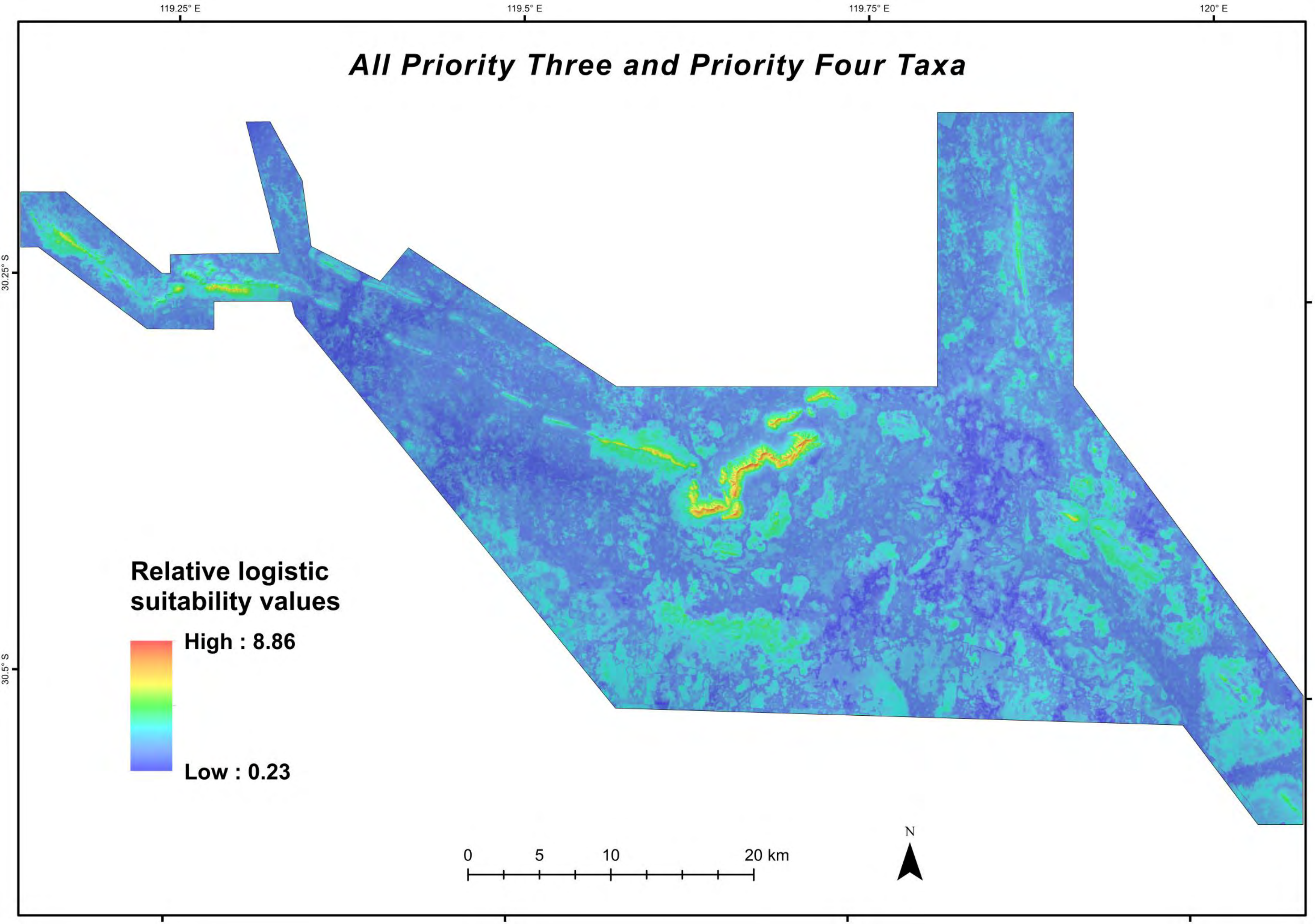

Figure 22. Predicted habitat suitability for all priority three and priority four taxa (restricted background sample selection).

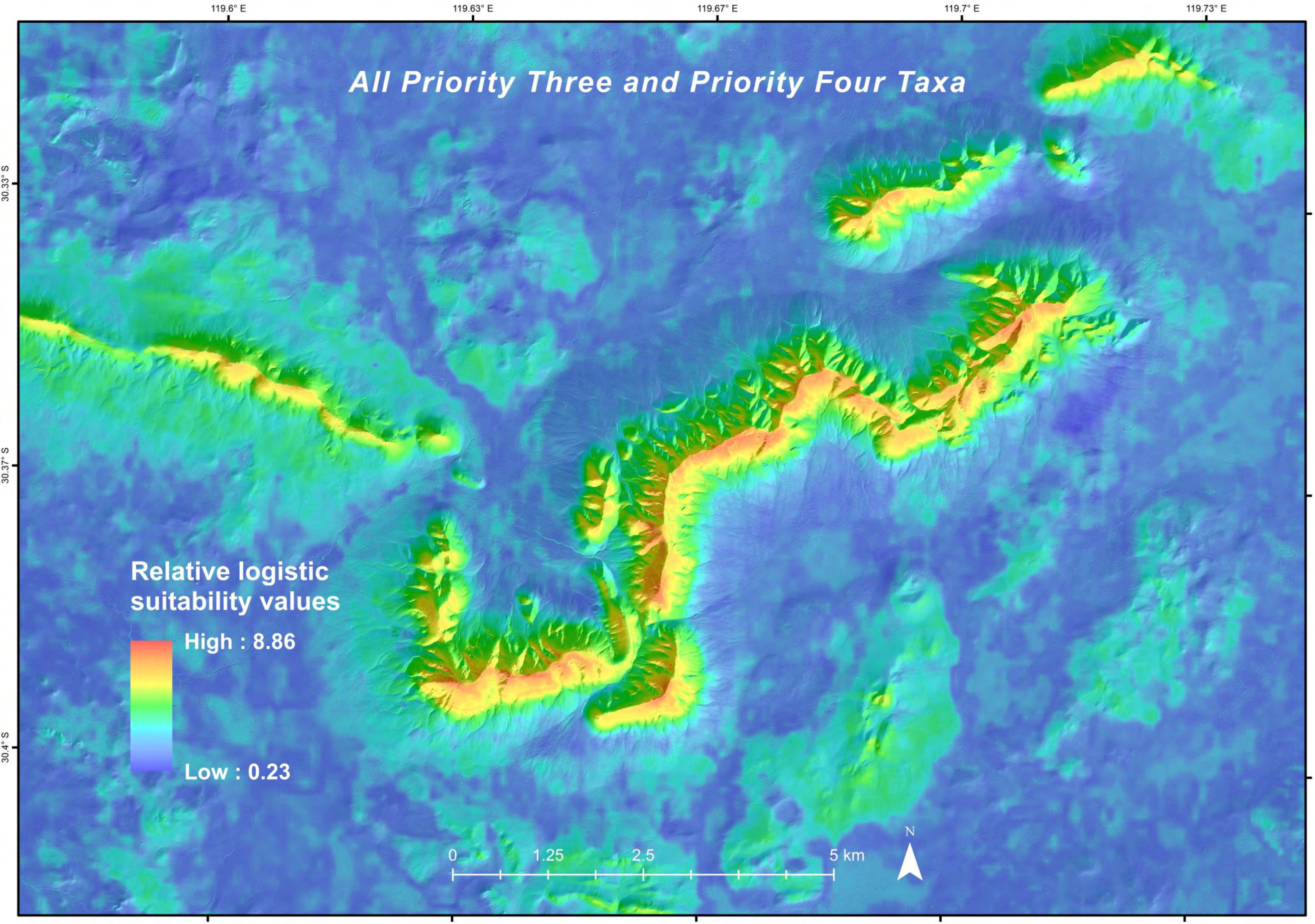

Figure 23. Predicted habitat suitability for all priority three and priority four taxa, focusing on the HAR (restricted background sample selection).

Supplementary Materials

Figures S1 – S54

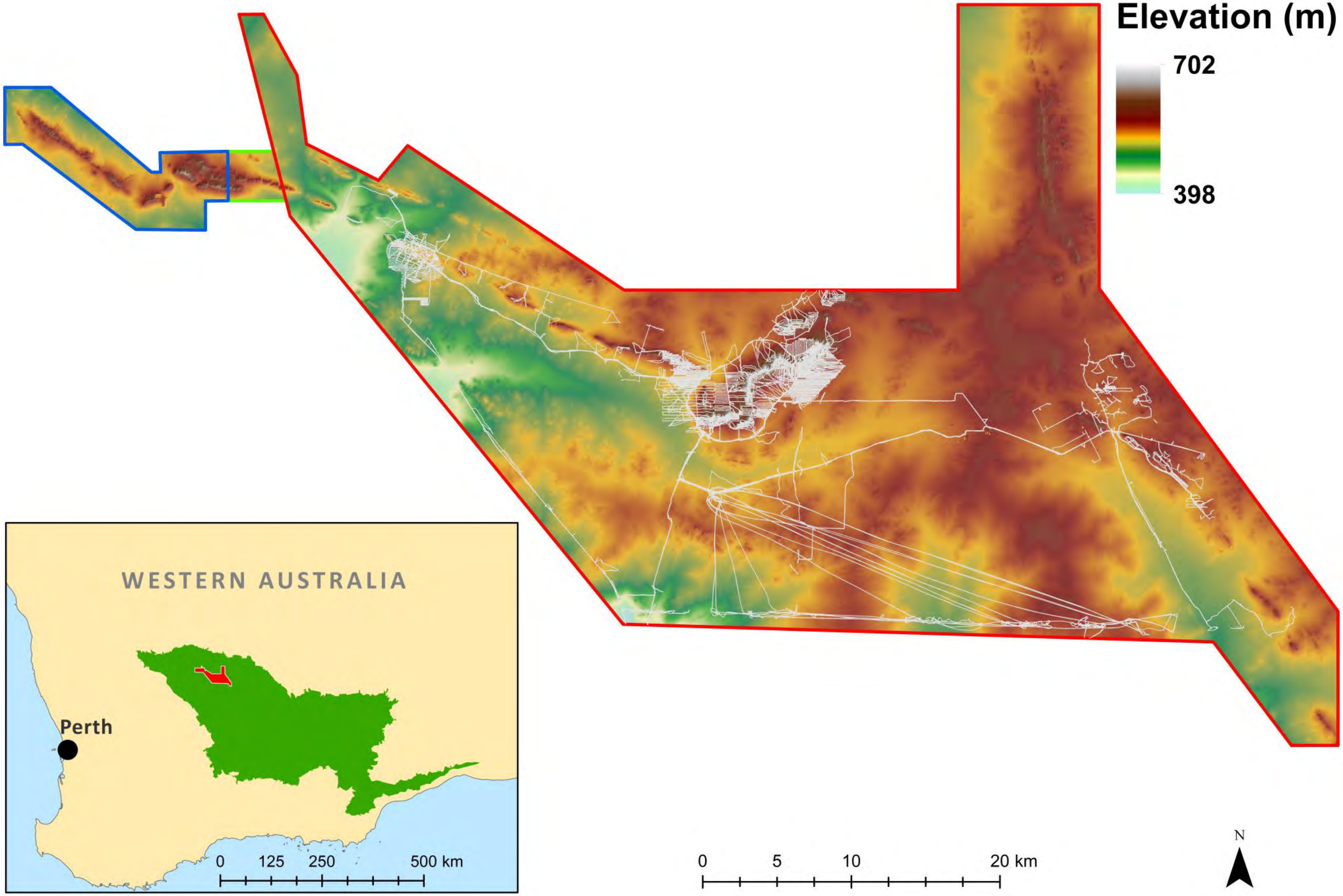

Figure S1. The study area comprises the Helena and Aurora Range banded ironstone formation (BIF) summits and surrounding BIFs and plains. Survey transects are shown in grey. The diagonal (north-west to south-east) transects in the south were flown by helicopter. Inset: study area location in the Coolgardie biogeographic region in south-western Australia.

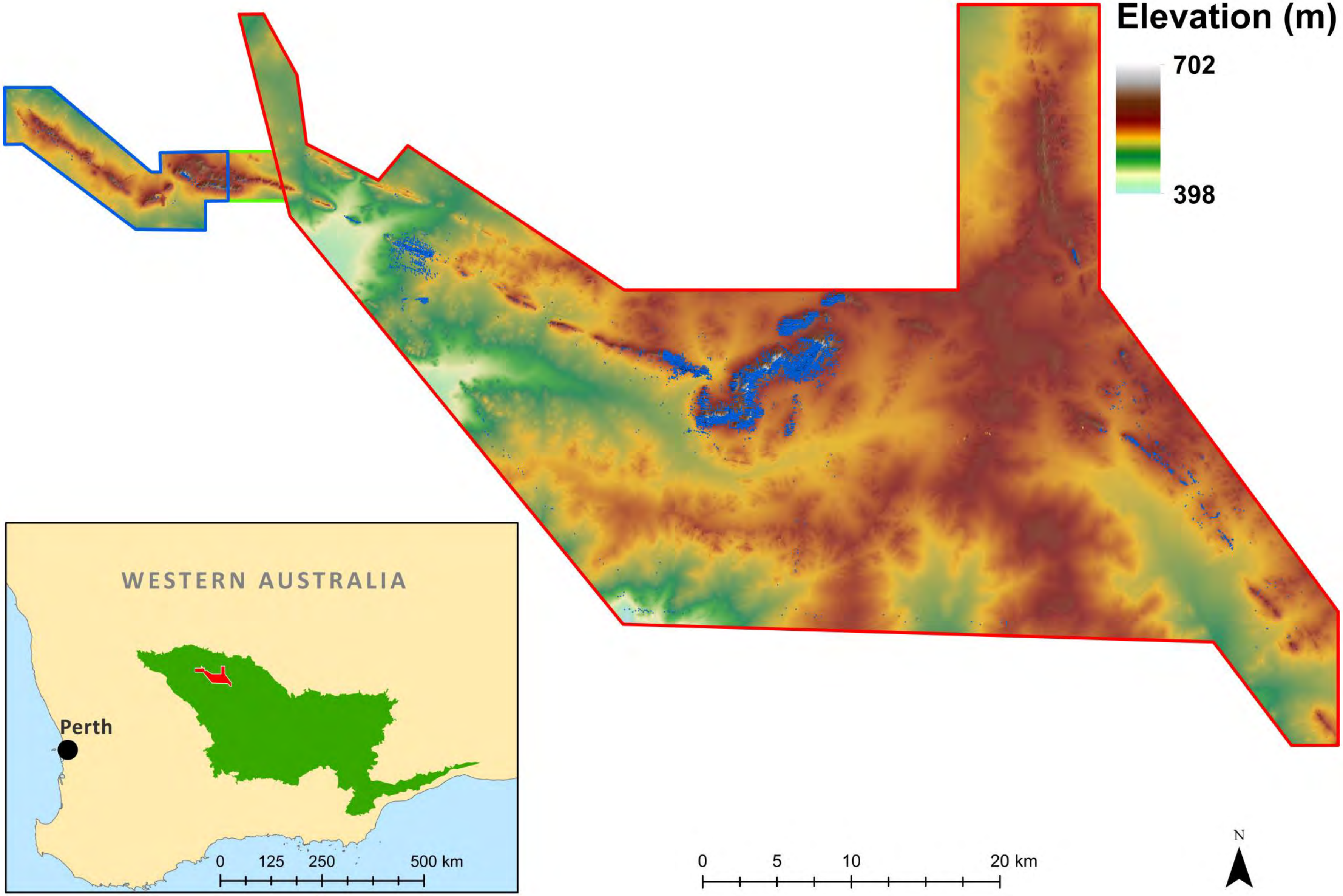

Figure S2. The study area comprises the Helena and Aurora Range banded ironstone formation (BIF) summits and surrounding BIFs and plains. Priority and threatened plant occurrences (n = 25,076) are shown as blue circles. Inset: the location of the study area in the Coolgardie biogeographic region in south-western Australia.

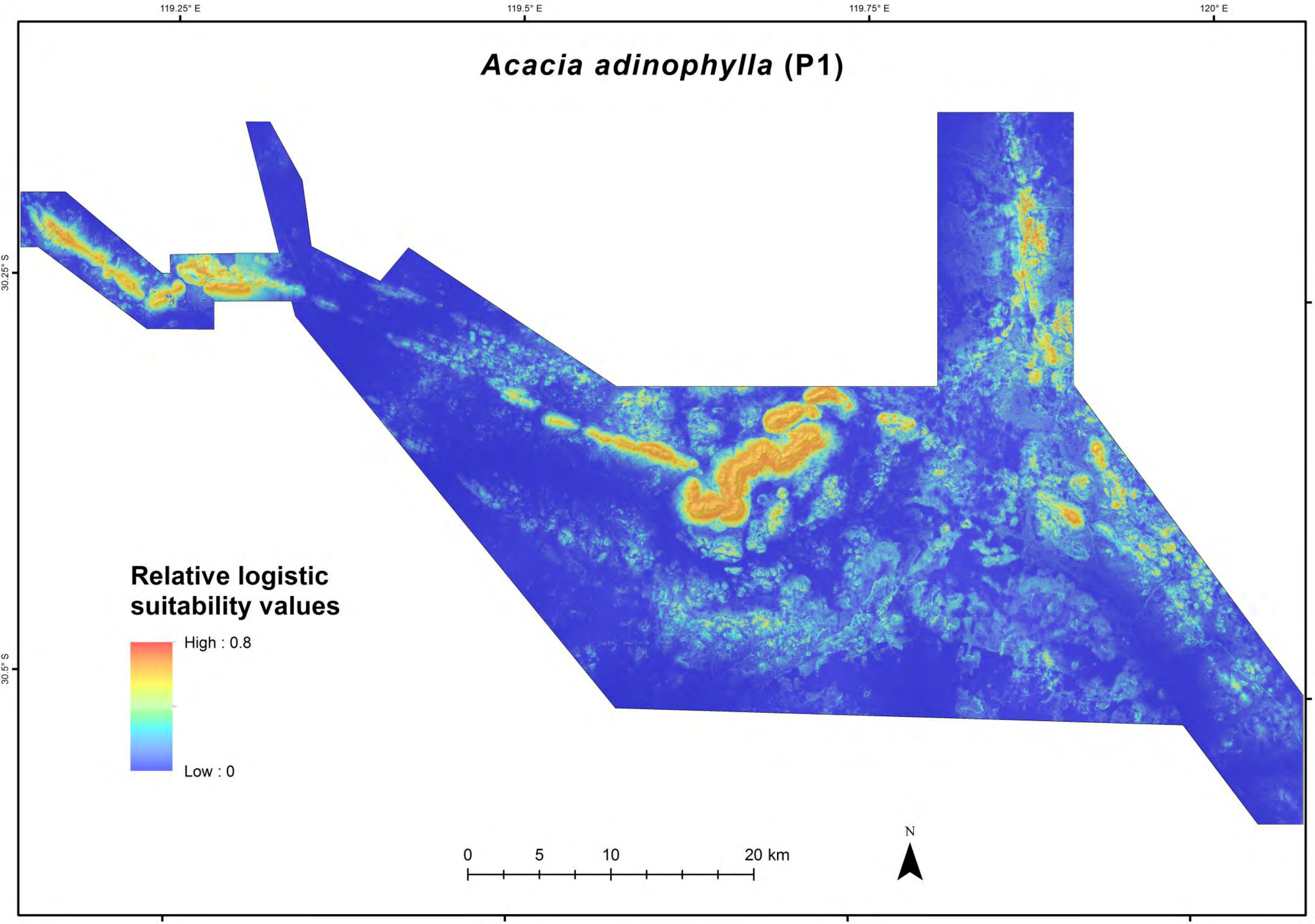

Figure S3. Predicted habitat suitability for *Acacia adinophylla* (default background sample selection).

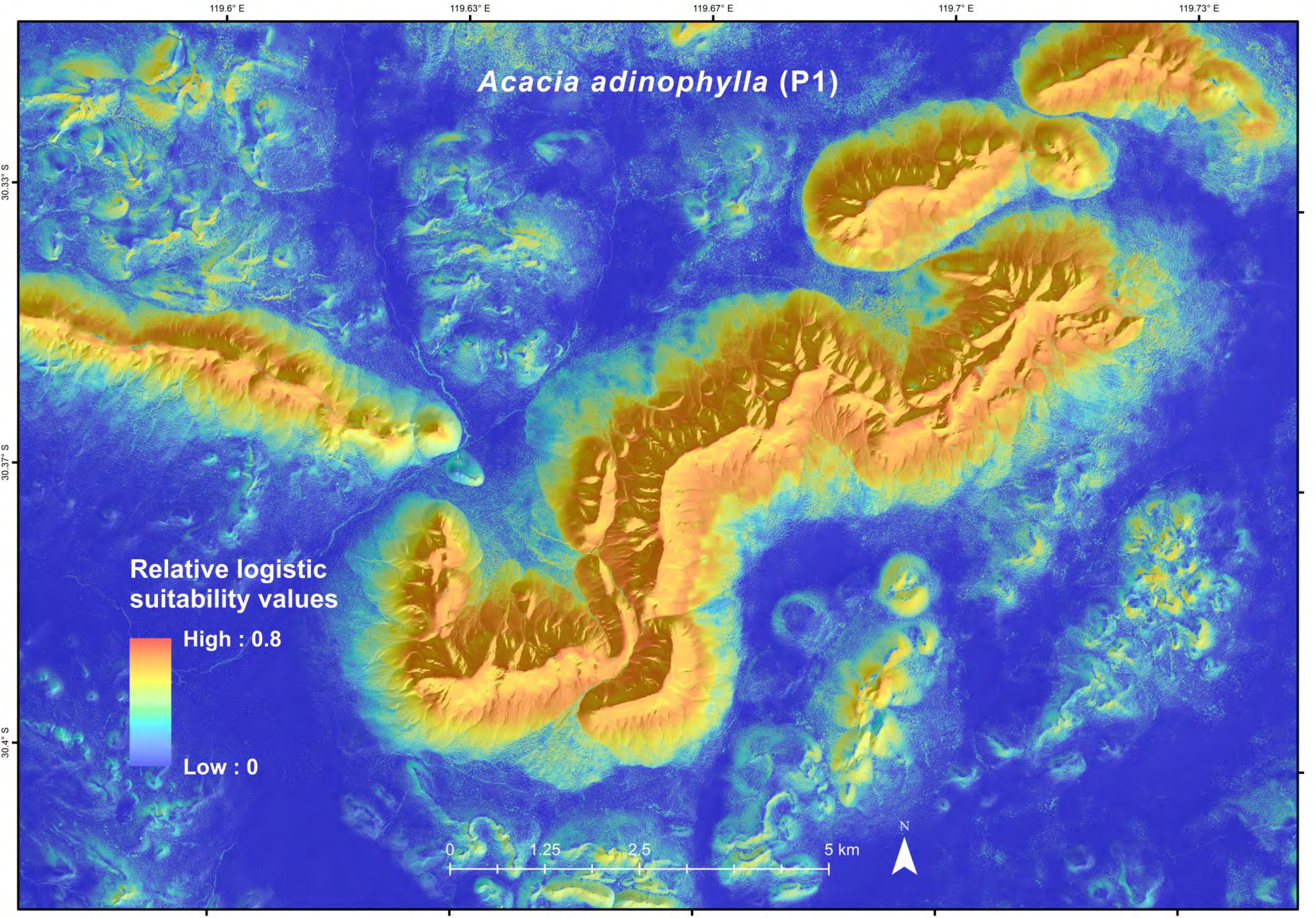

Figure S4. Predicted habitat suitability for *Acacia adinophylla* (default background sample selection).

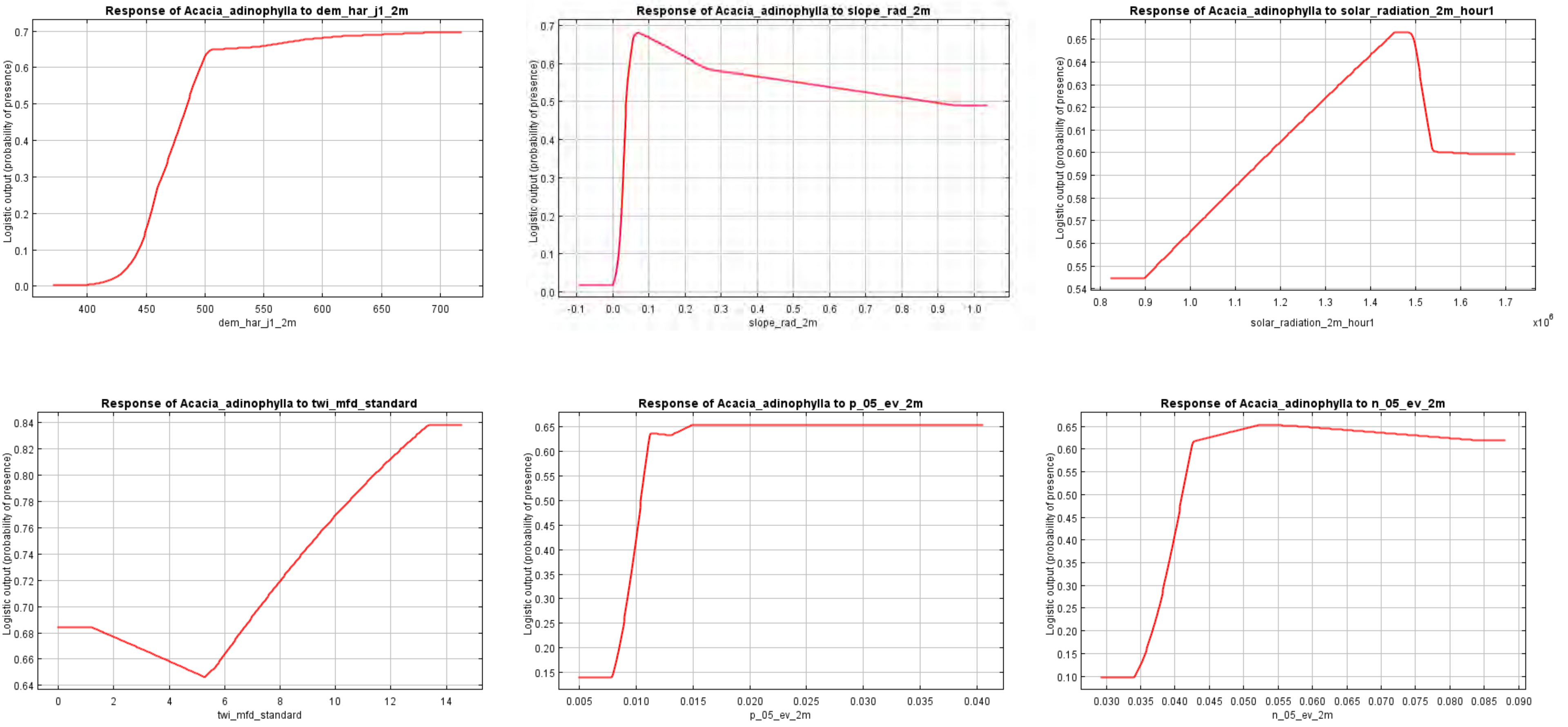

Figure S5. Partial dependence plots showing how the marginal response of *A. adinophylla* changes as each predictor is varied whilst the values of the remaining variables are fixed at their average sample values.

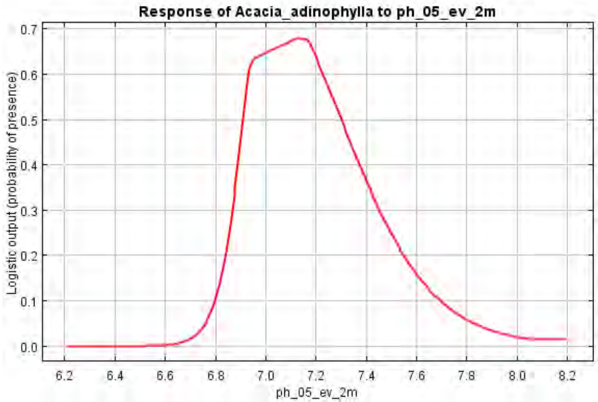

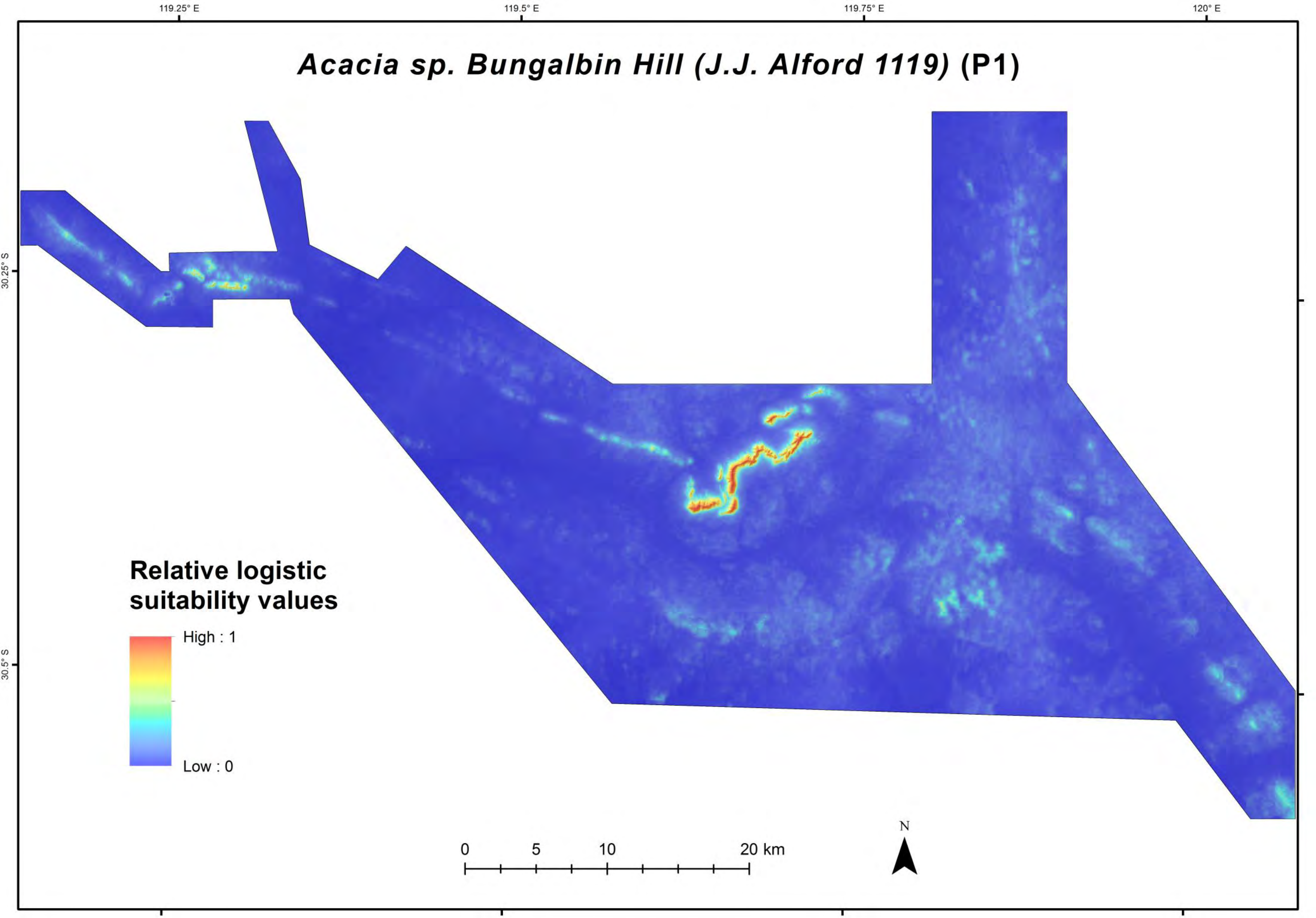

Figure S6. Predicted habitat suitability for *Acacia sp. Bungalbin Hill* for each 2 × 2 m grid cell (default background sample selection)

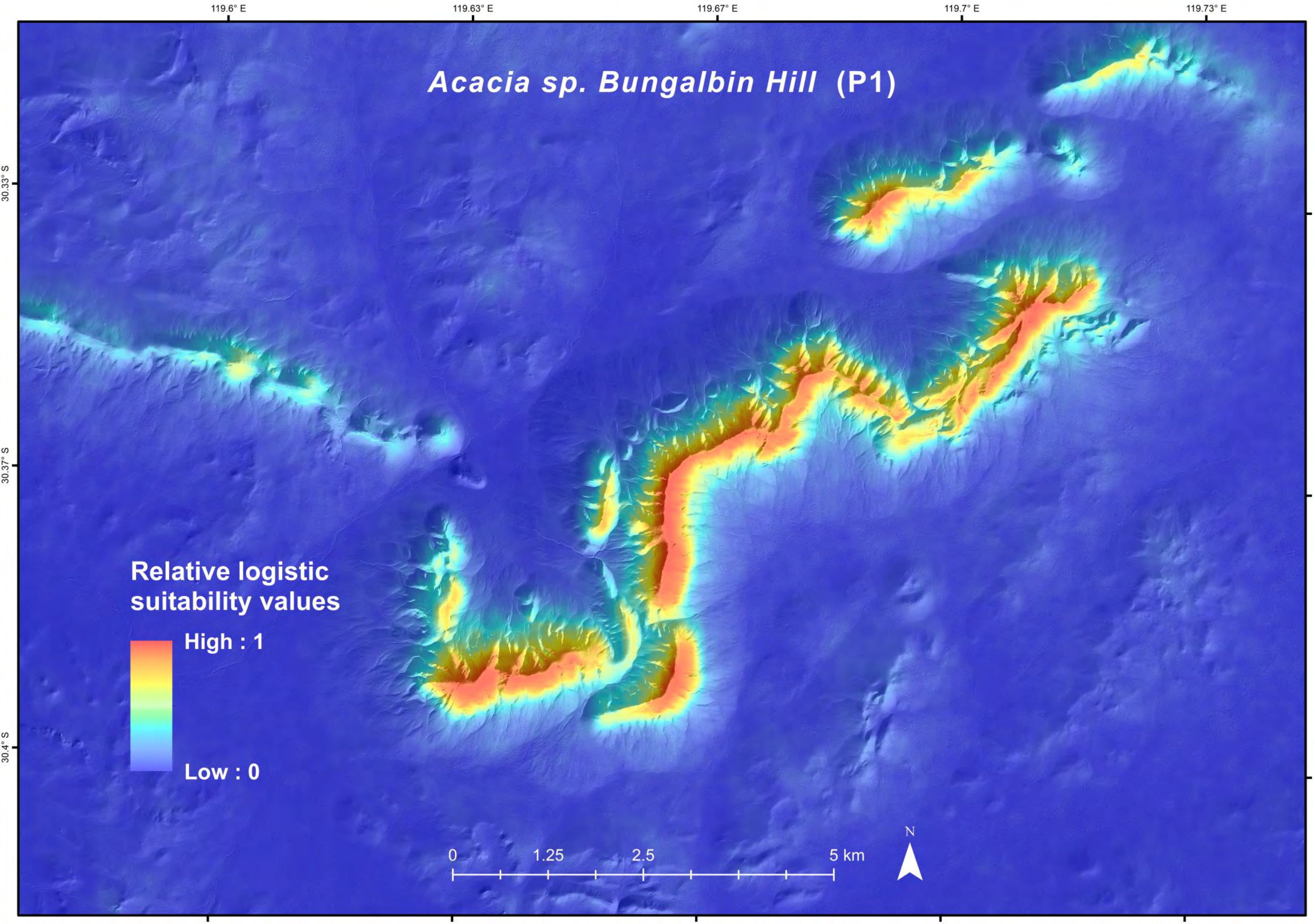

Figure S7. Predicted habitat suitability for *Acacia sp. Bungalbin Hill* for each 2 × 2 m grid cell (default background sample selection)

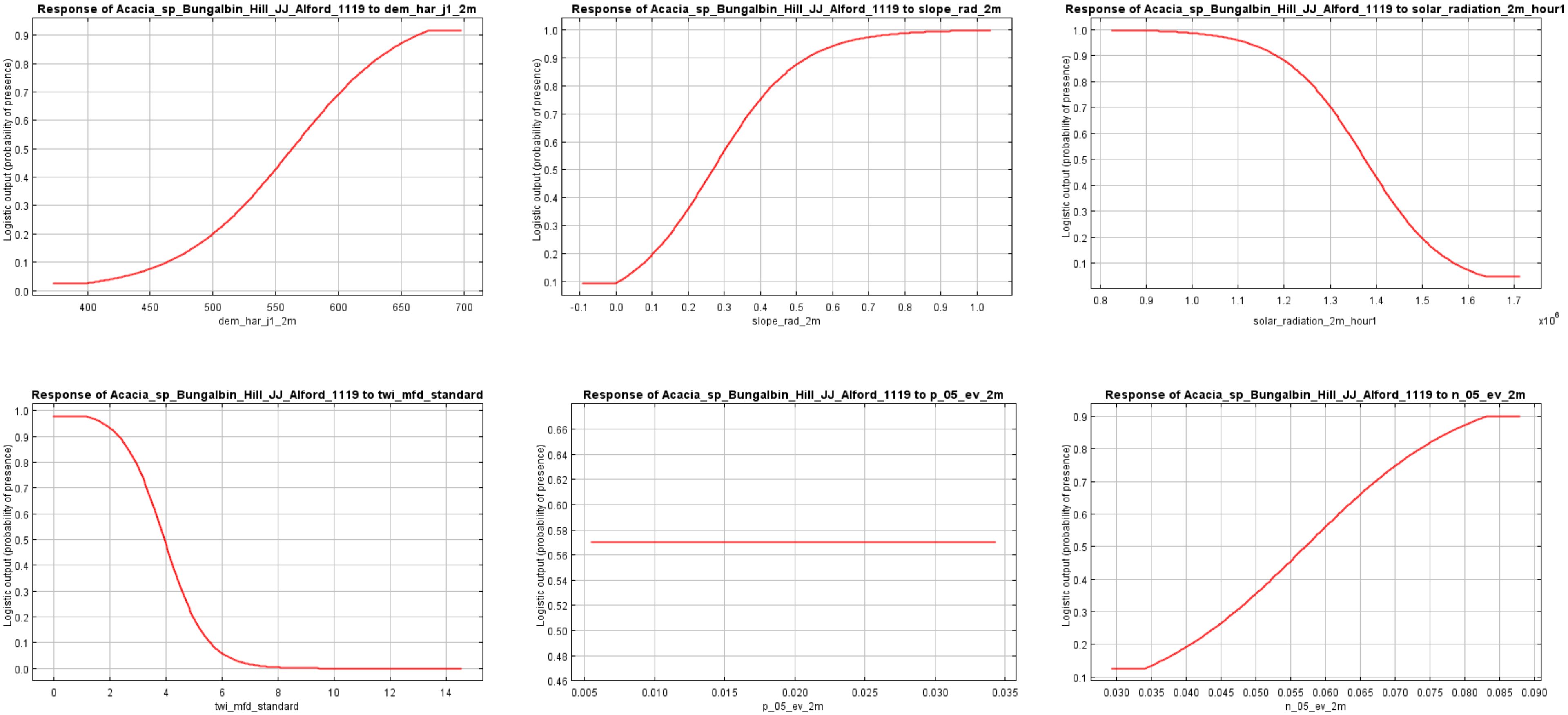

Figure S8. Partial dependence plots showing how the marginal response of *Acacia sp. Bungalbin Hill* changes as each predictor is varied whilst the values of the remaining variables are fixed at their average sample values.

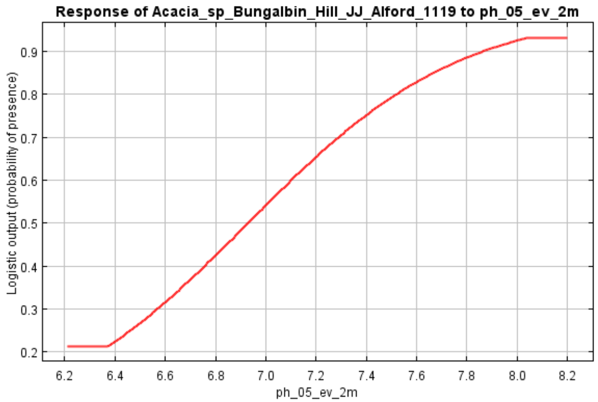

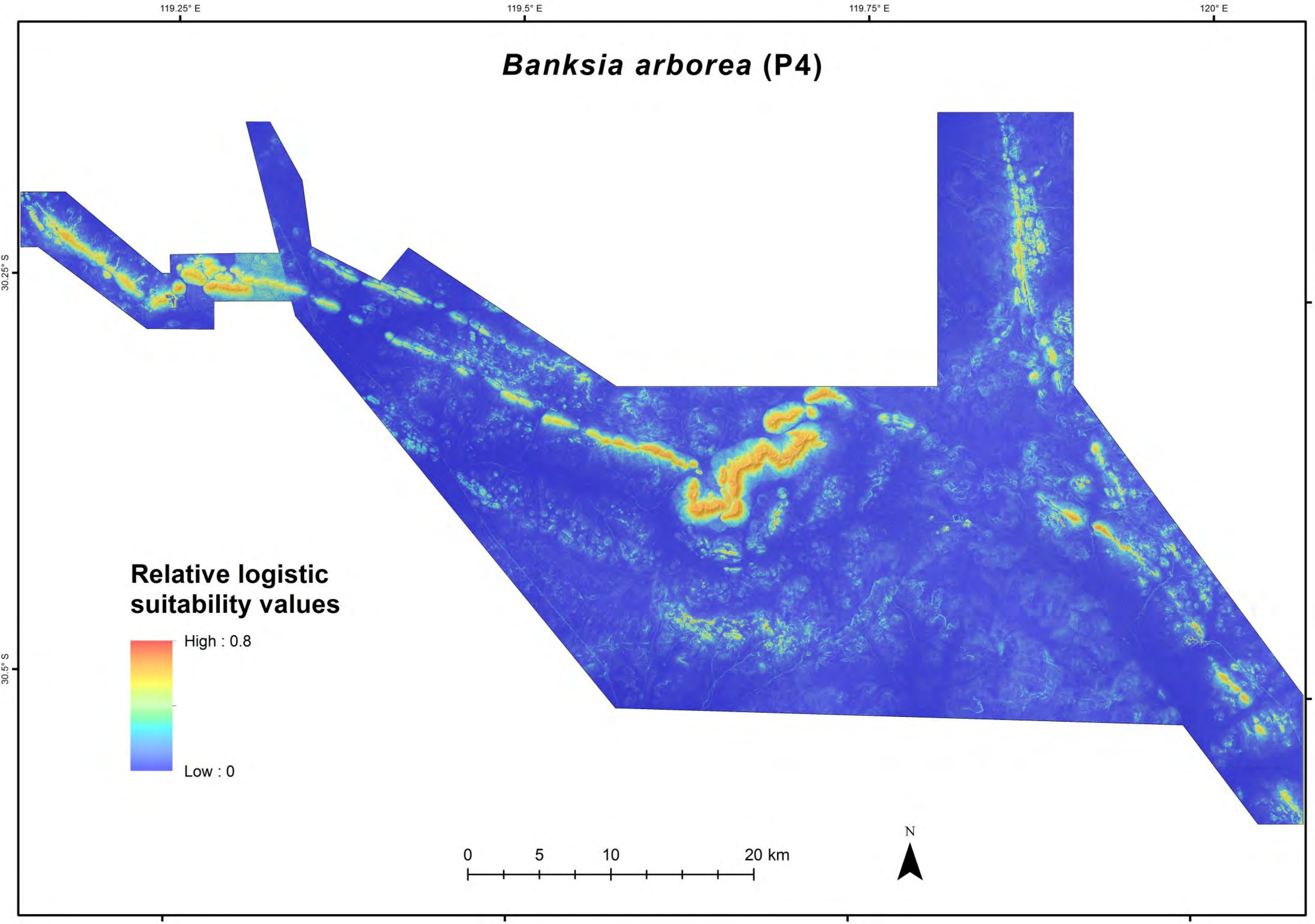

Figure S9. Predicted habitat suitability for *Banksia arborea* for each 2 × 2 m grid cell (default background sample selection).

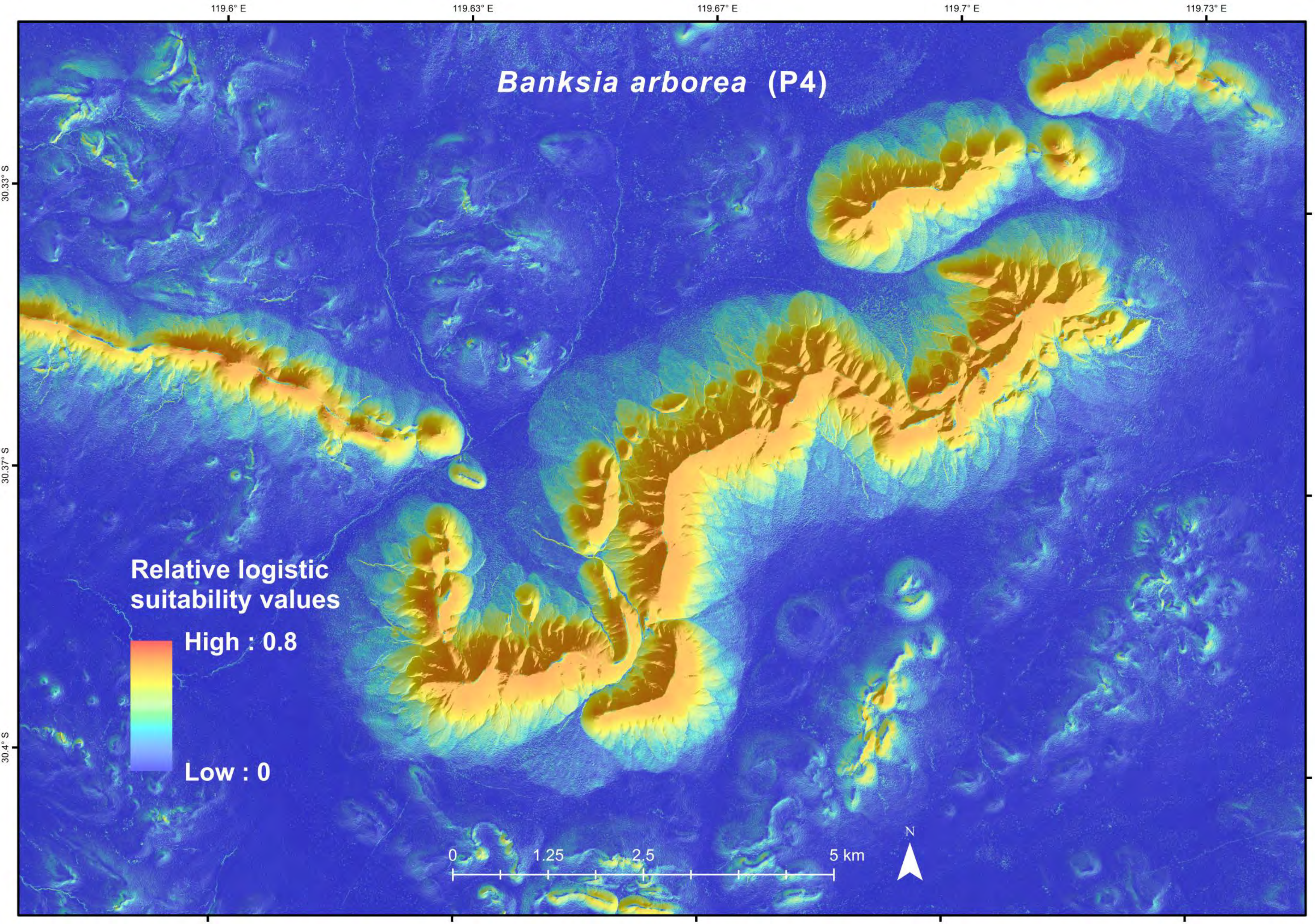

Figure S10. Predicted habitat suitability for *Banksia arborea* for each 2 × 2 m grid cell (default background sample selection).

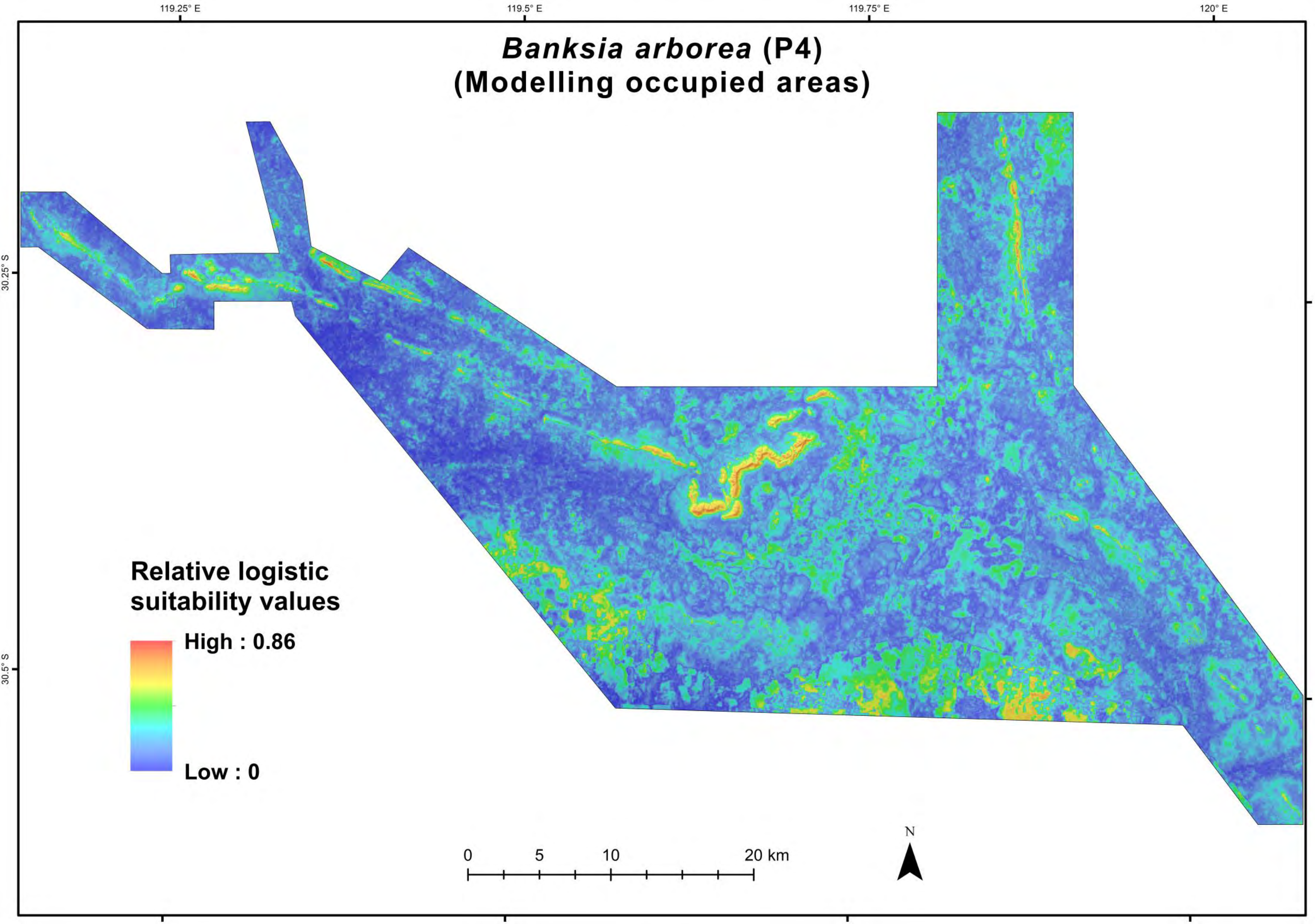

Figure S11. Predicted habitat suitability for *Banksia arborea* for each 2 × 2 m grid cell (restricted background sample selection).

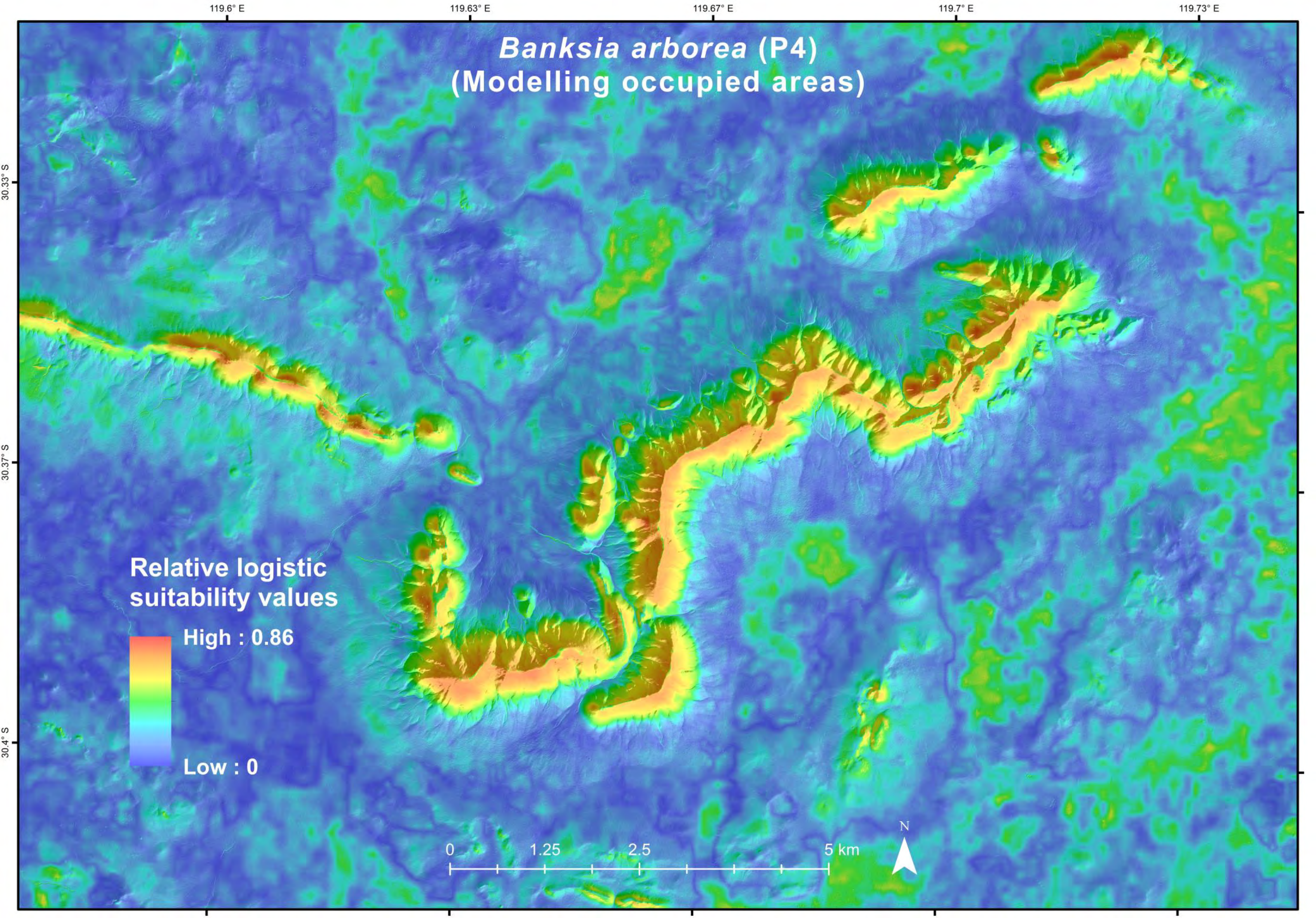

Figure S12. Predicted habitat suitability for *Banksia arborea* for each 2 × 2 m grid cell (restricted background sample selection).

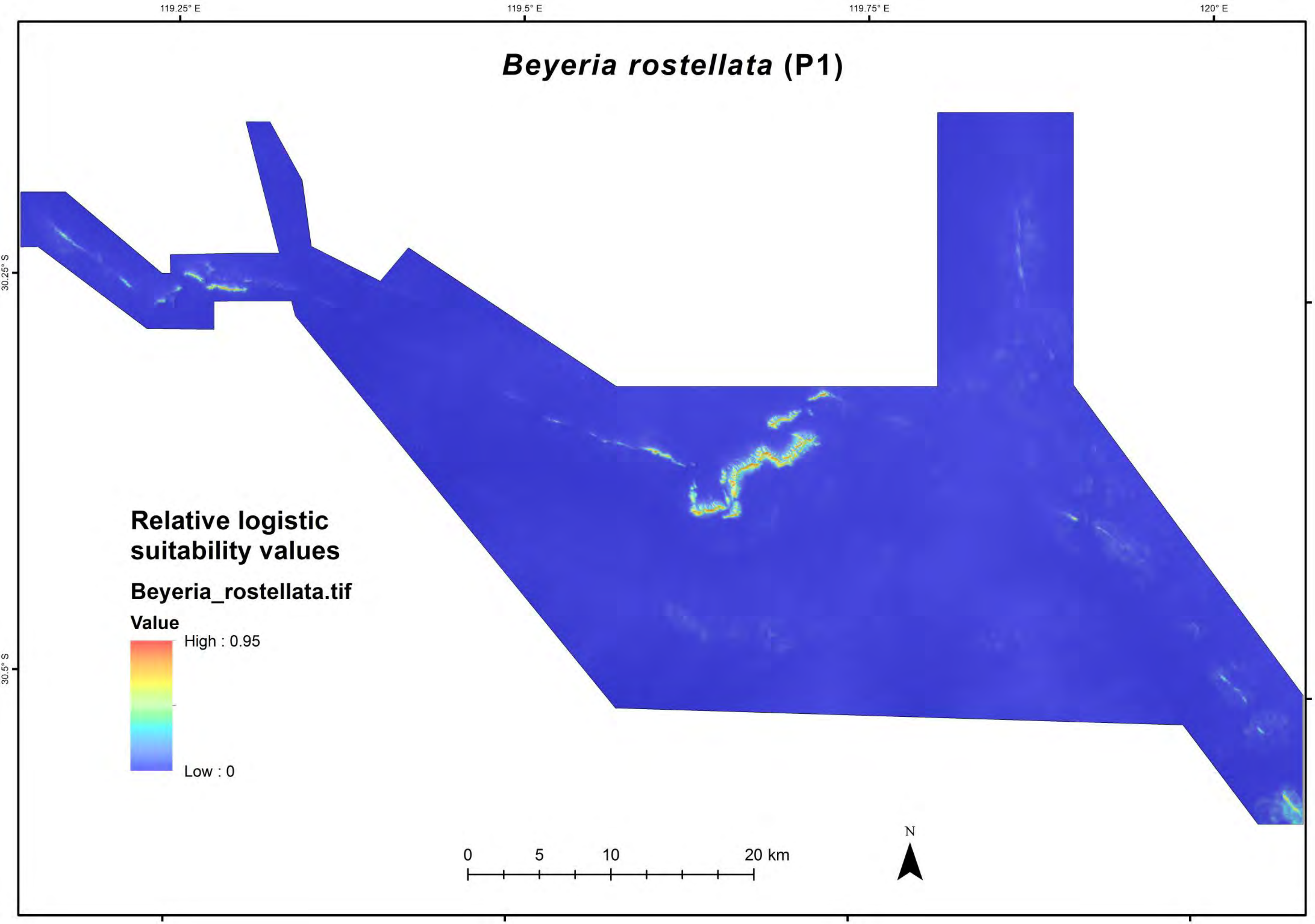

Figure S13. Predicted habitat suitability for *Beyeria rostellata* for each 2 × 2 m grid cell (default background sample selection).

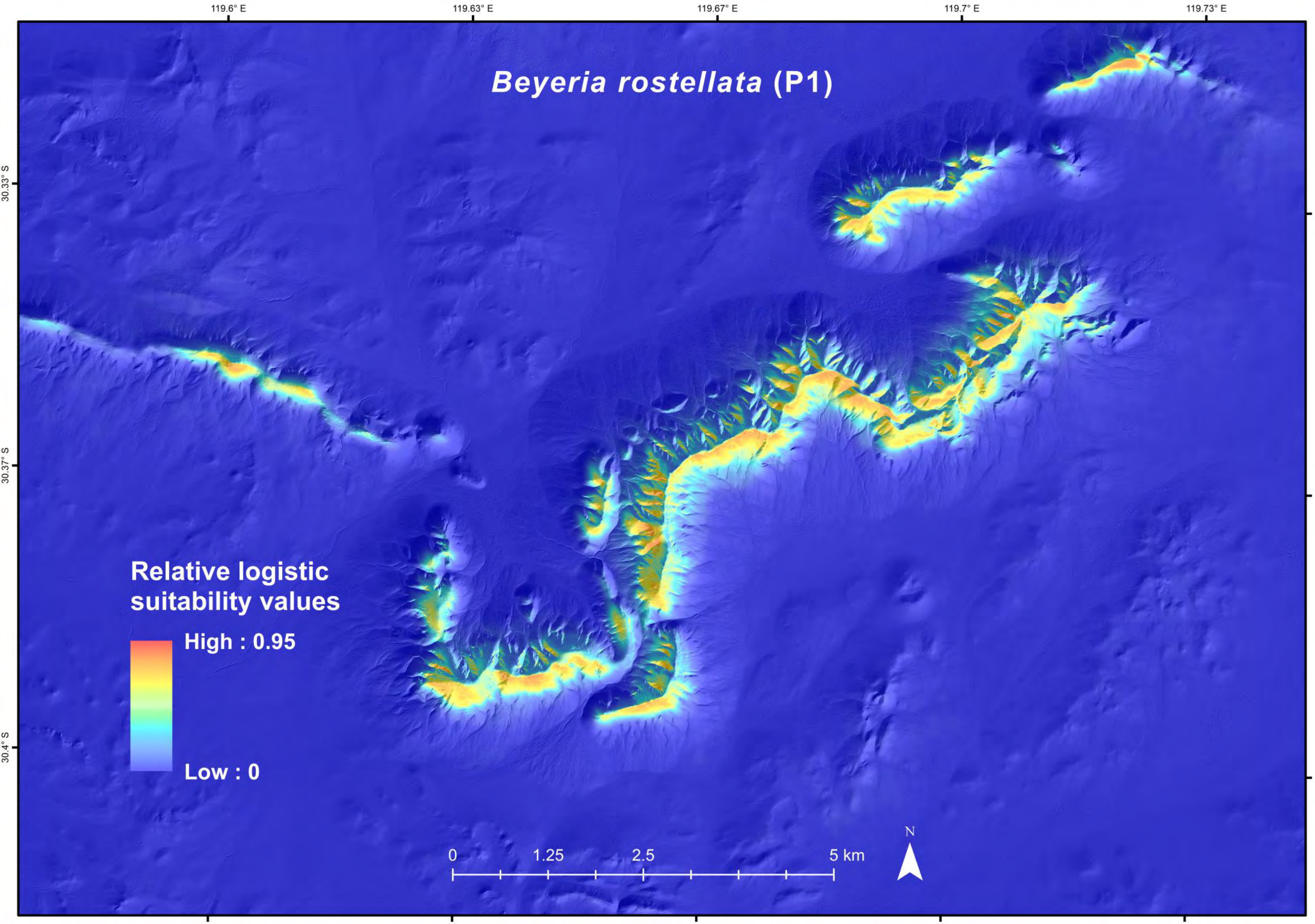

Figure S14. Predicted habitat suitability for *Beyeria rostellata* for each 2 × 2 m grid cell (default background sample selection).

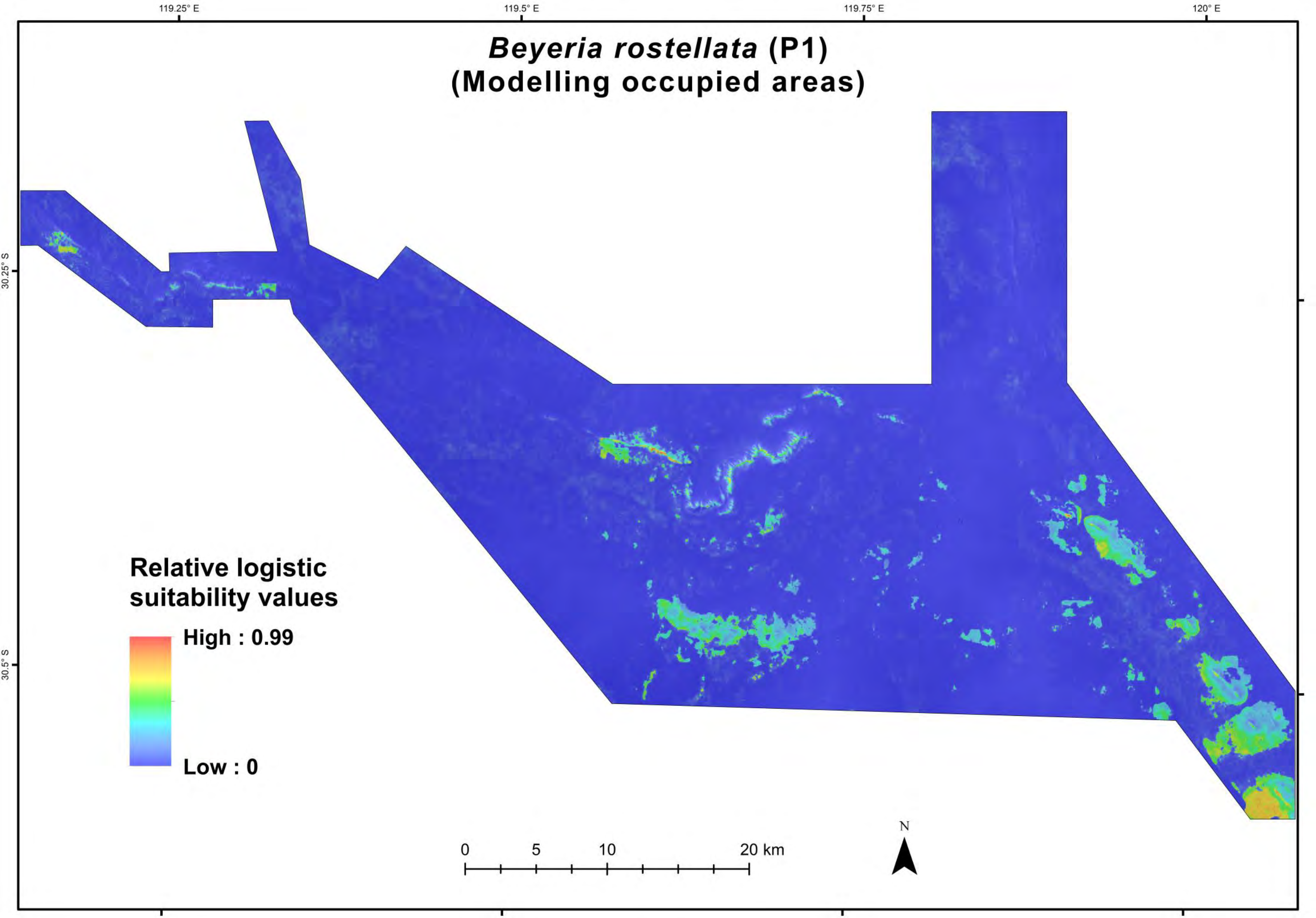

Figure S15. Predicted habitat suitability for *Beyeria rostellata* for each 2 × 2 m grid cell (restricted background sample selection).

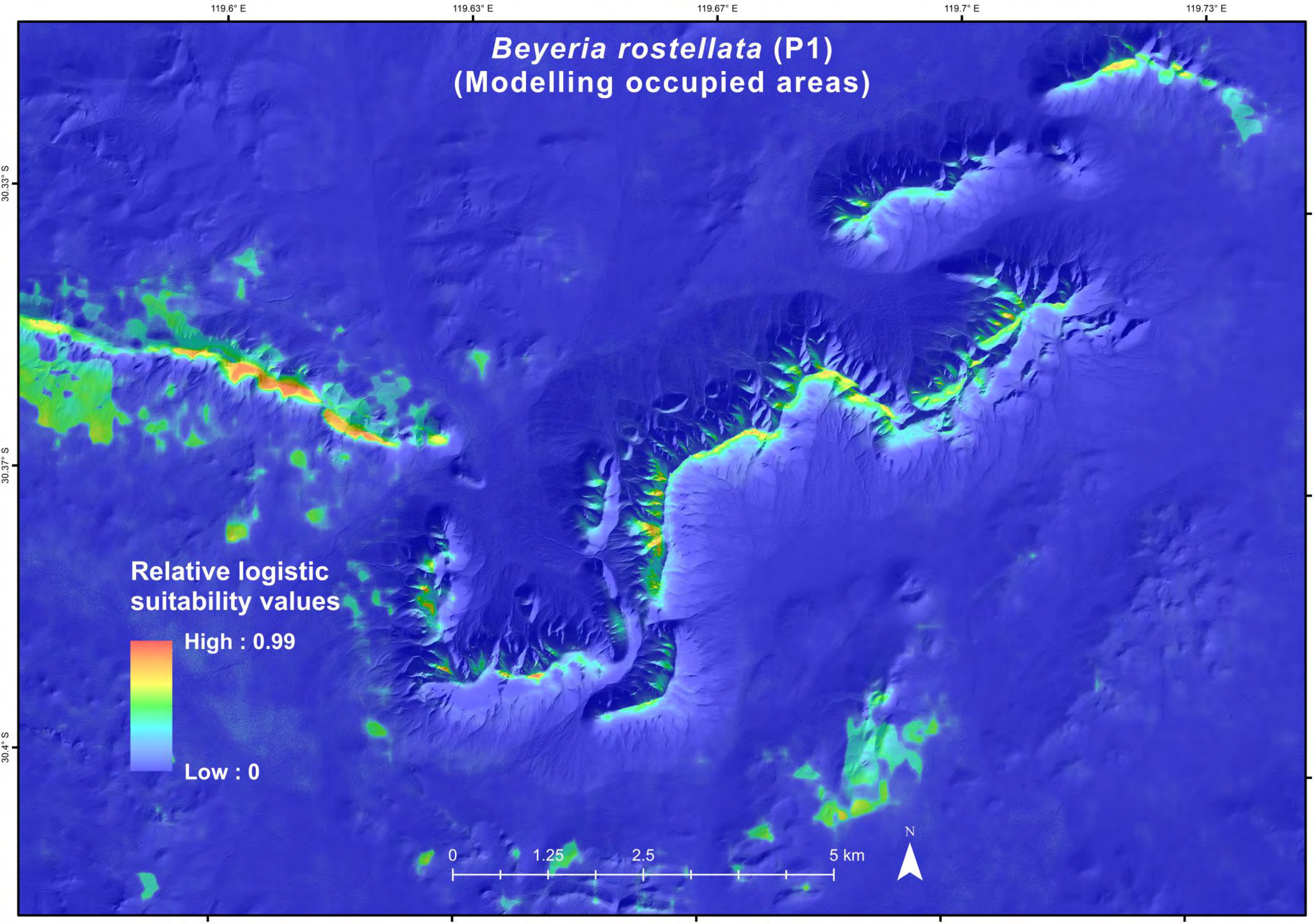

Figure S16. Predicted habitat suitability for *Beyeria rostellata* for each 2 × 2 m grid cell (restricted background sample selection).

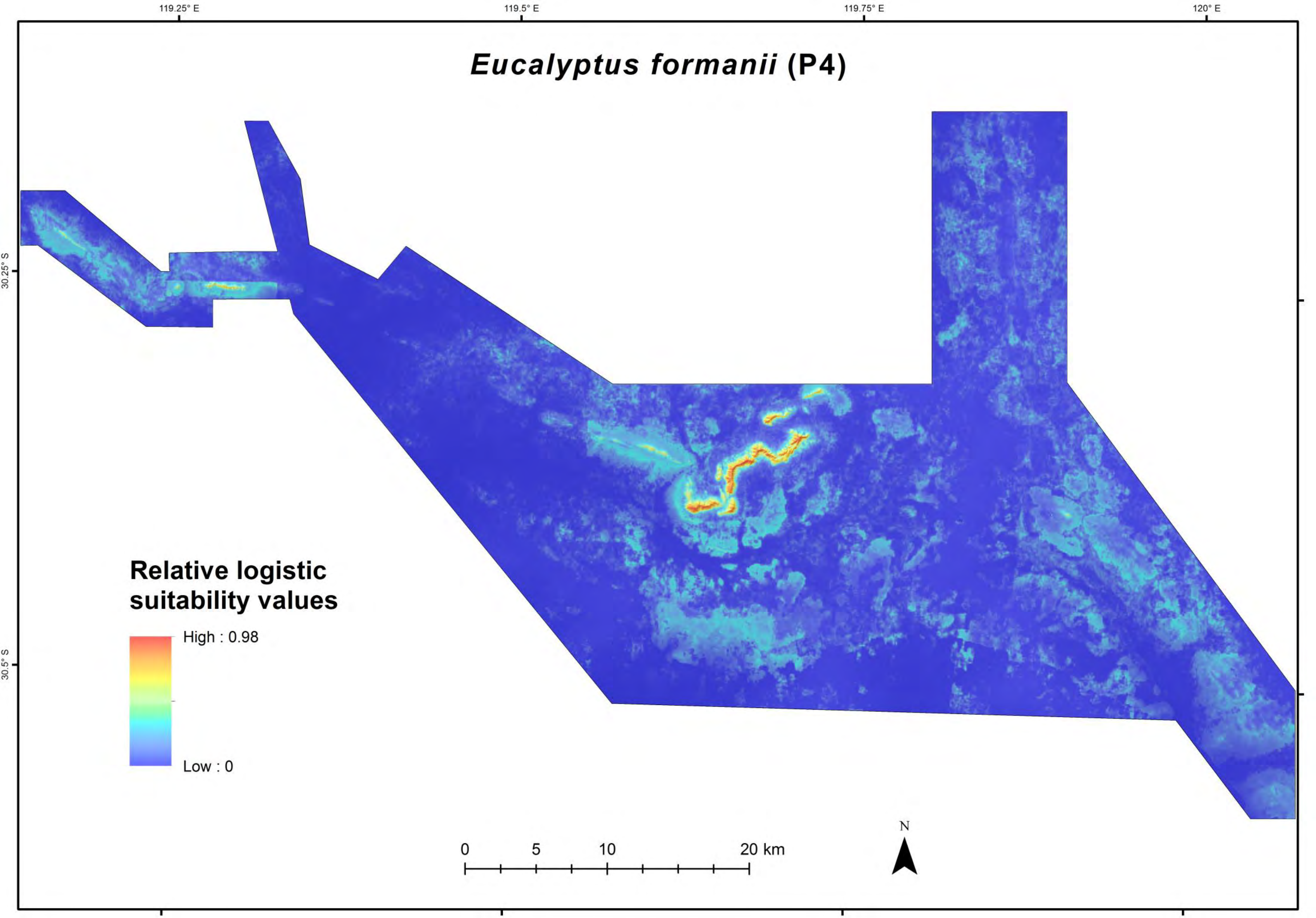

Figure S17. Predicted habitat suitability for *Eucalyptus formanii* for each 2 × 2 m grid cell

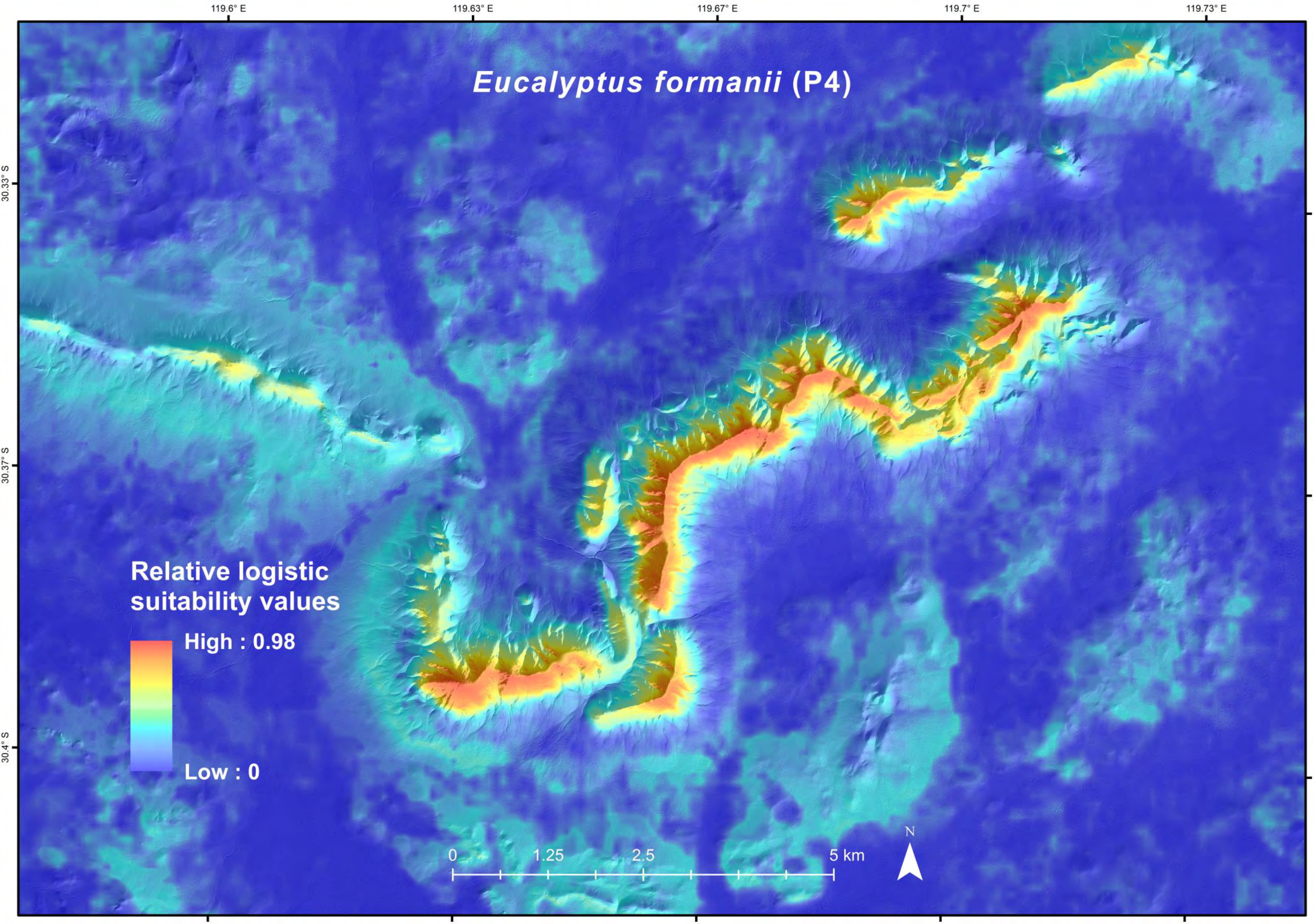

Figure S18. Predicted habitat suitability for *Eucalyptus formanii* for each 2 × 2 m grid cell

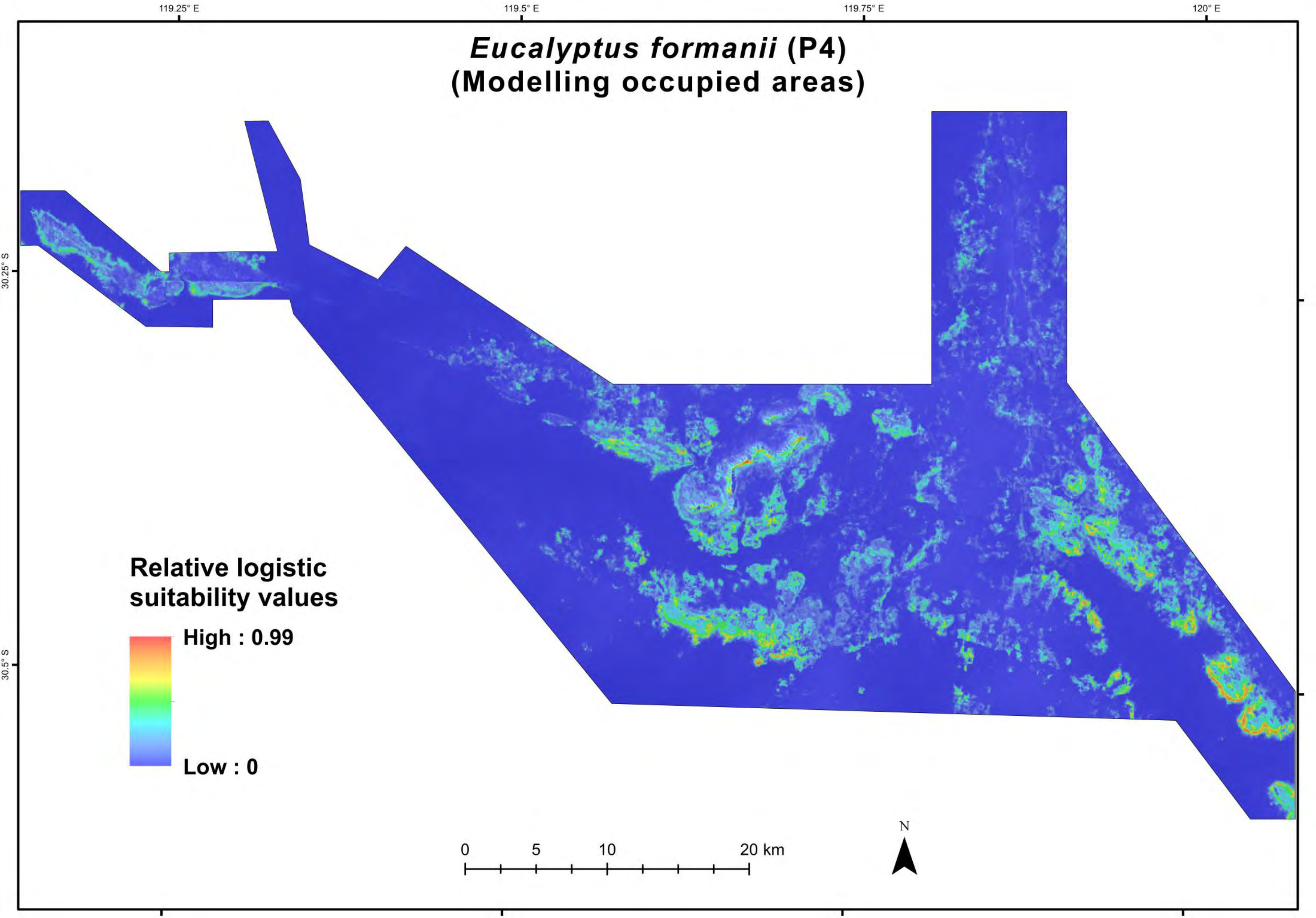

Figure S19. Predicted habitat suitability for *Eucalyptus formanii* for each 2 × 2 m grid cell (restricted background sample selection).

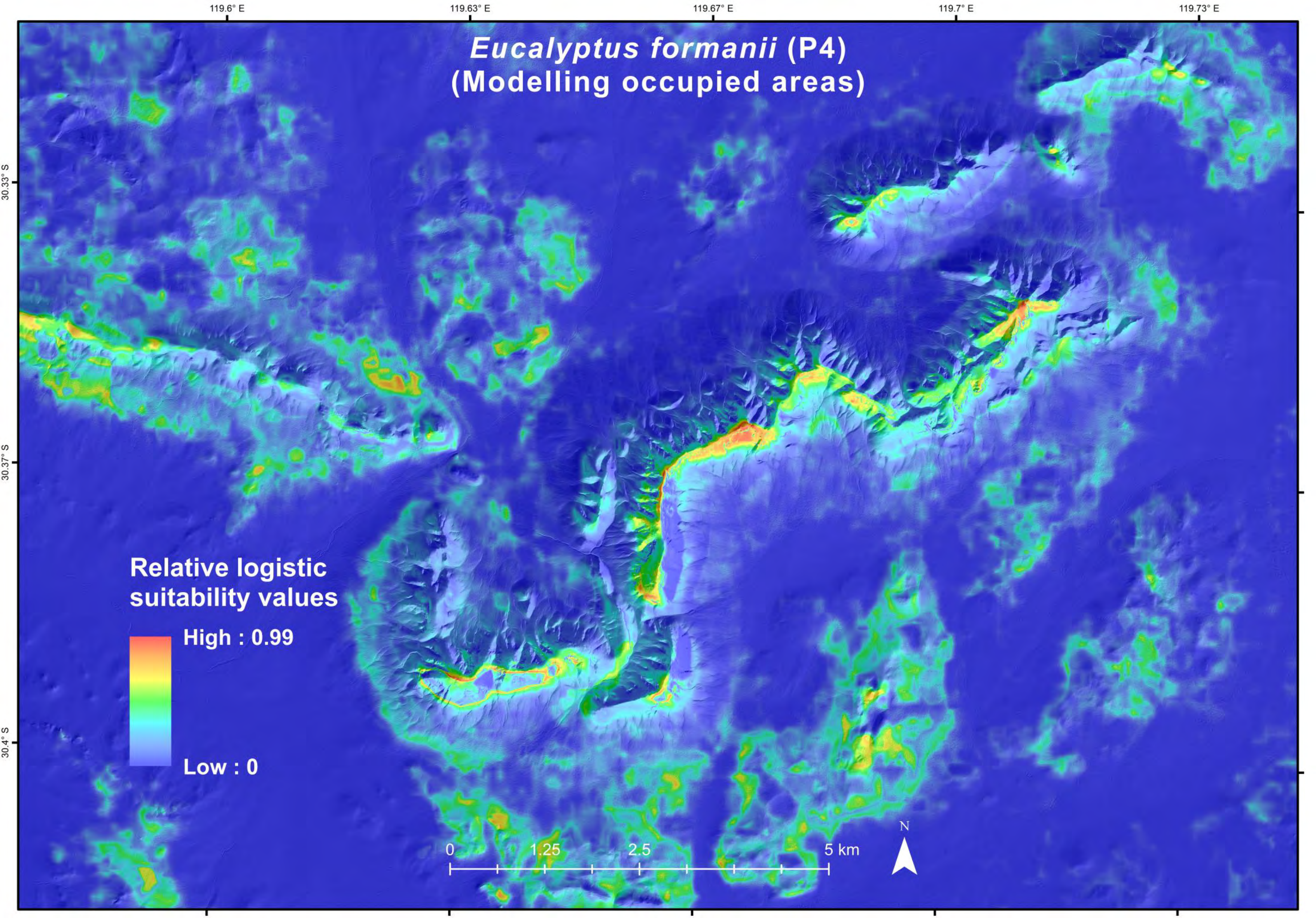

Figure S20. Predicted habitat suitability for *Eucalyptus formanii* for each 2 × 2 m grid cell (restricted background sample selection).

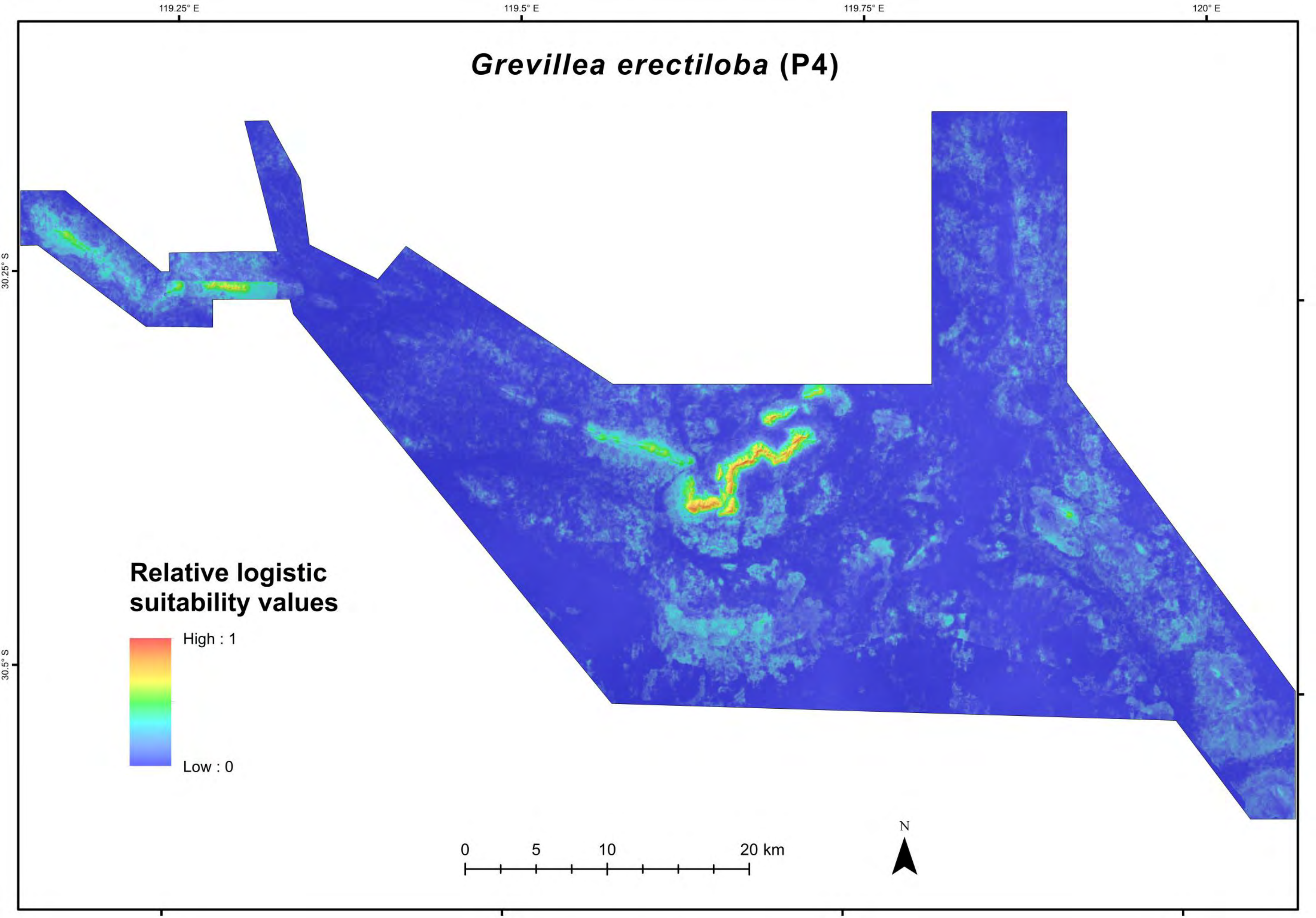

Figure S21. Predicted habitat suitability for *Grevillea erectiloba.*

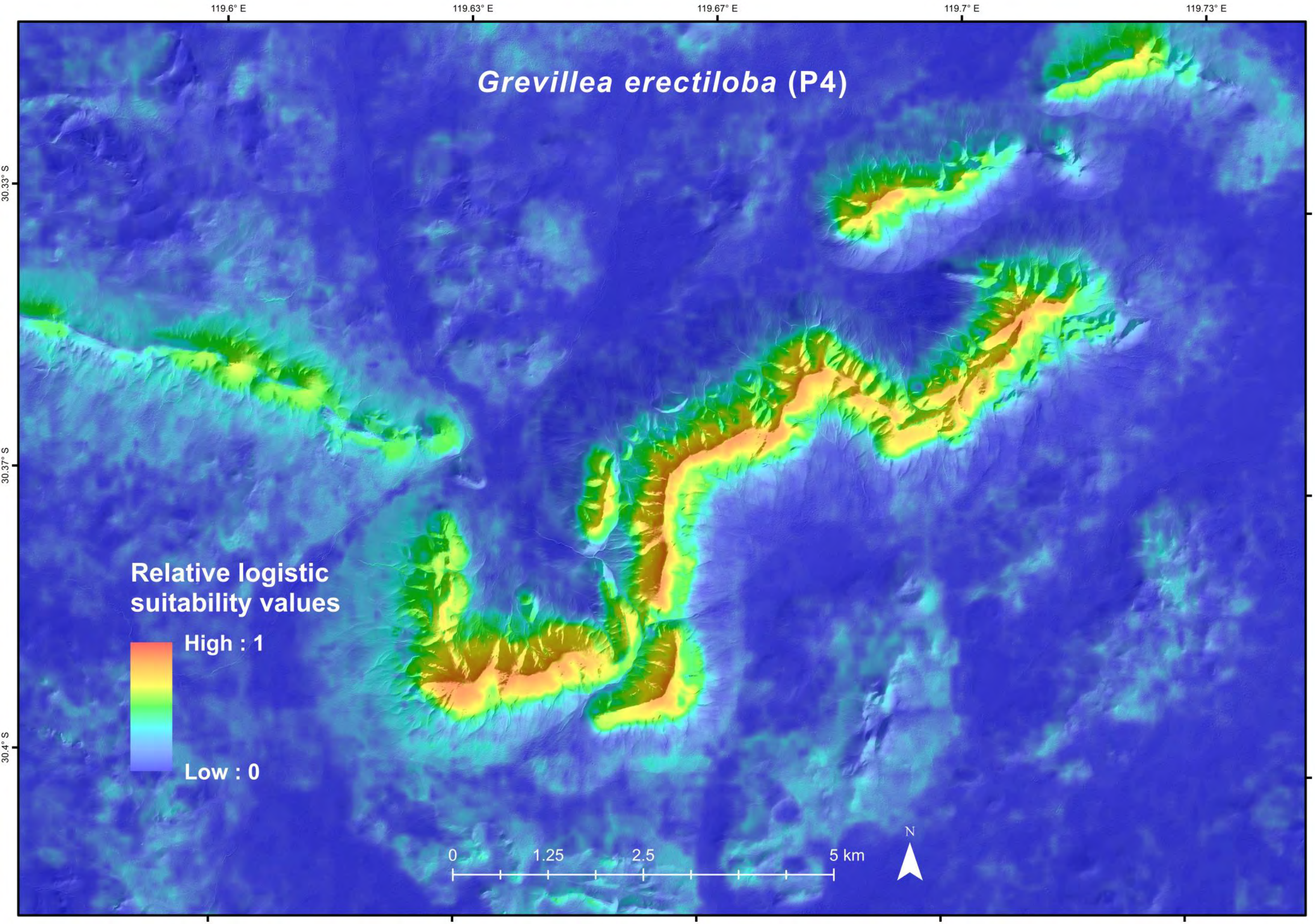

Figure S22. Predicted habitat suitability for *Grevillea erectiloba.*

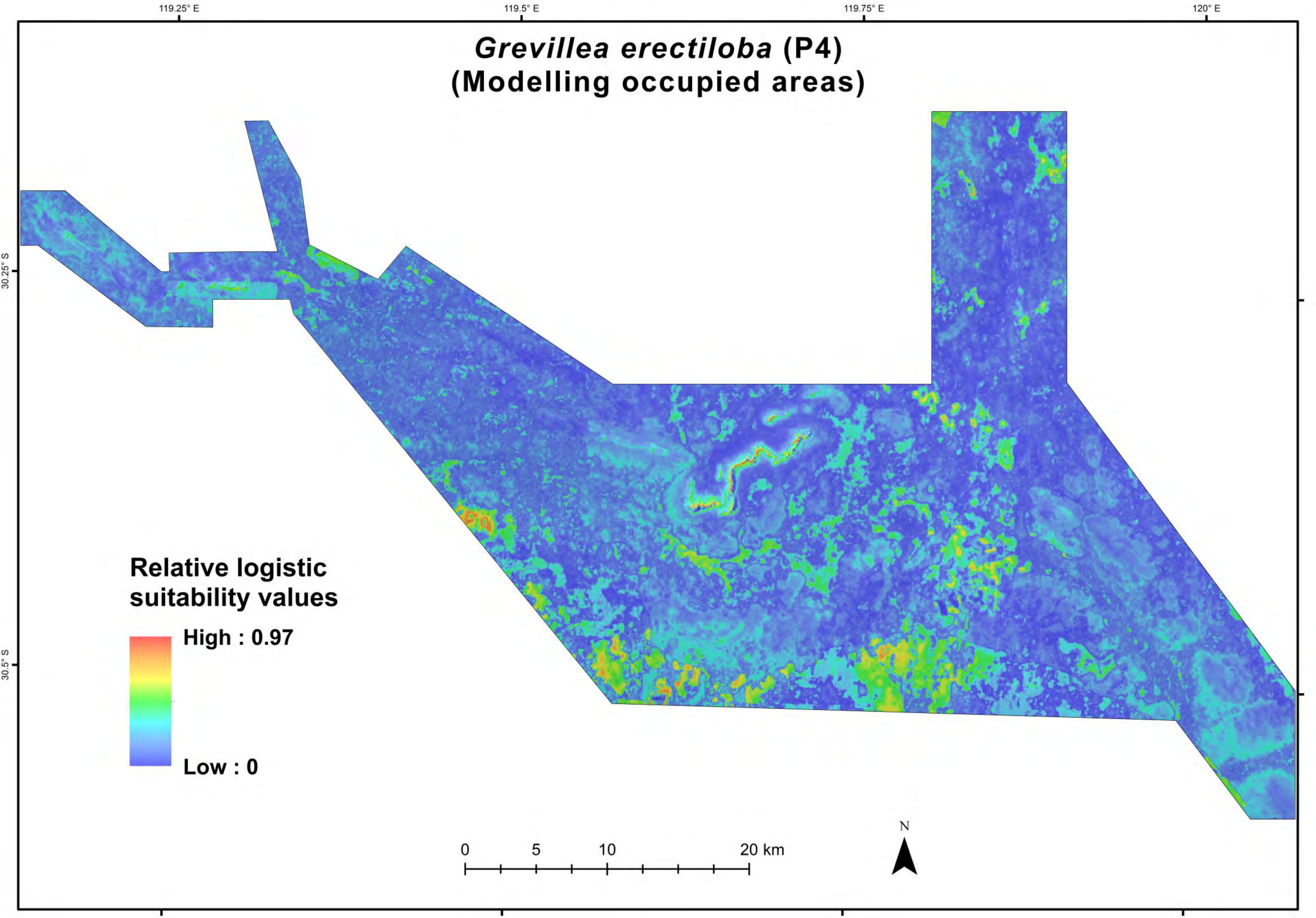

Figure S23. Predicted habitat suitability for *Grevillea erectiloba* (restricted background sample selection).

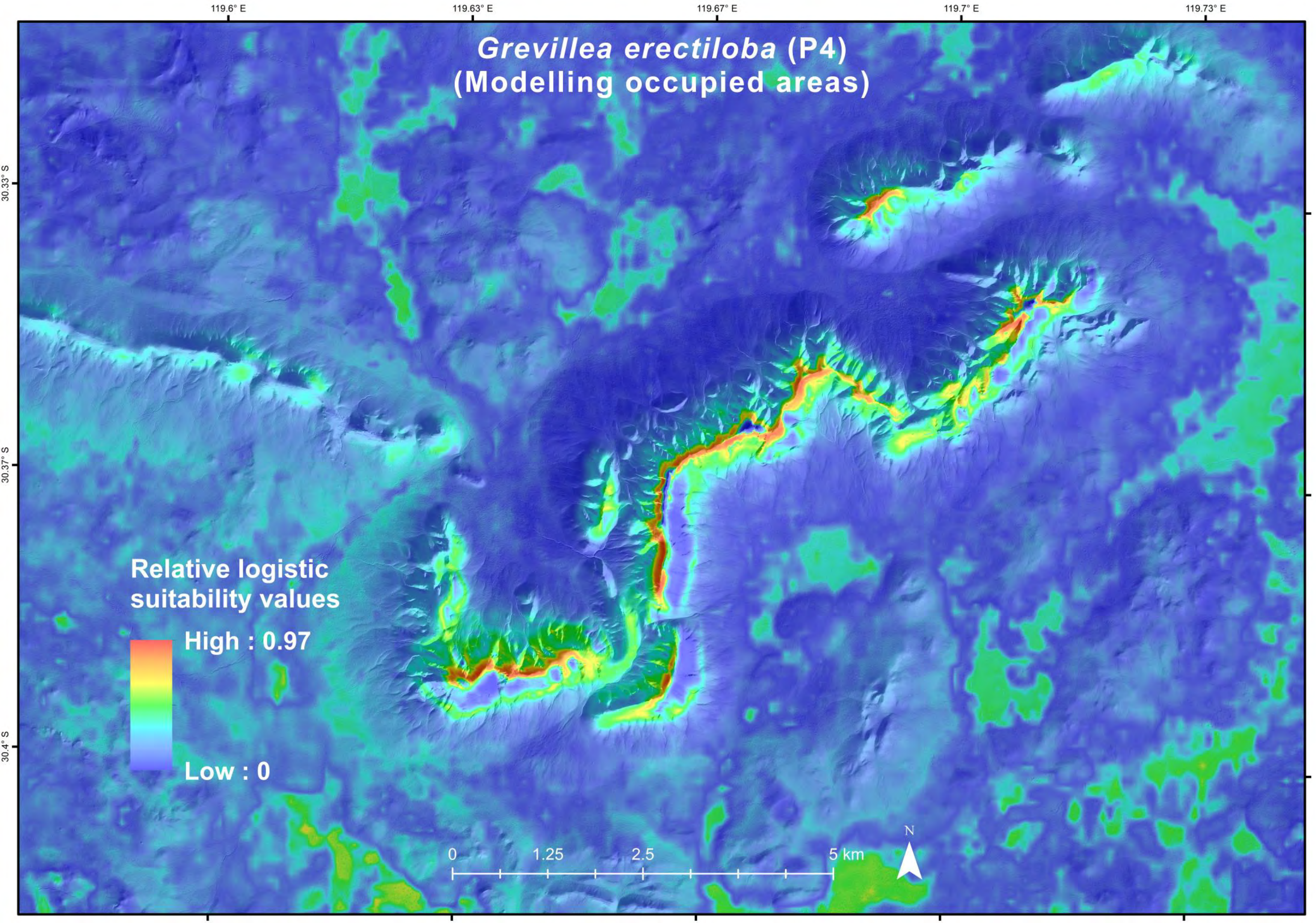

Figure S24. Predicted habitat suitability for *Grevillea erectiloba* (restricted background sample selection).

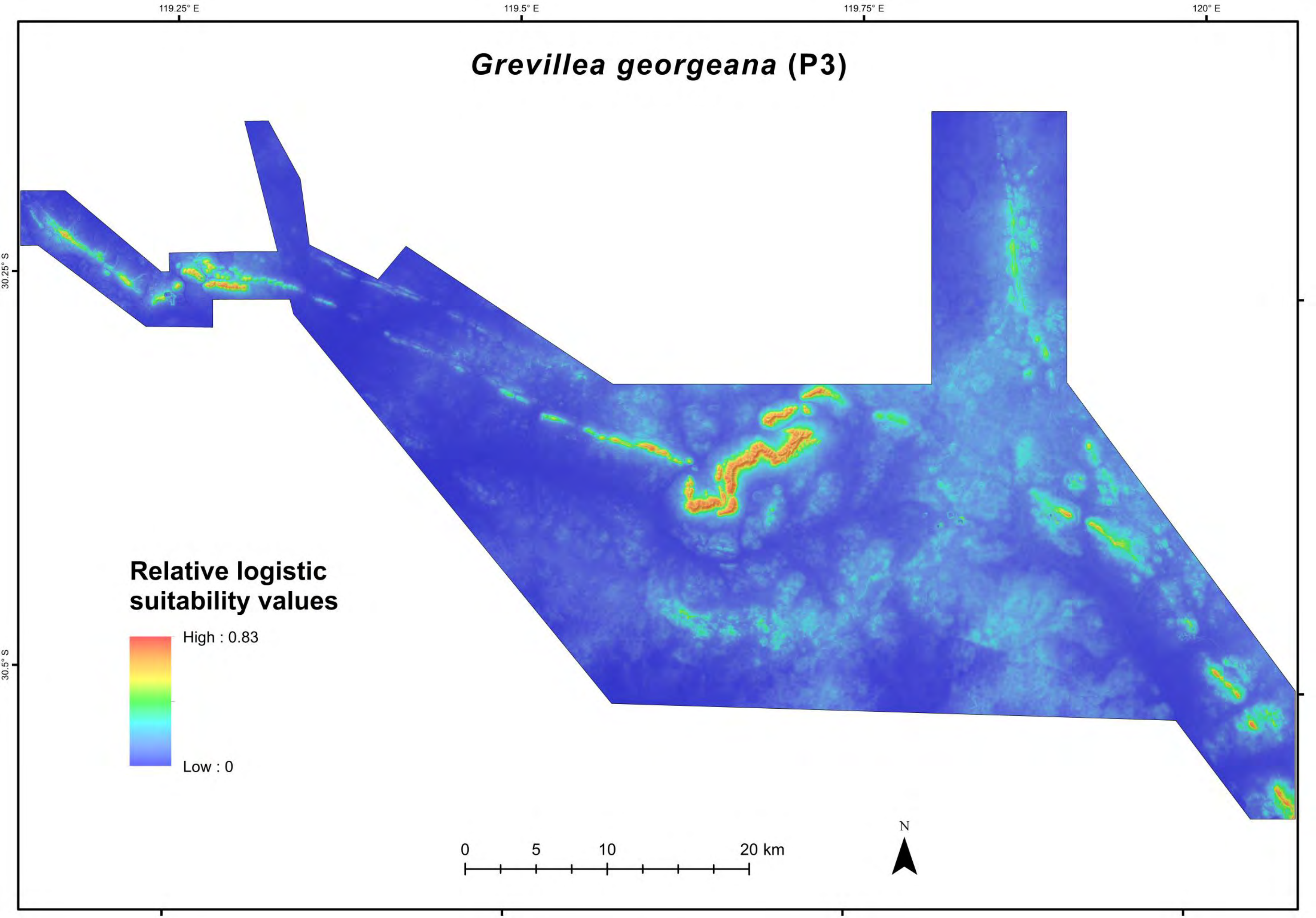

Figure S25. Predicted habitat suitability for *Grevillea georgeana.*

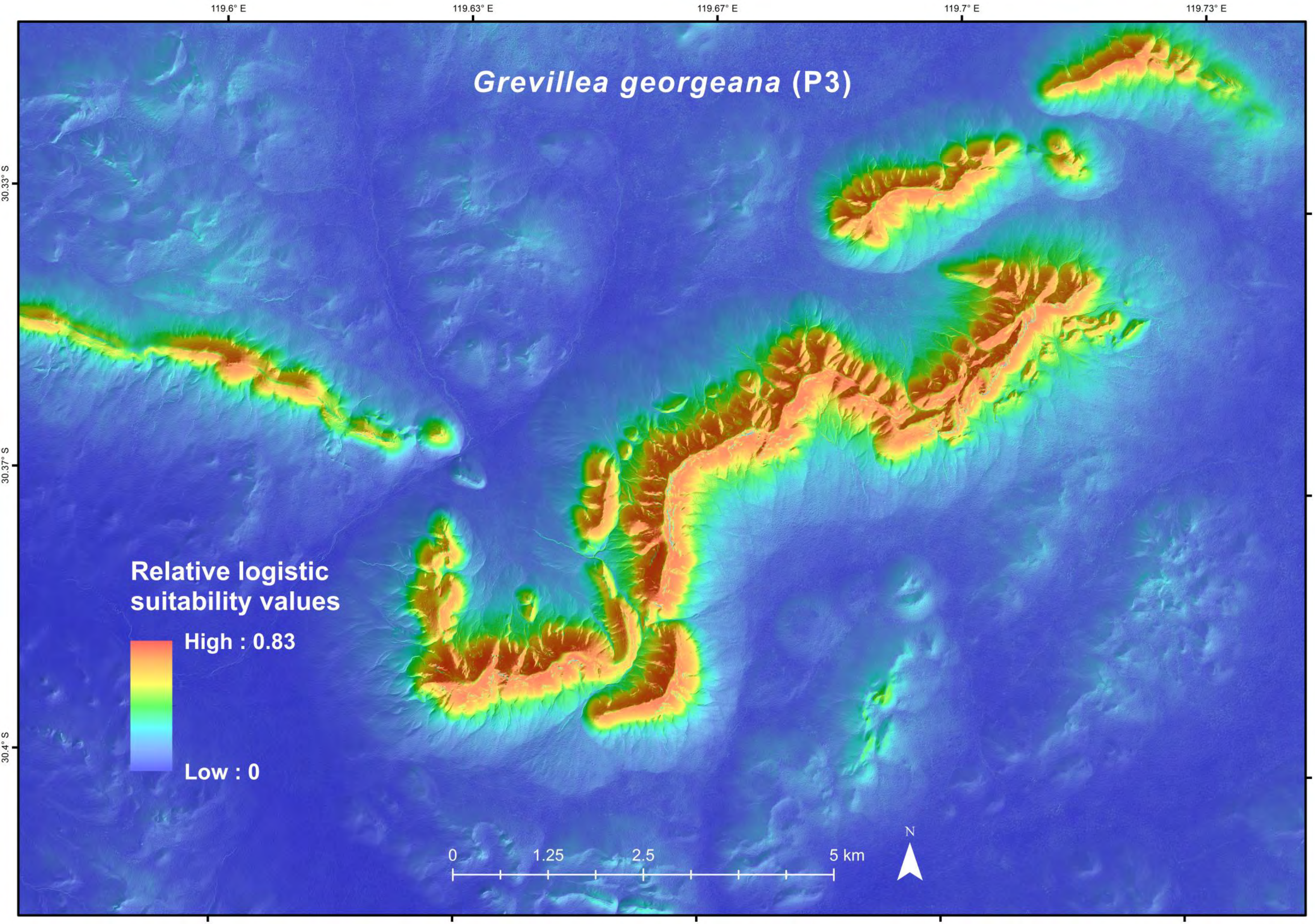

Figure S26. Predicted habitat suitability for *Grevillea georgeana.*

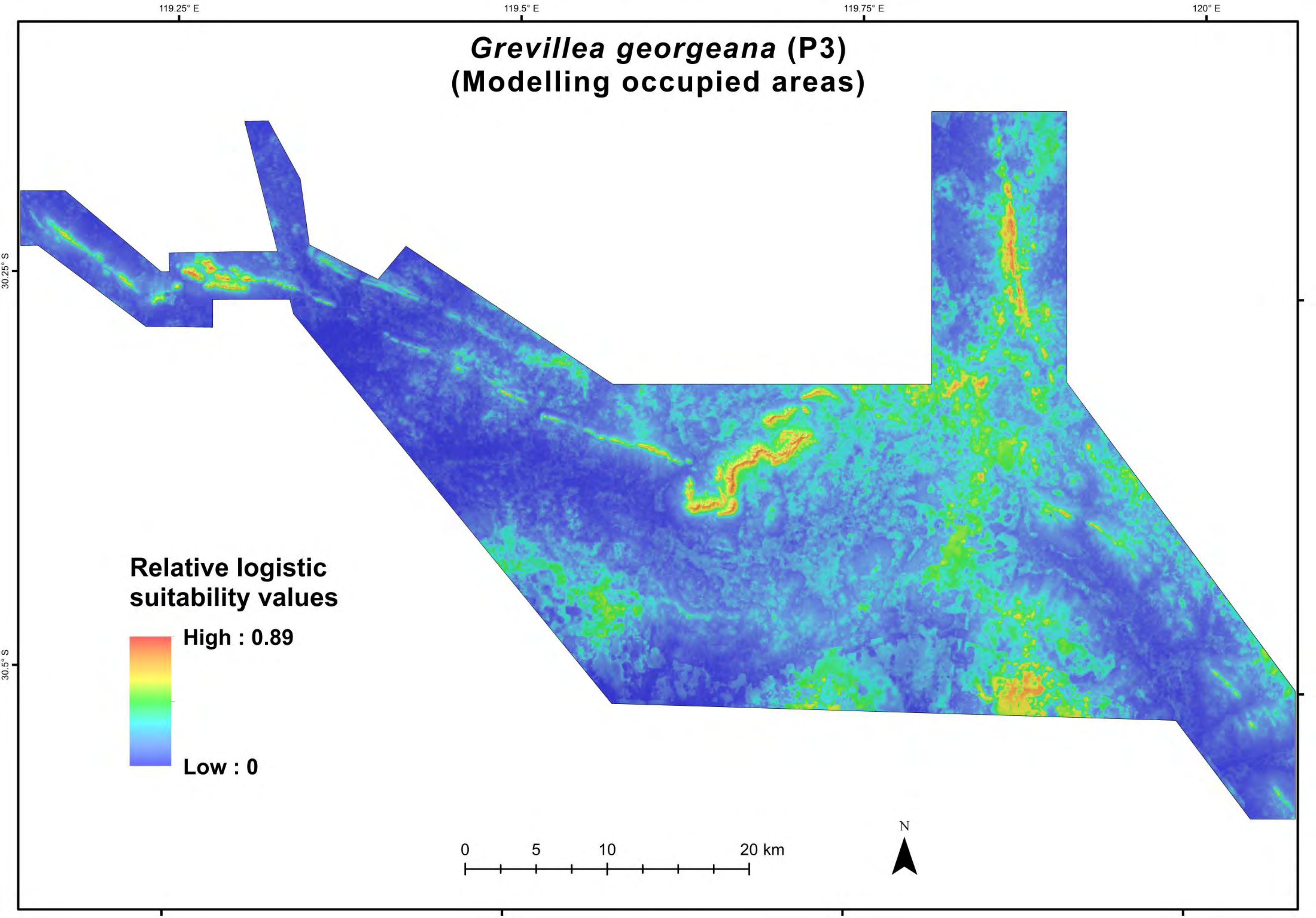

Figure S27. Predicted habitat suitability for *Grevillea georgeana* (restricted background sample selection).

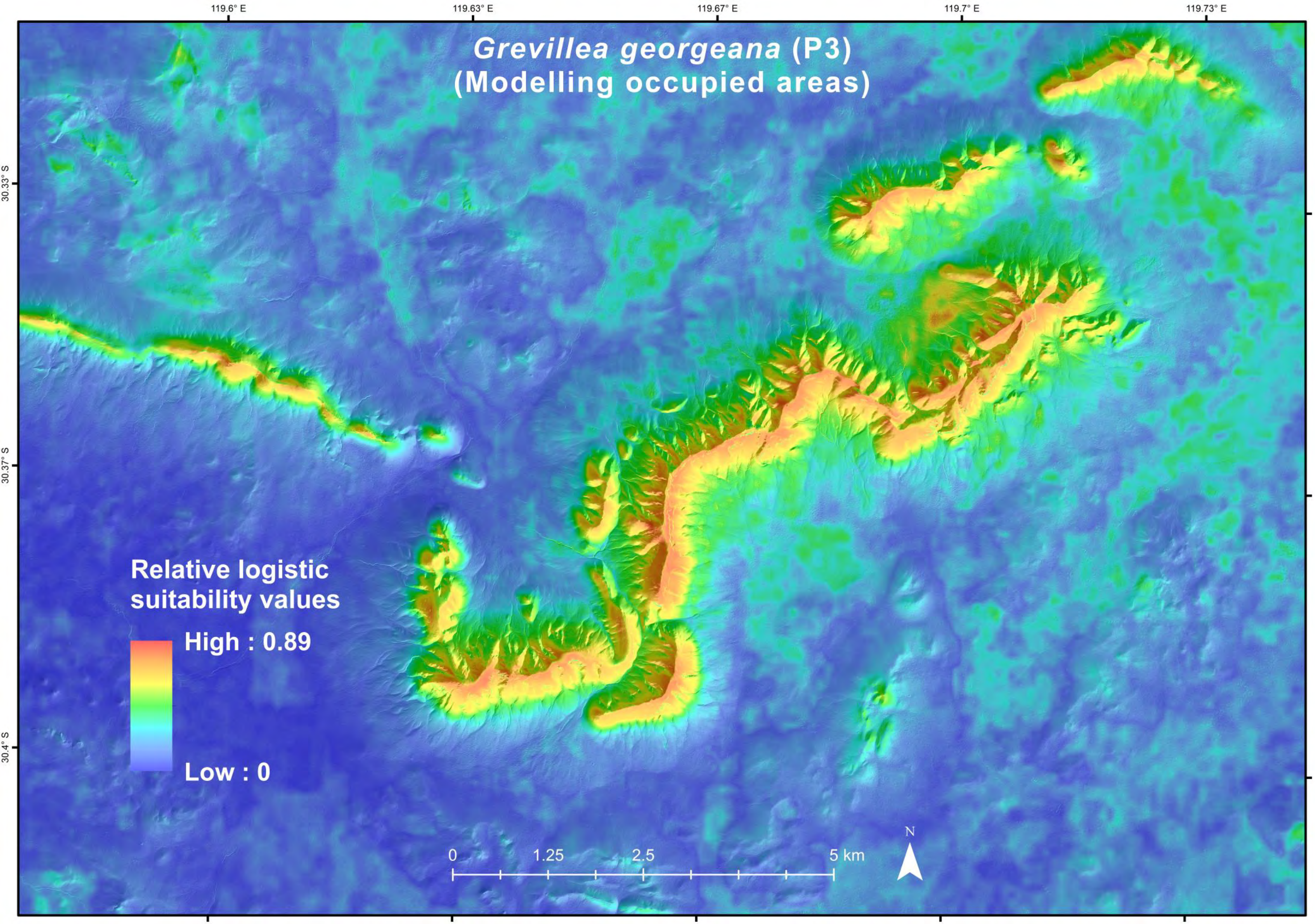

Figure S28. Predicted habitat suitability for *Grevillea georgeana* (restricted background sample selection).

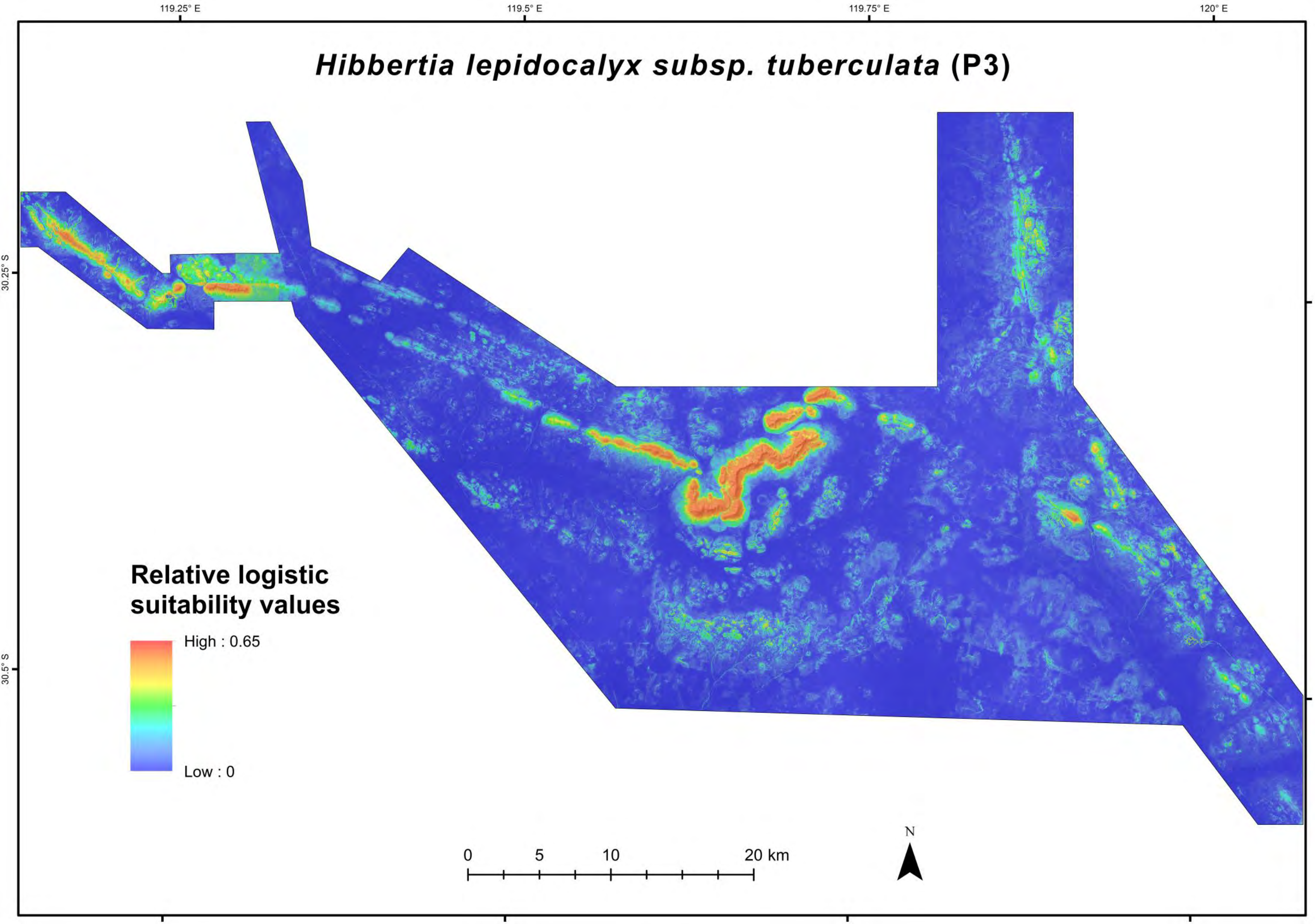

Figure S29. Predicted habitat suitability for *Hibbertia lepidocalyx subsp. Tuberculata* (default background sample selection).

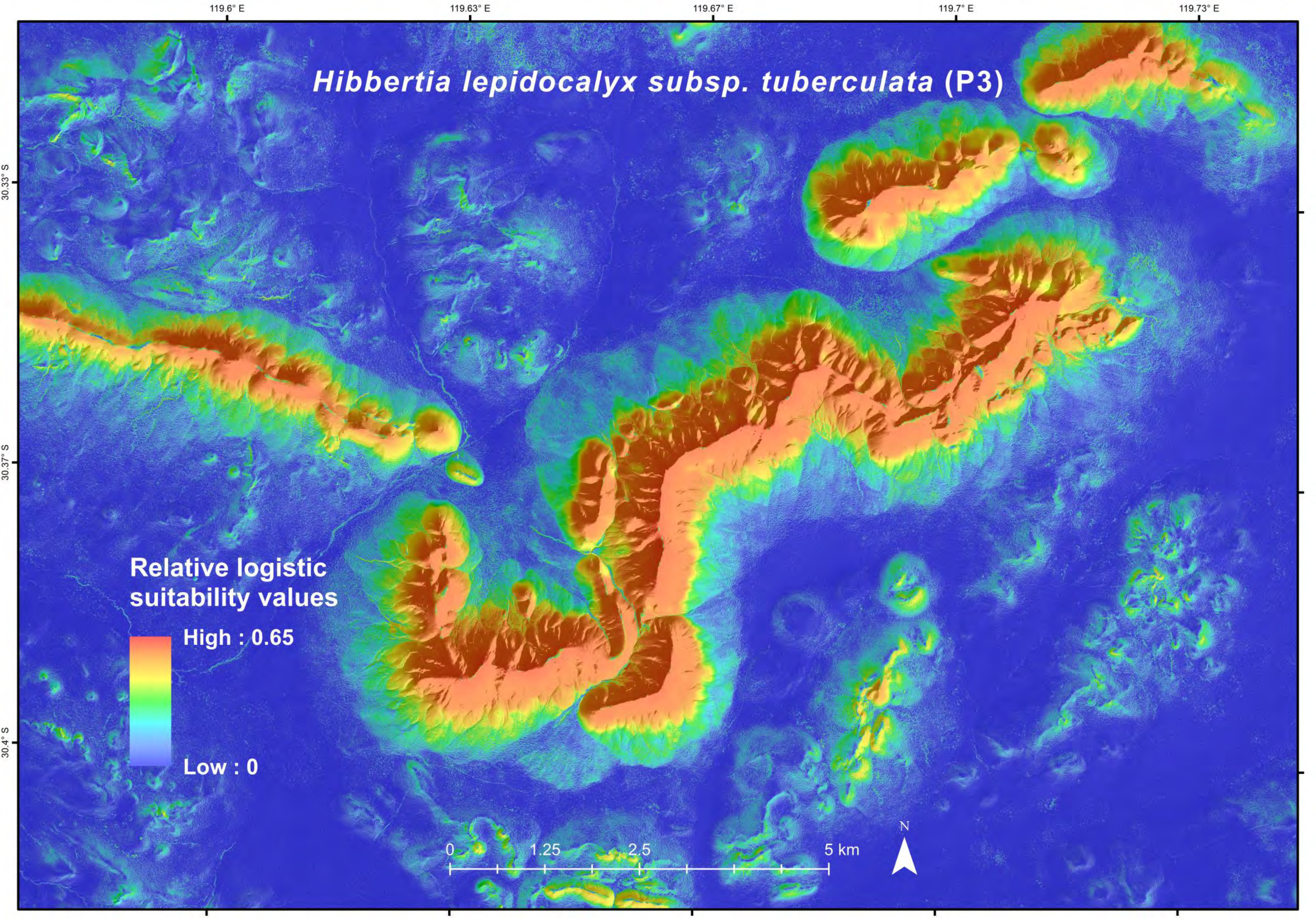

Figure S30. Predicted habitat suitability for *Hibbertia lepidocalyx subsp. Tuberculata* (default background sample selection).

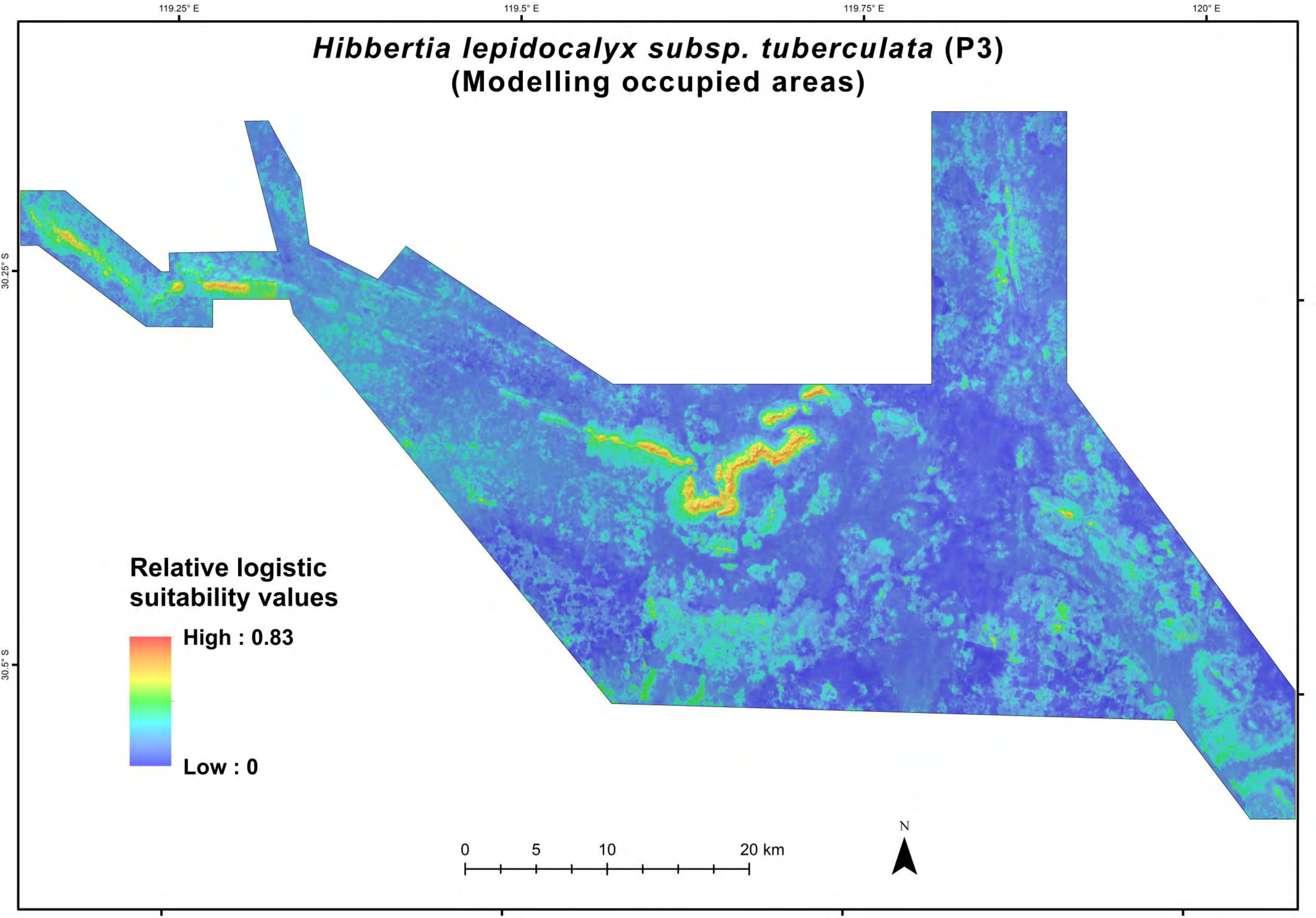

Figure S31. Predicted habitat suitability for *Hibbertia lepidocalyx subsp. Tuberculata* (restricted background sample selection).

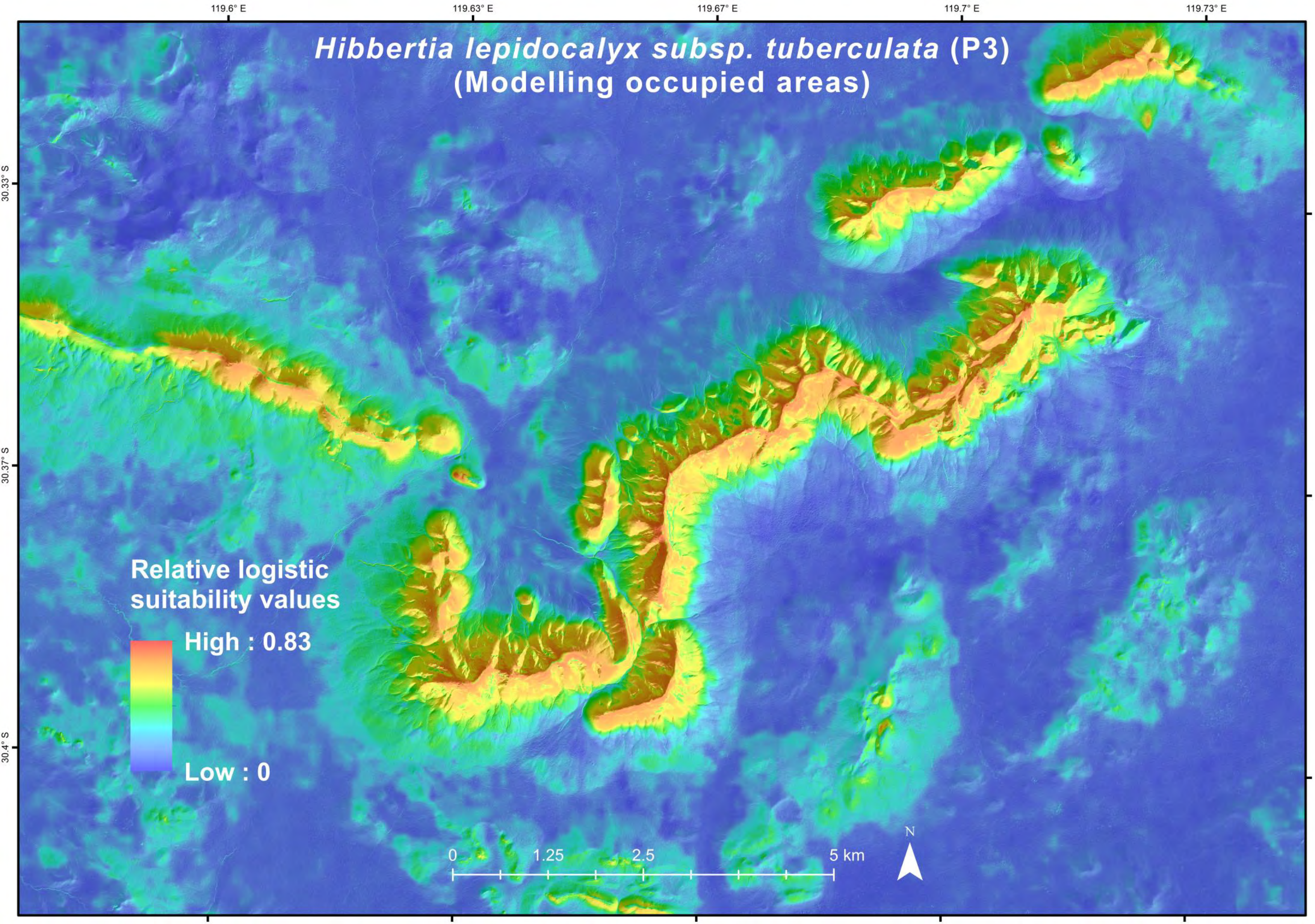

Figure S32. Predicted habitat suitability for *Hibbertia lepidocalyx subsp. Tuberculata* (restricted background sample selection).

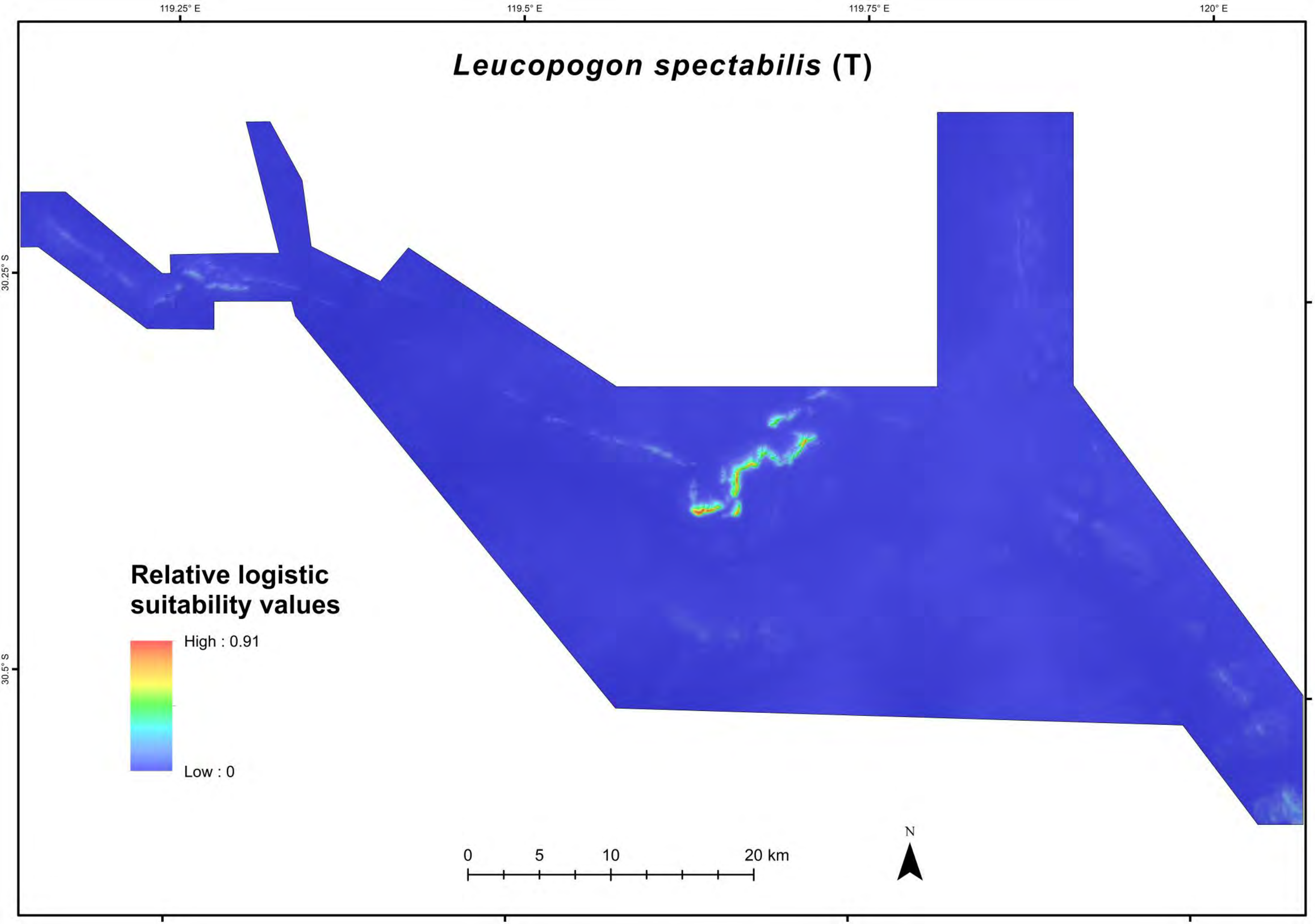

Figure S33. Predicted habitat suitability for *Leucopogon spectabilis* (default background sample selection).

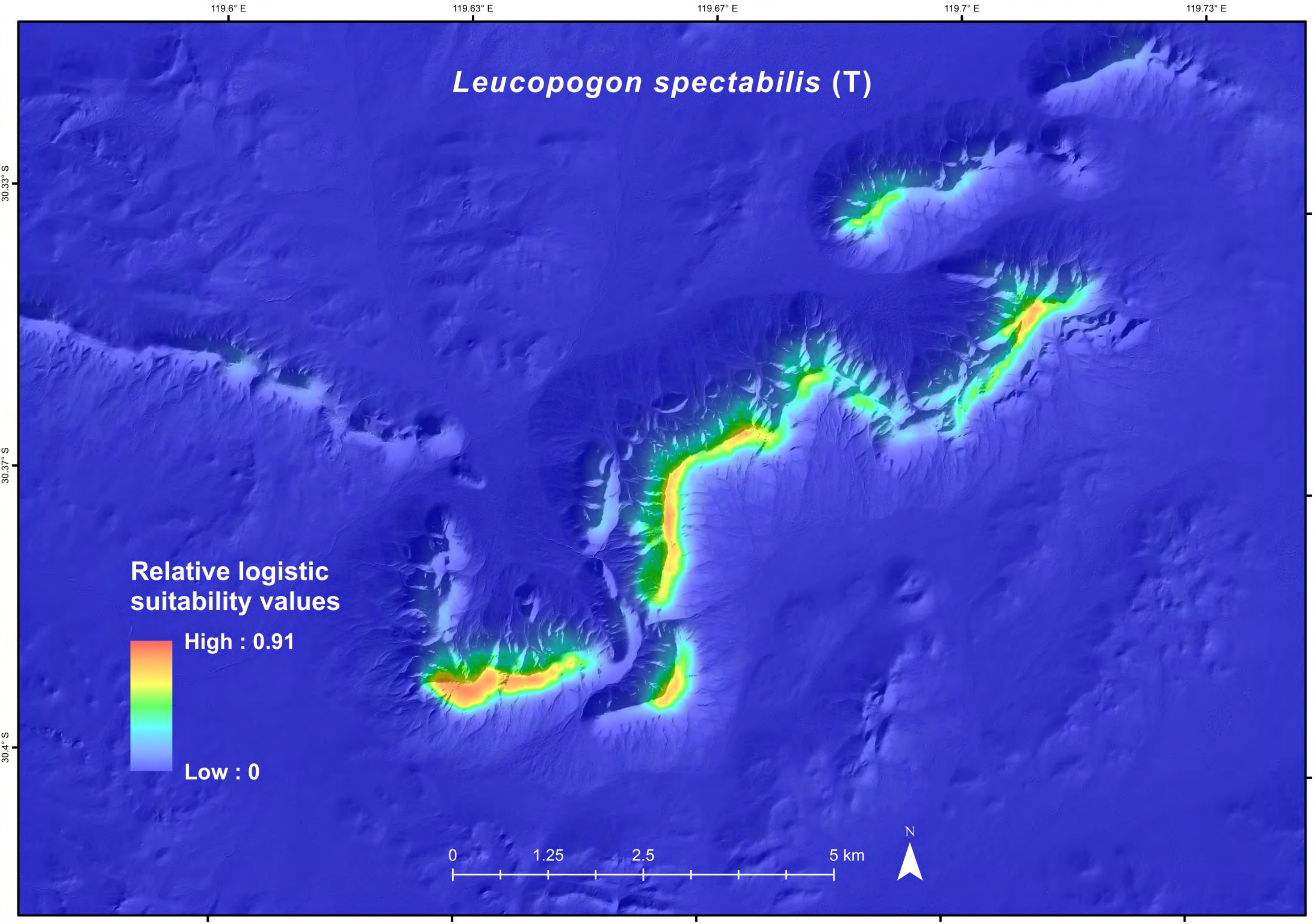

Figure S34. Predicted habitat suitability for *Leucopogon spectabilis* (default background sample selection).

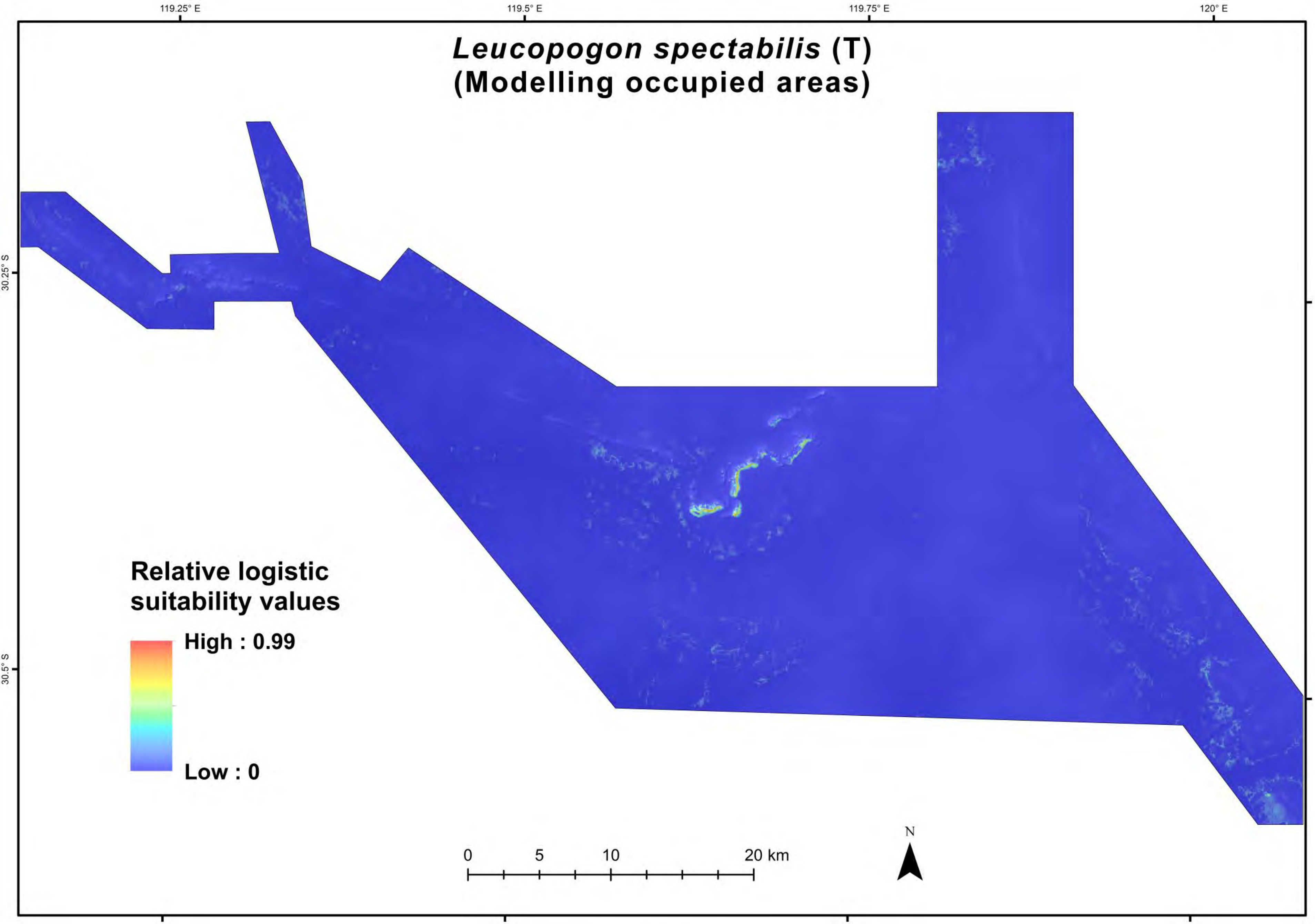

Figure S35. Predicted habitat suitability for *Leucopogon spectabilis* (restricted background sample selection).

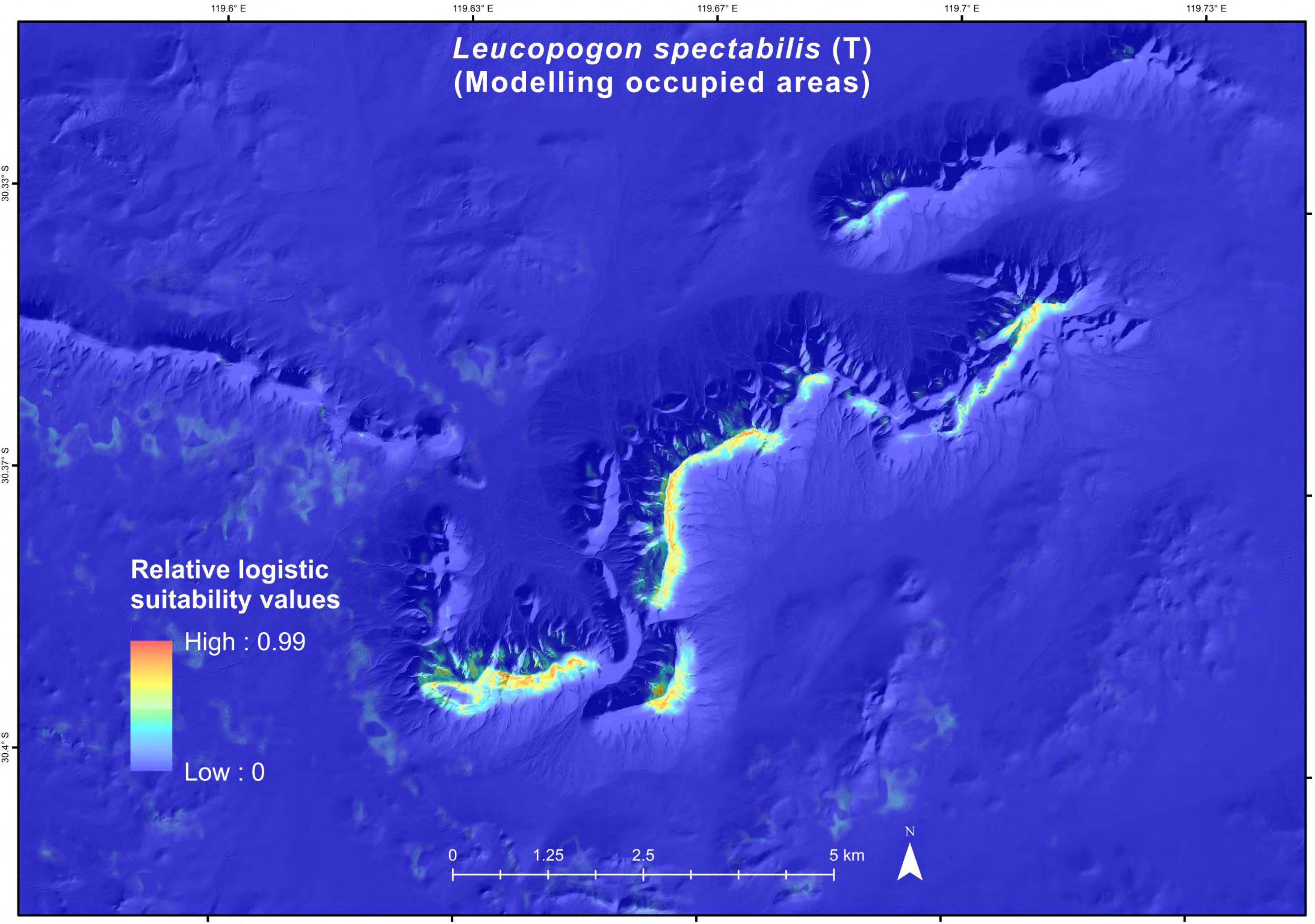

Figure S36. Predicted habitat suitability for *Leucopogon spectabilis* (restricted background sample selection).

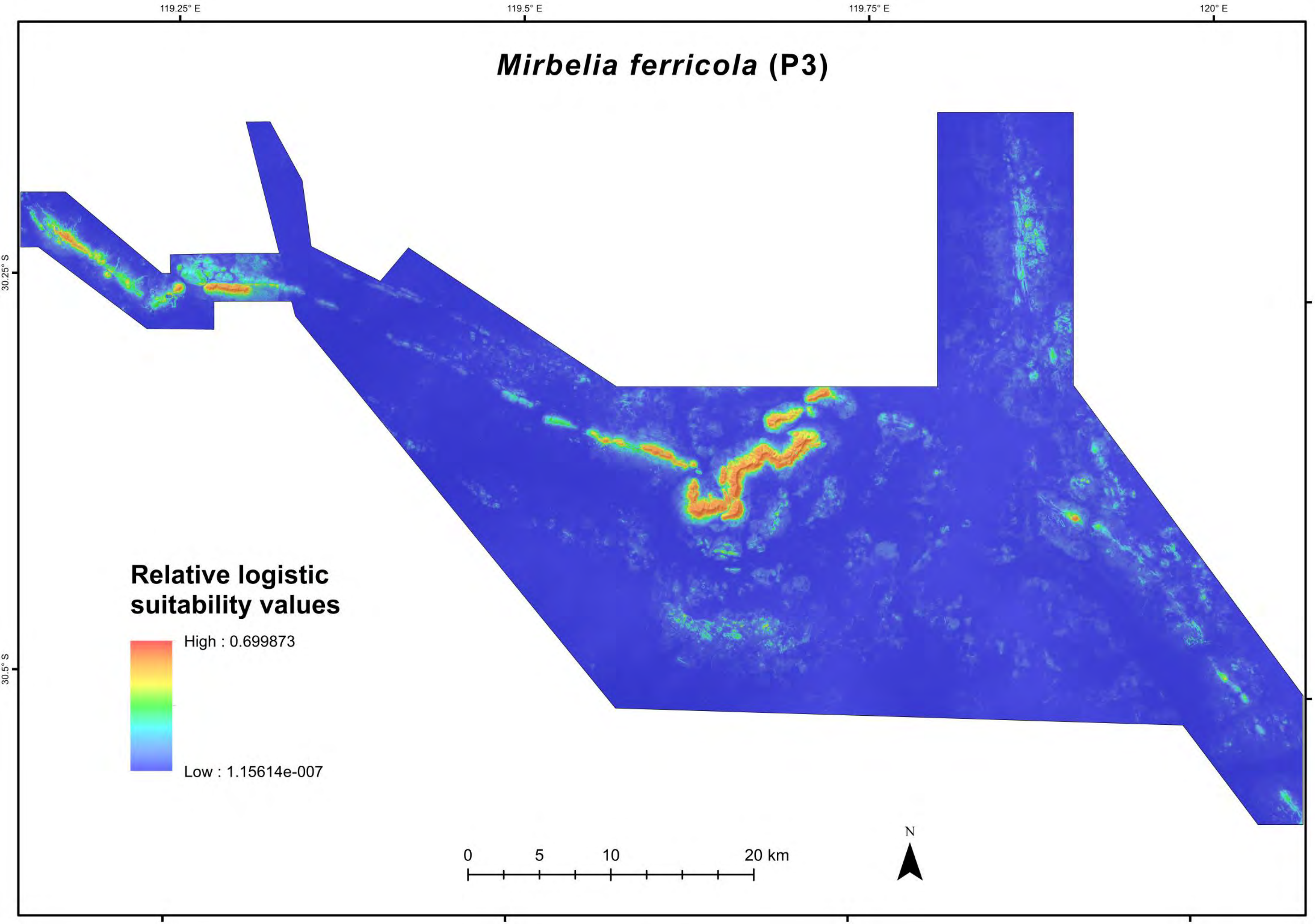

Figure S37. Predicted habitat suitability for *Mirbelia ferricola* (default background sample selection).

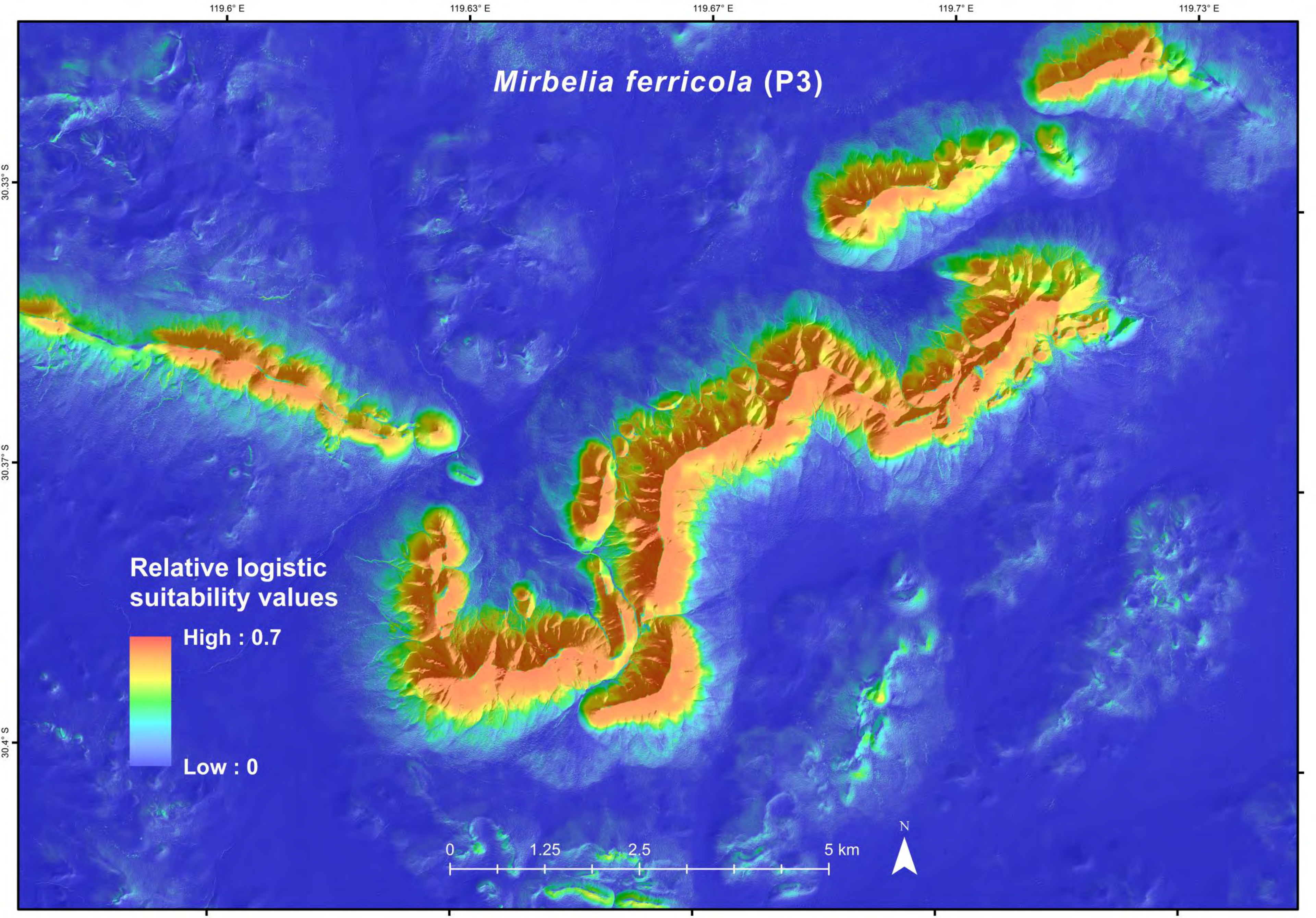

Figure S38. Predicted habitat suitability for *Mirbelia ferricola* (default background sample selection).

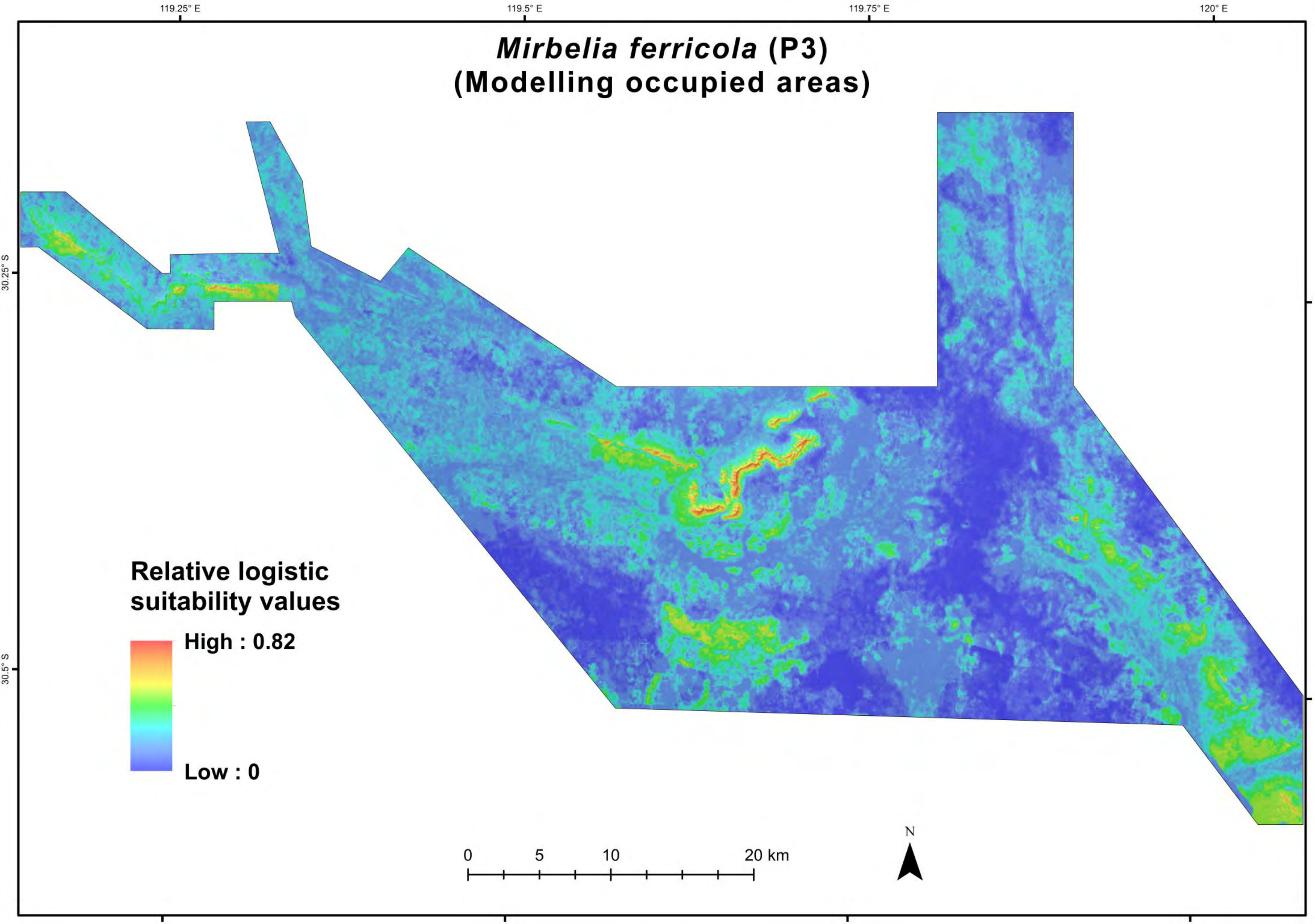

Figure S39. Predicted habitat suitability for *Mirbelia ferricola* (restricted background sample selection).

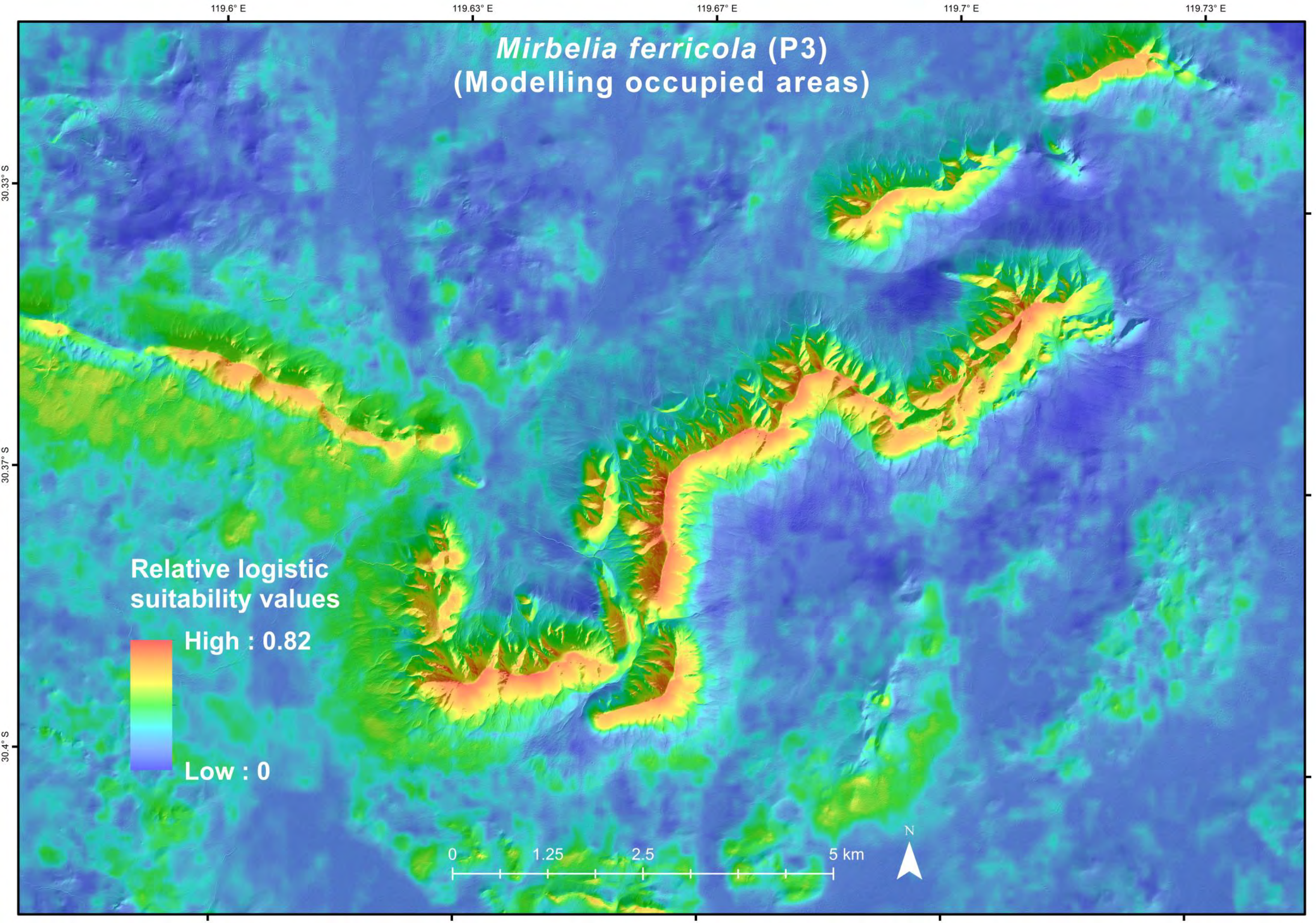

Figure S40. Predicted habitat suitability for *Mirbelia ferricola* (restricted background sample selection).

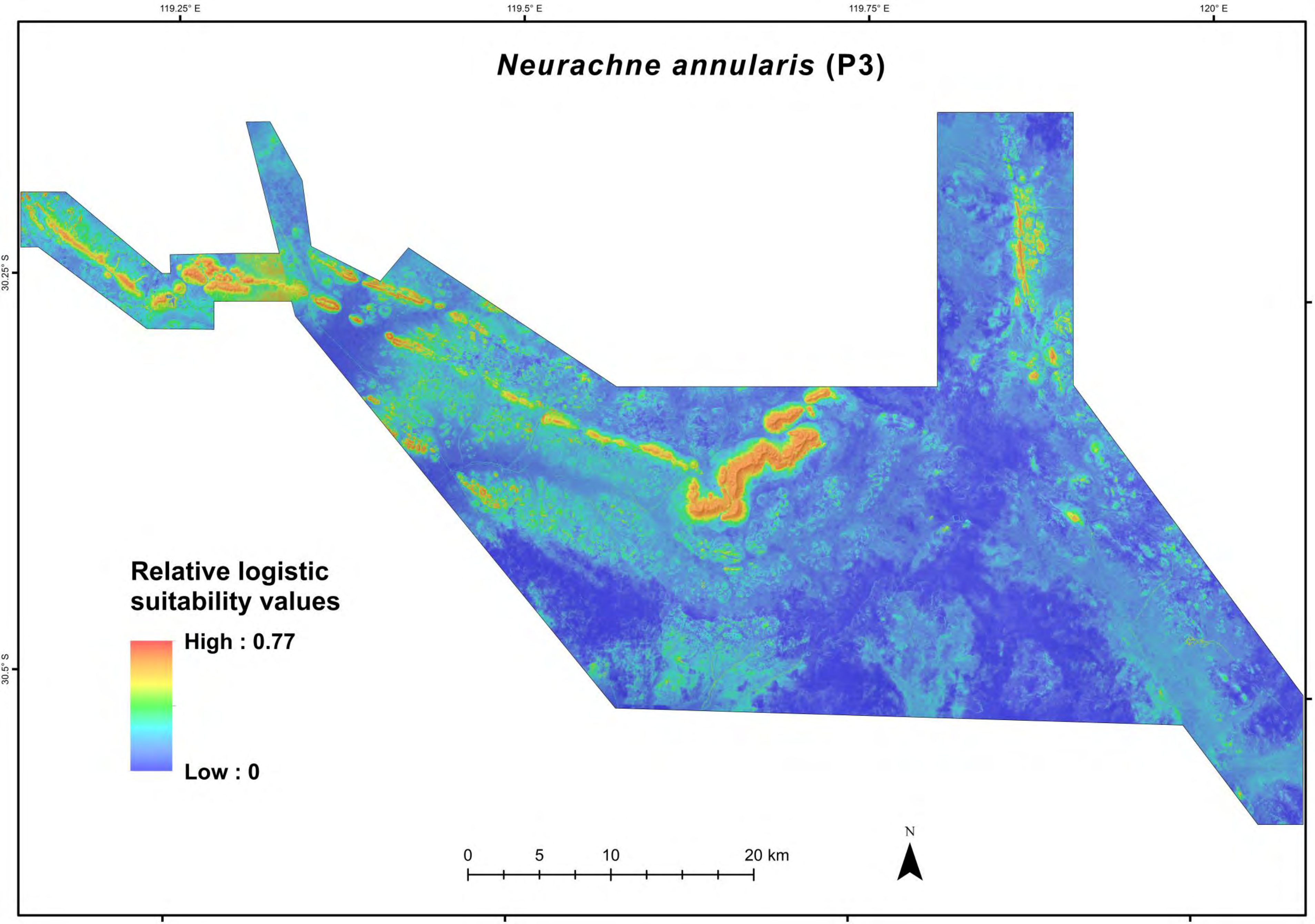

Figure S41. Predicted habitat suitability for *Neurachne annularis* (default background sample selection).

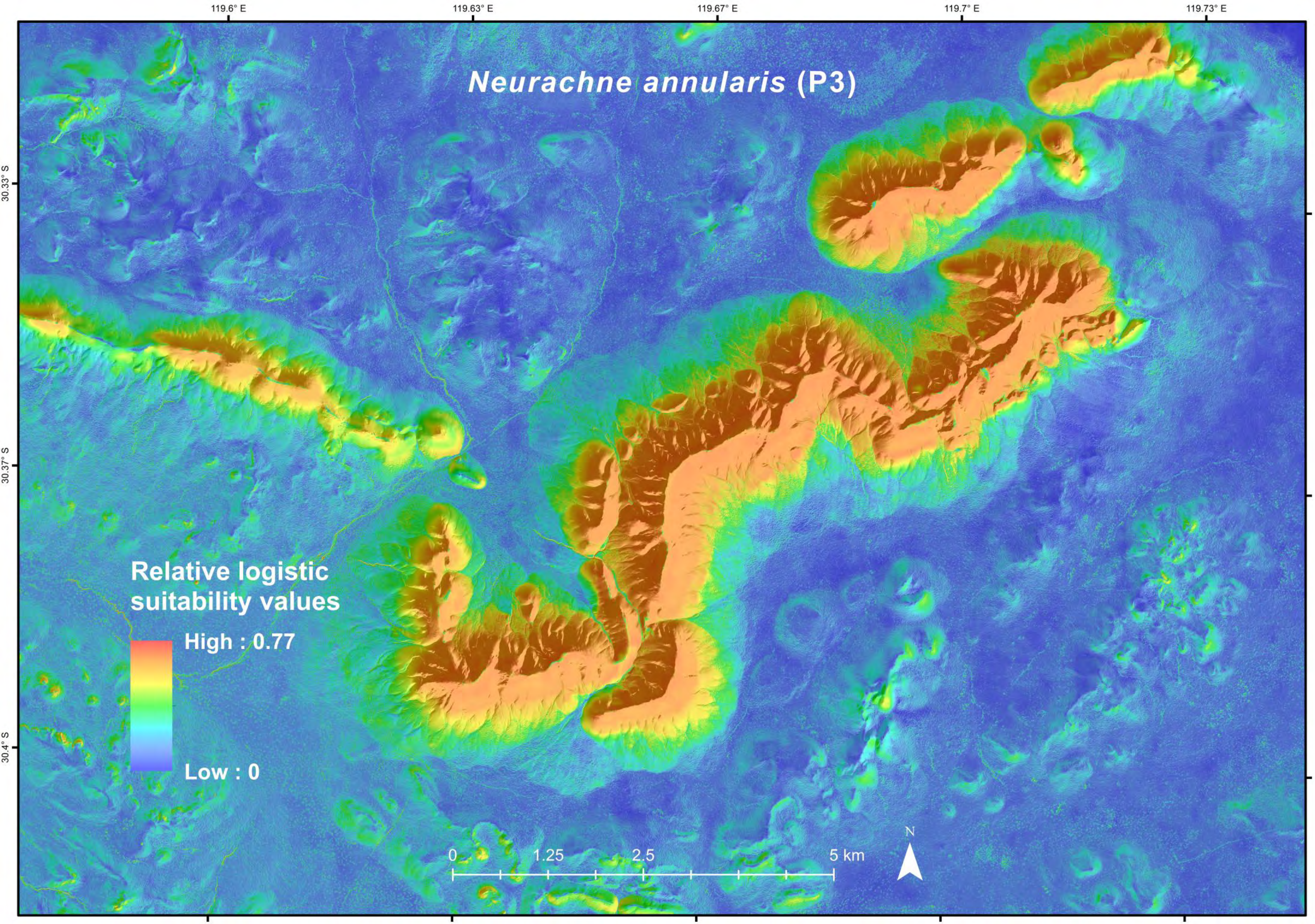

Figure S42. Predicted habitat suitability for *Neurachne annularis* (default background sample selection).

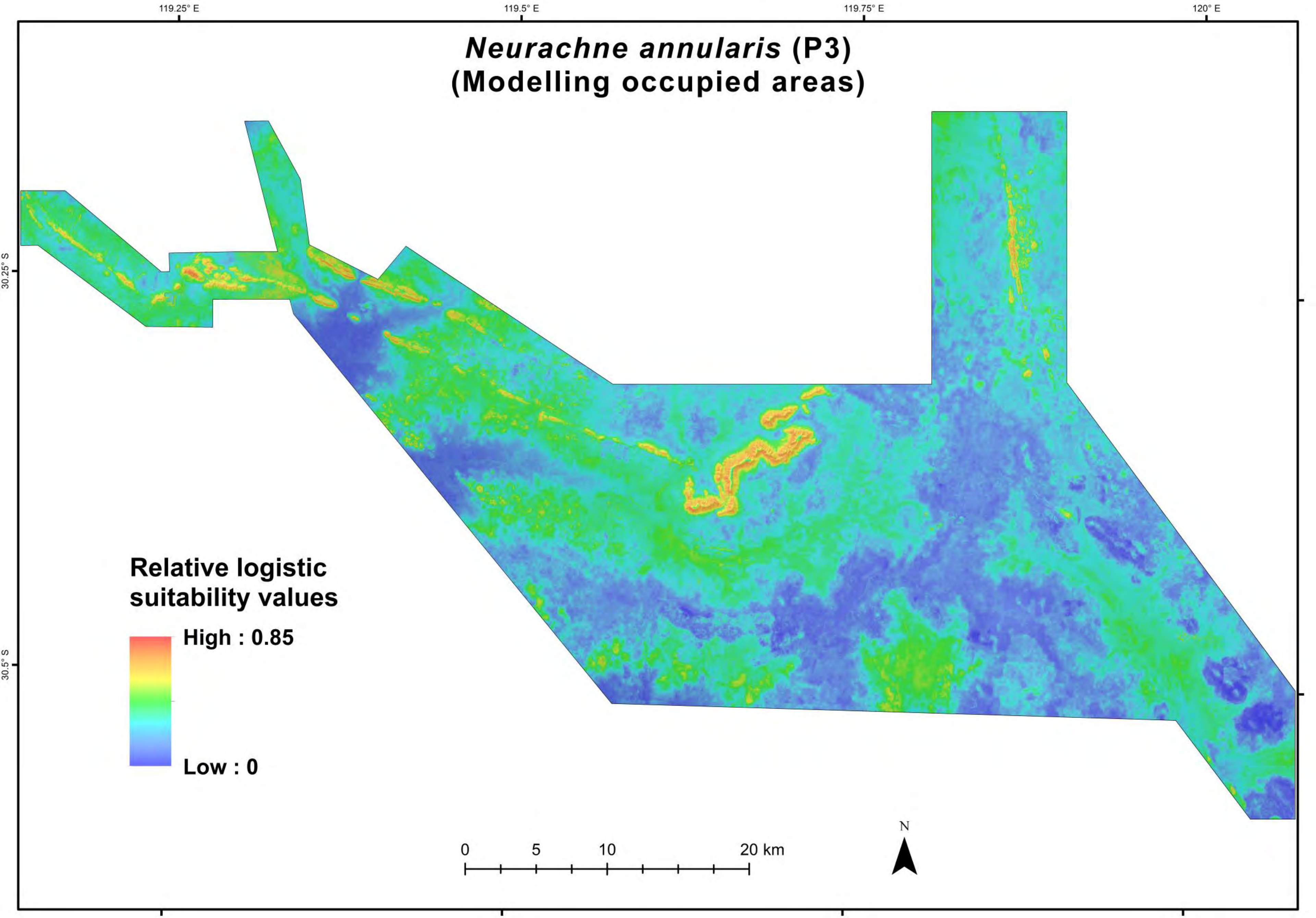

Figure S43. Predicted habitat suitability for *Neurachne annularis* (restricted background sample selection).

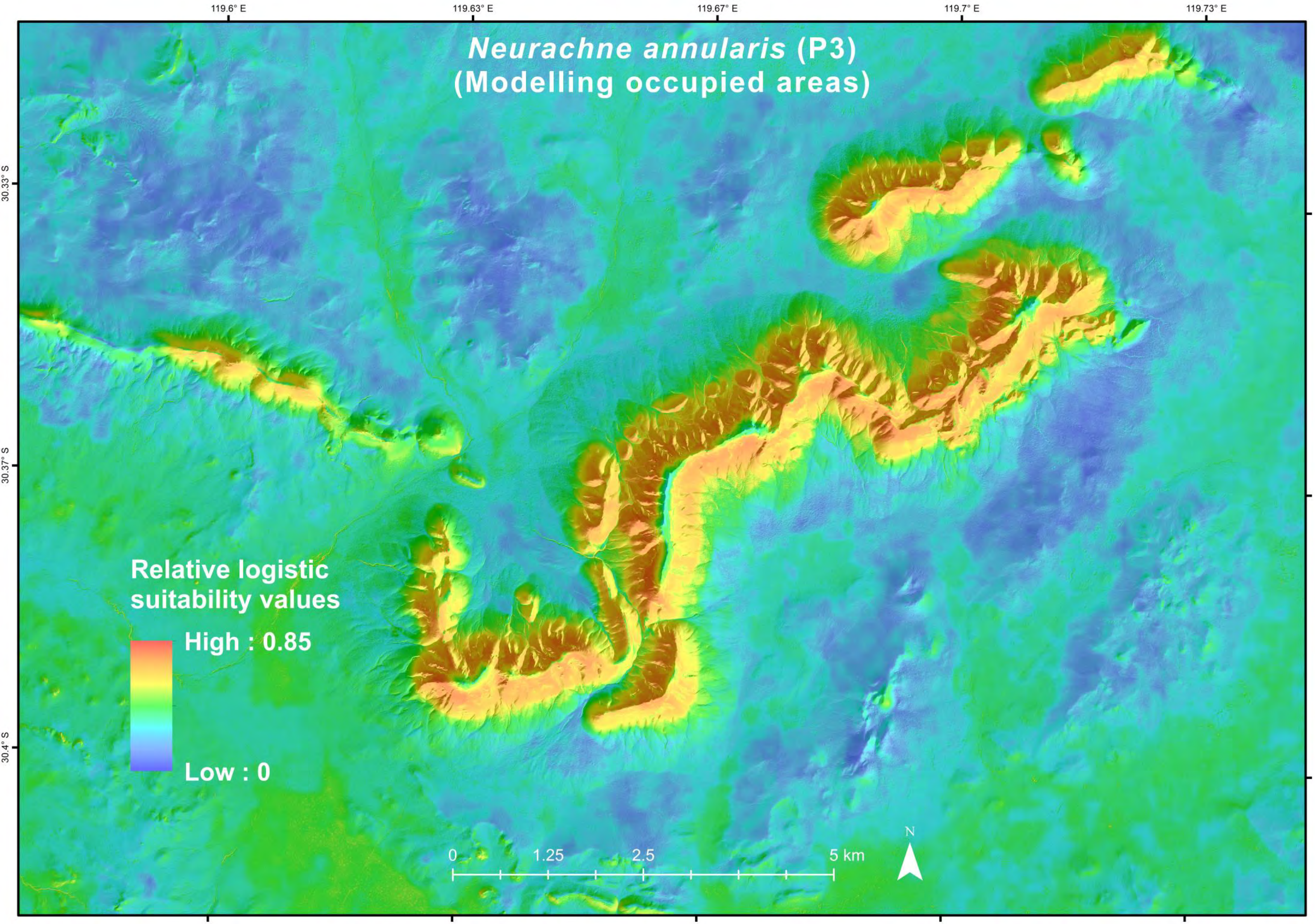

Figure S44. Predicted habitat suitability for *Neurachne annularis* (restricted background sample selection).

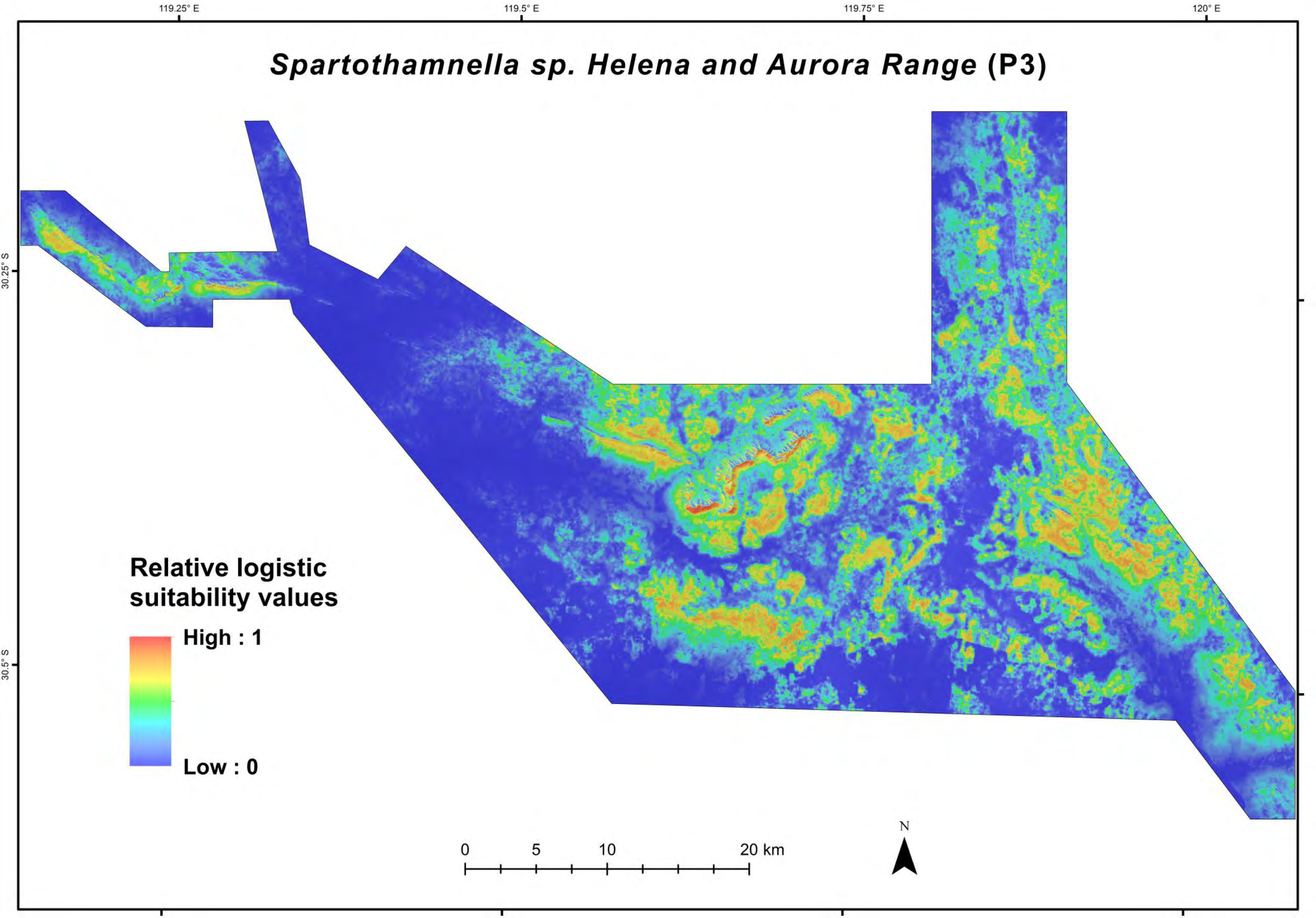

Figure S45. Predicted habitat suitability for *Spartothamnella sp. Helena & Aurora Range* (default background sample selection).

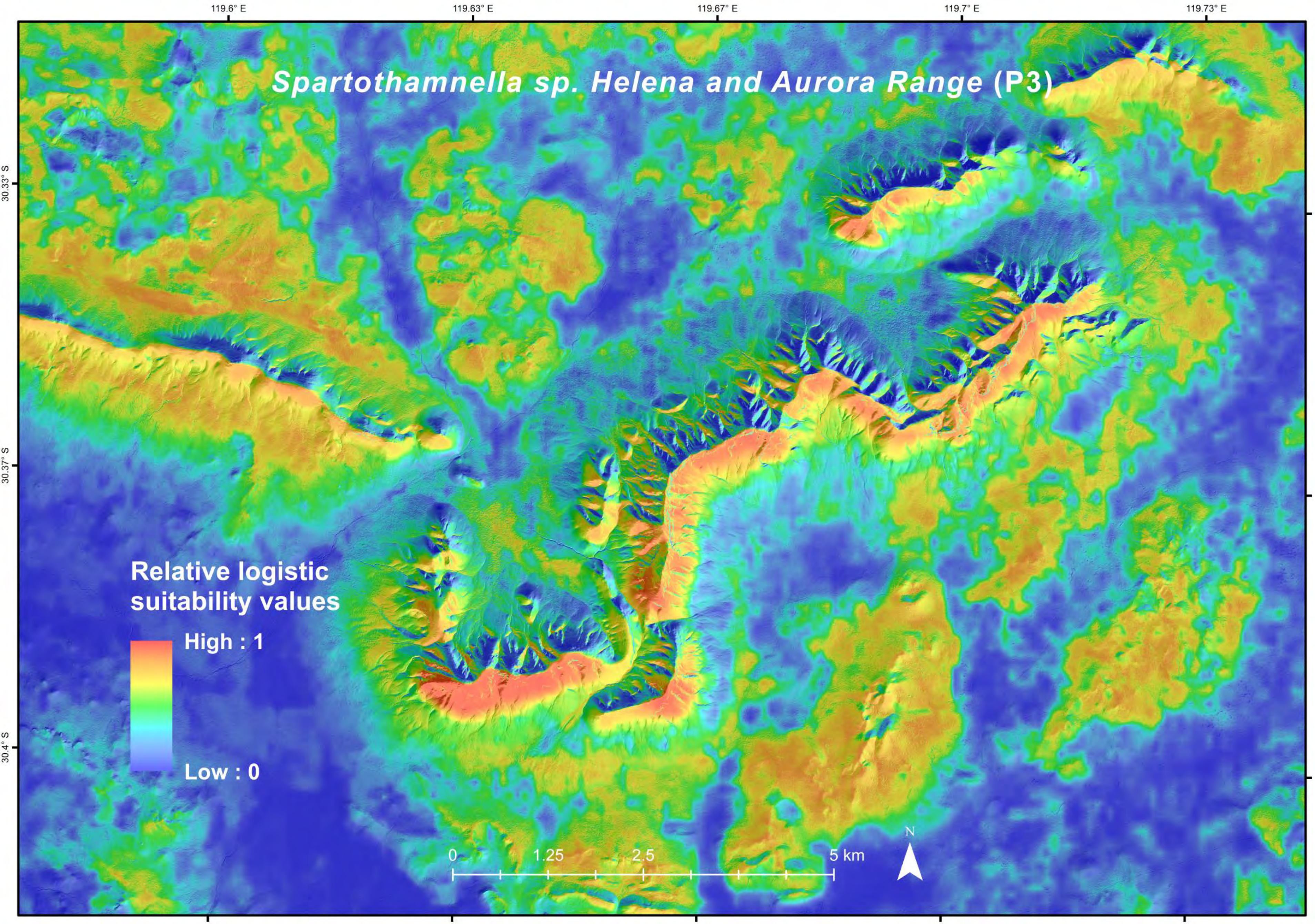

Figure S46. Predicted habitat suitability for *Spartothamnella sp. Helena & Aurora Range* (default background sample selection).

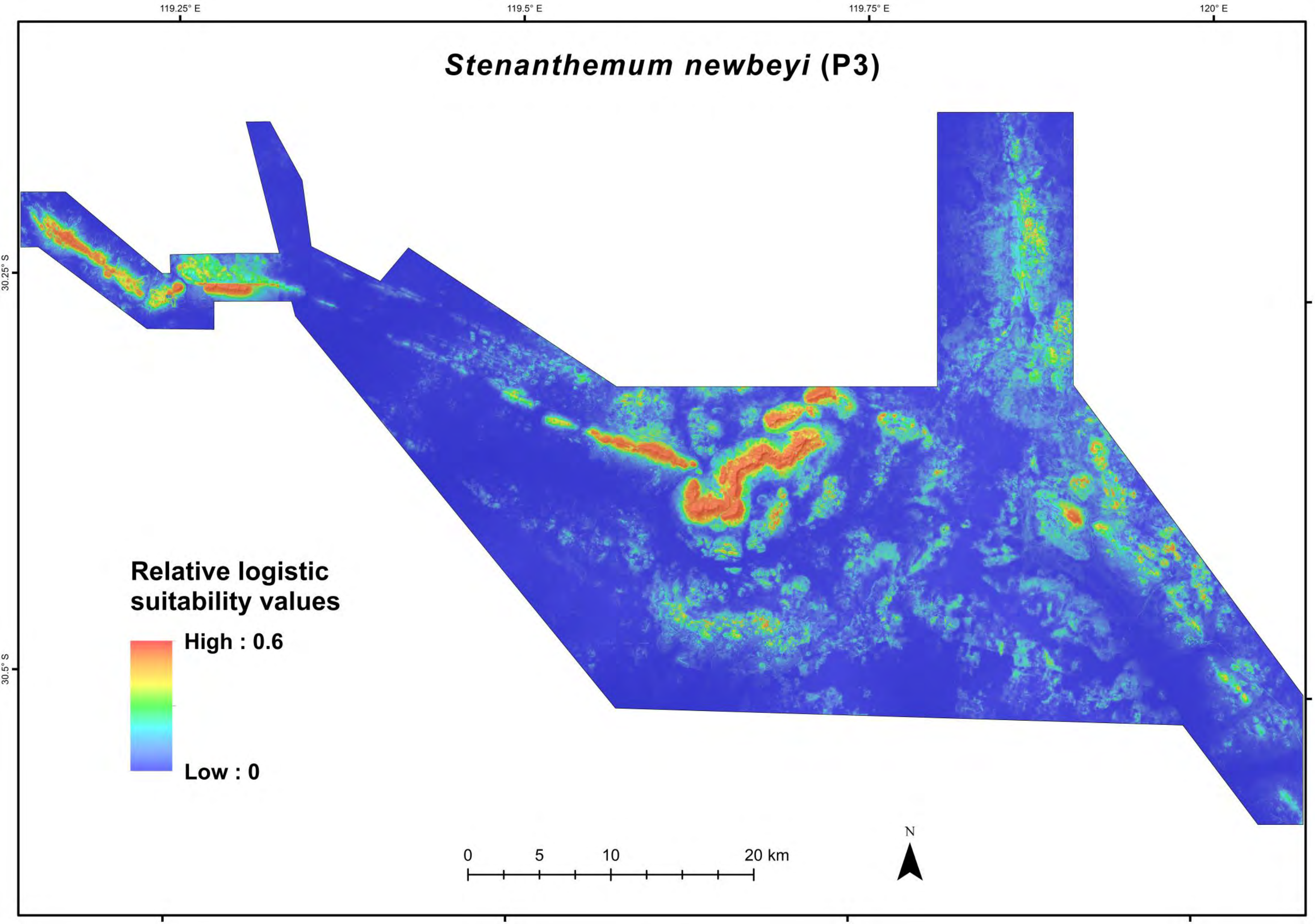

Figure S47. Predicted habitat suitability for *Stenanthemum newbeyi* (default background sample selection).

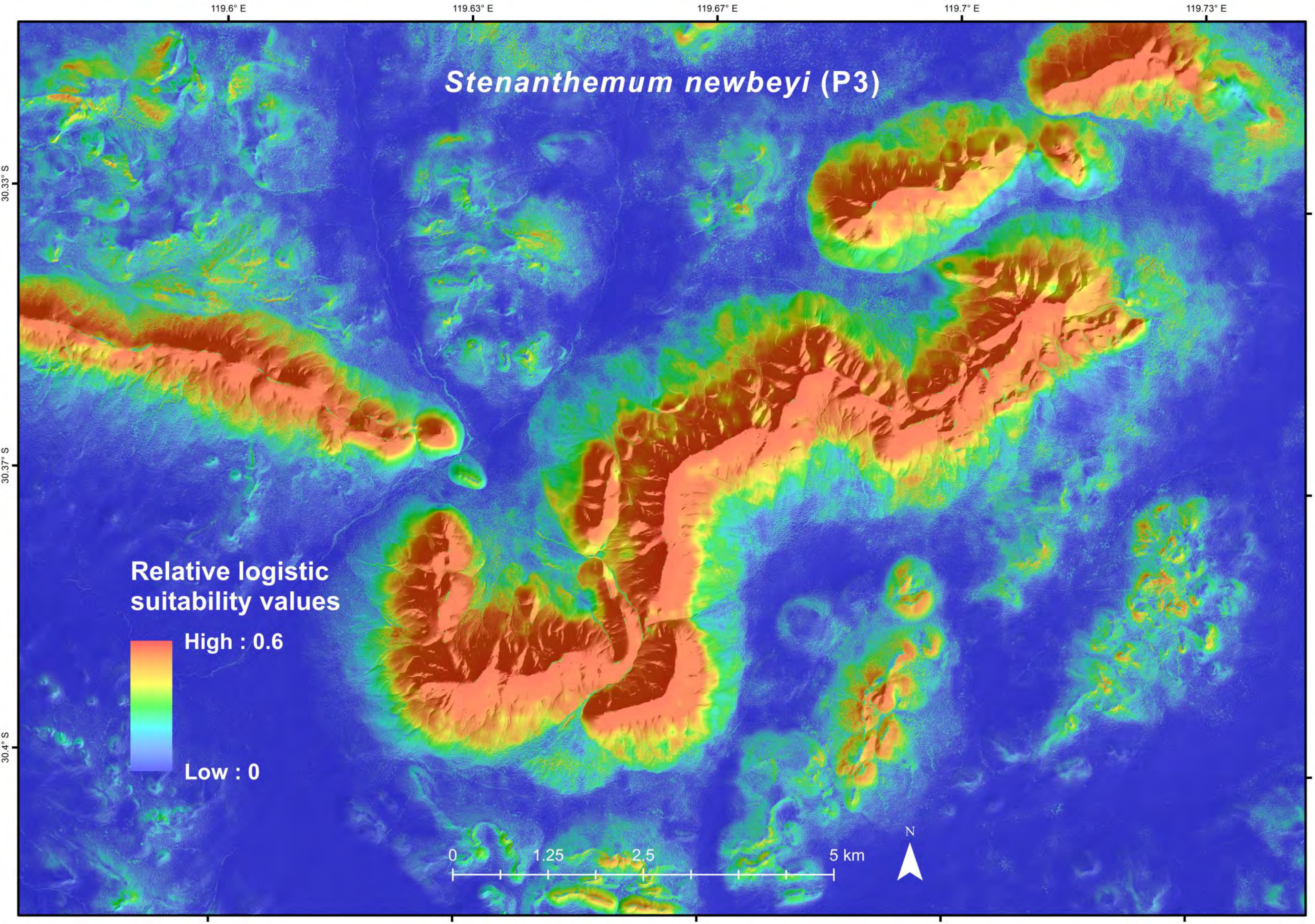

Figure S48. Predicted habitat suitability for *Stenanthemum newbeyi* (default background sample selection).

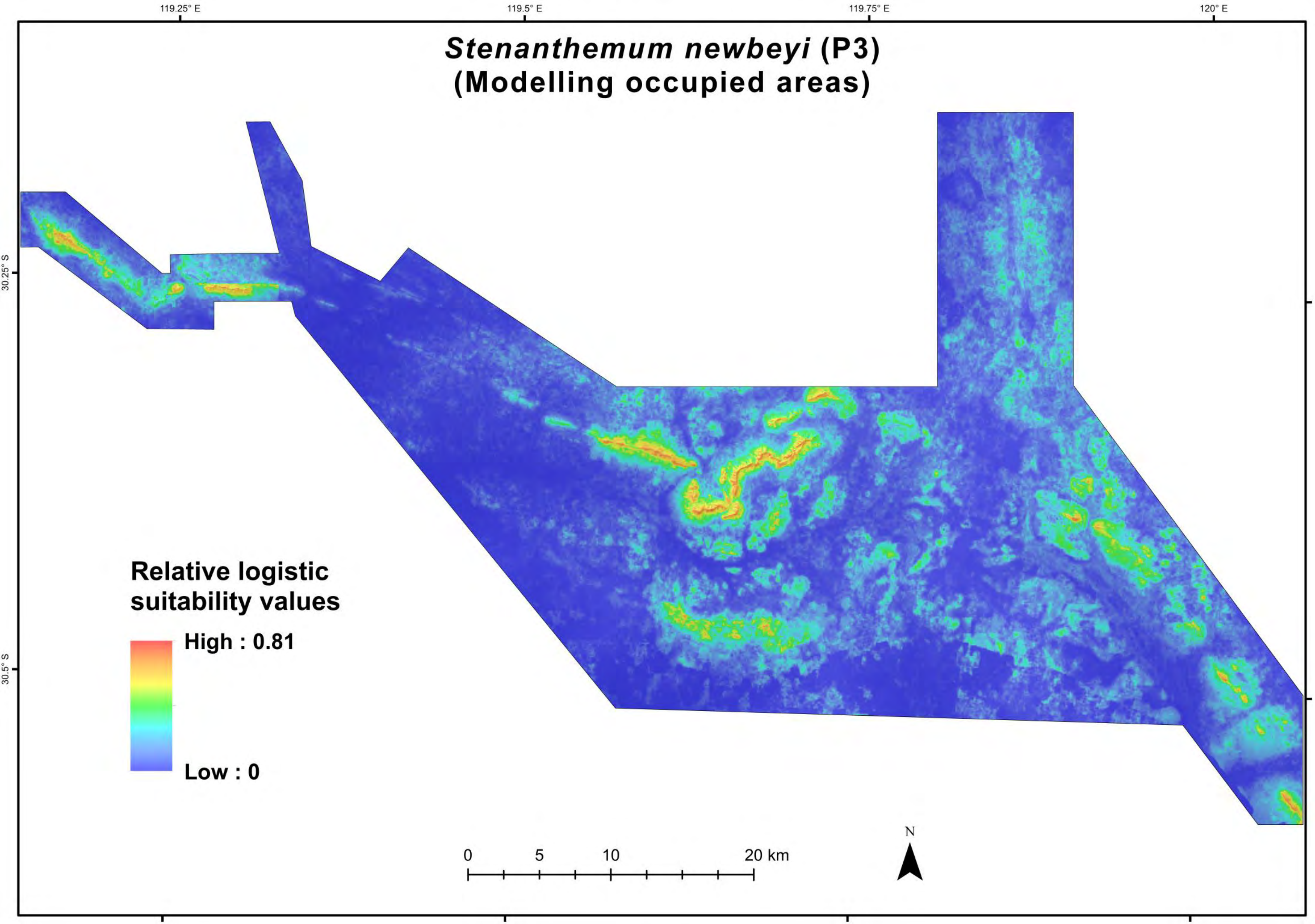

Figure S49. Predicted habitat suitability for *Stenanthemum newbeyi* (restricted background sample selection).

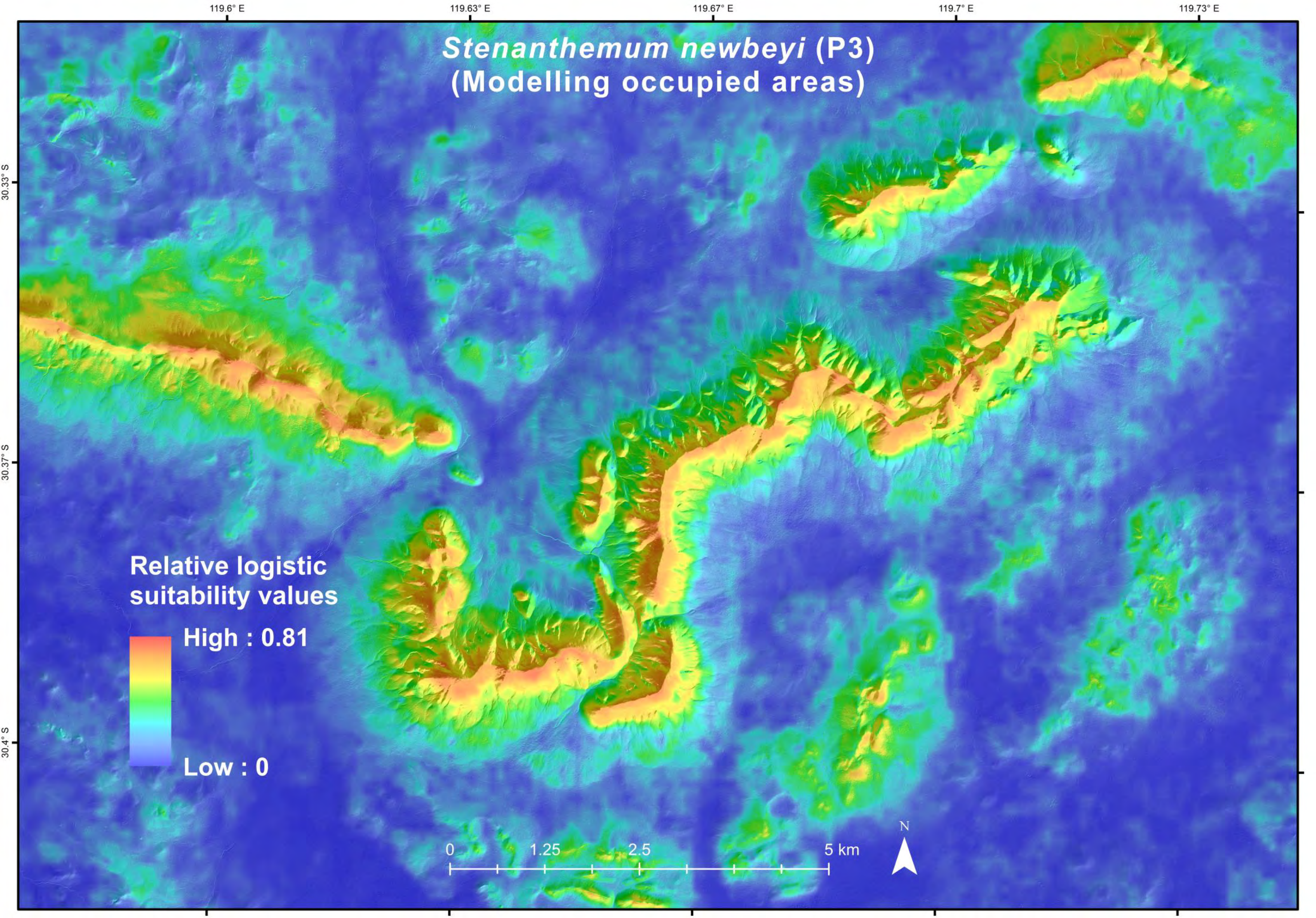

Figure S50. Predicted habitat suitability for *Stenanthemum newbeyi* (restricted background sample selection).

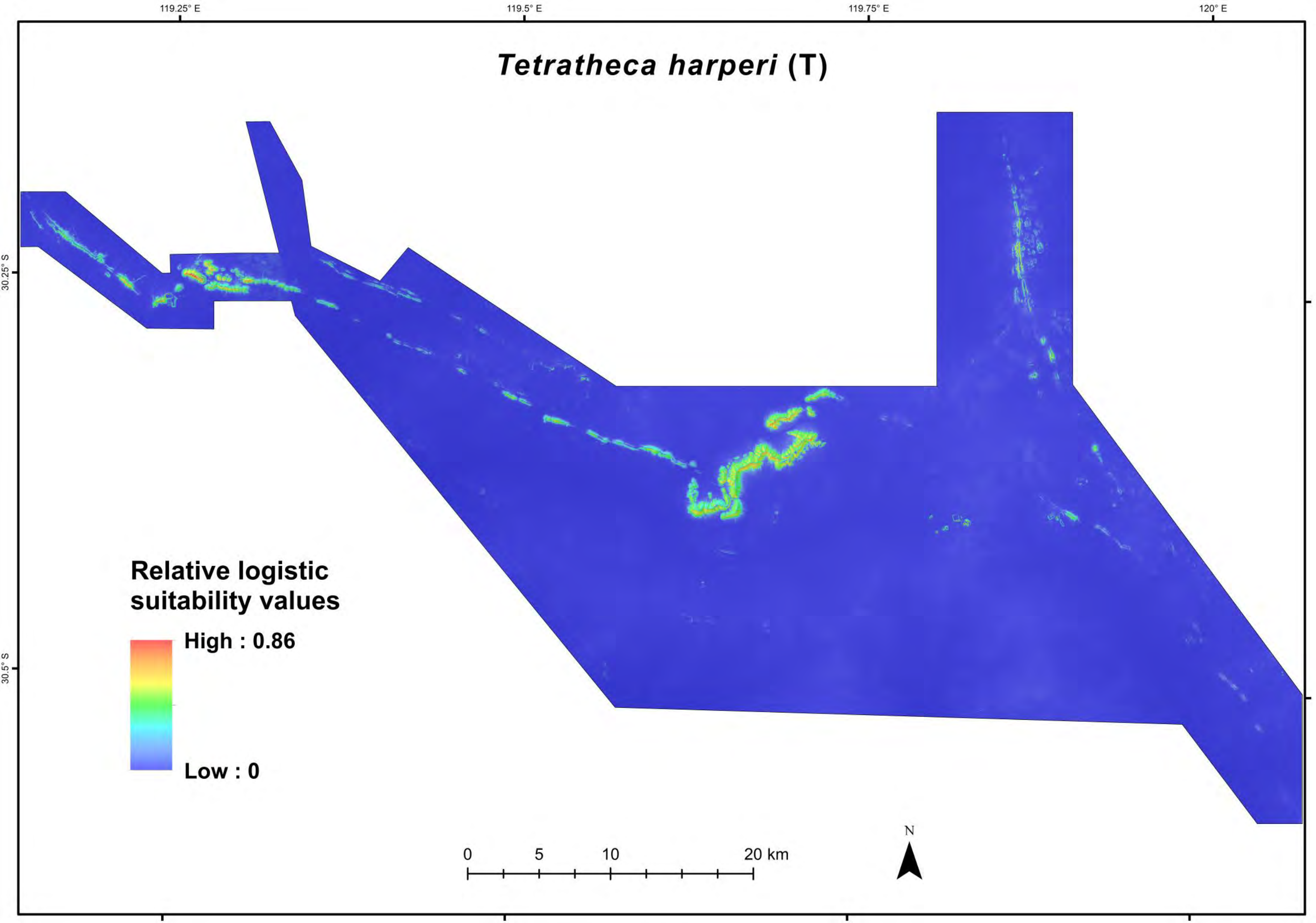

Figure S51. Predicted habitat suitability for *Tetratheca harperi* (default background sample selection).

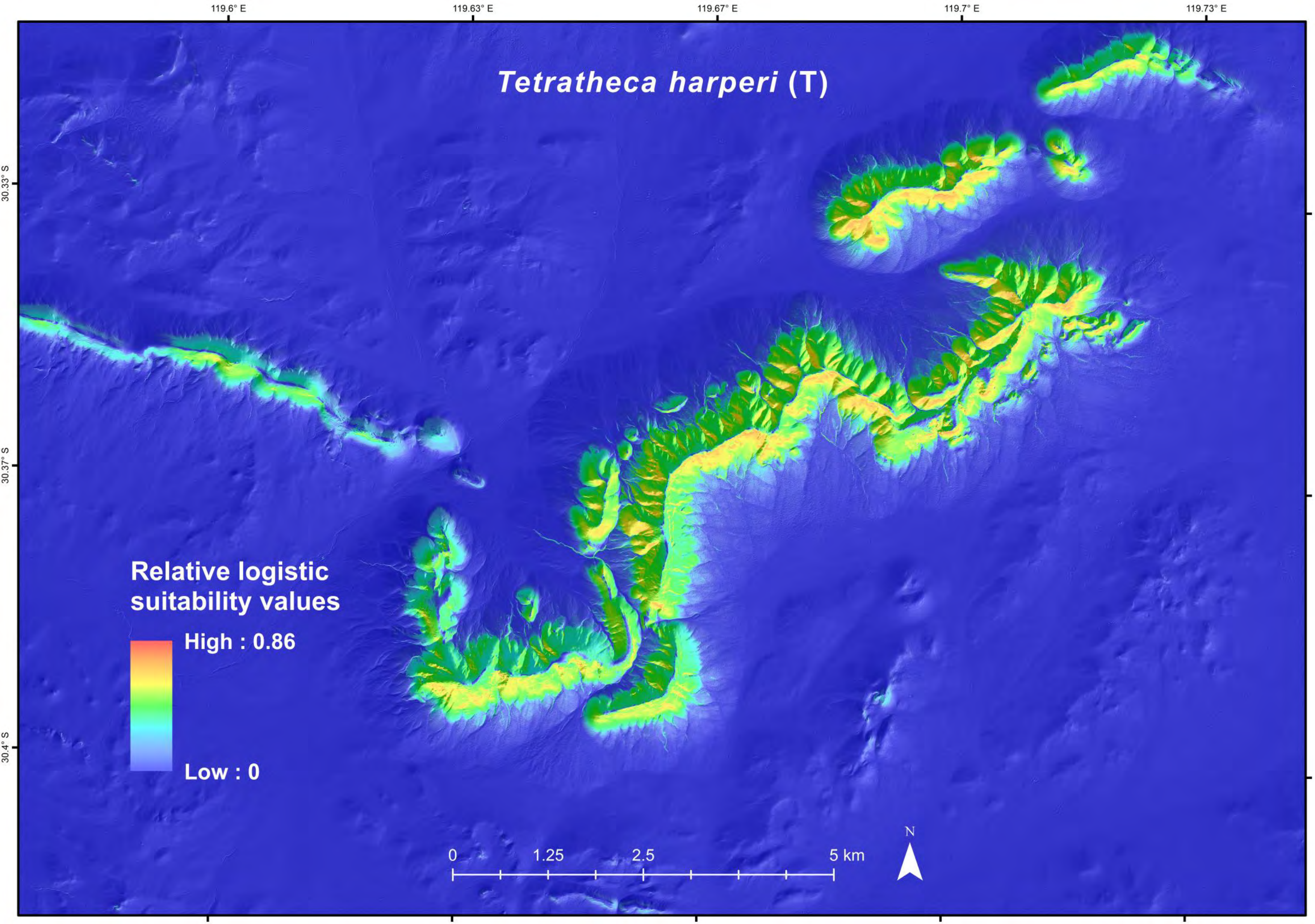

Figure S52. Predicted habitat suitability for *Tetratheca harperi* (default background sample selection).

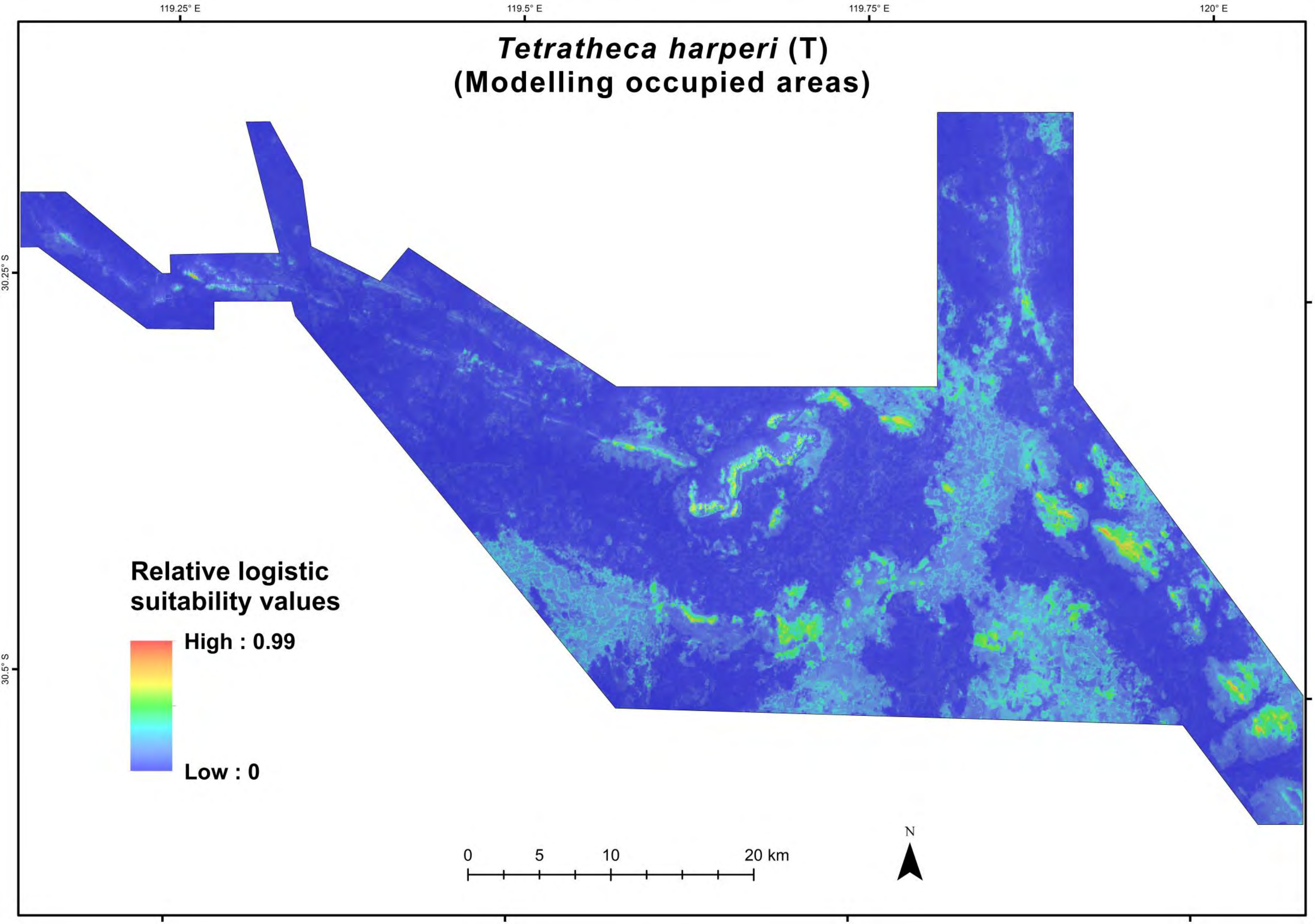

Figure S53. Predicted habitat suitability for *Tetratheca harperi* (restricted background sample selection).

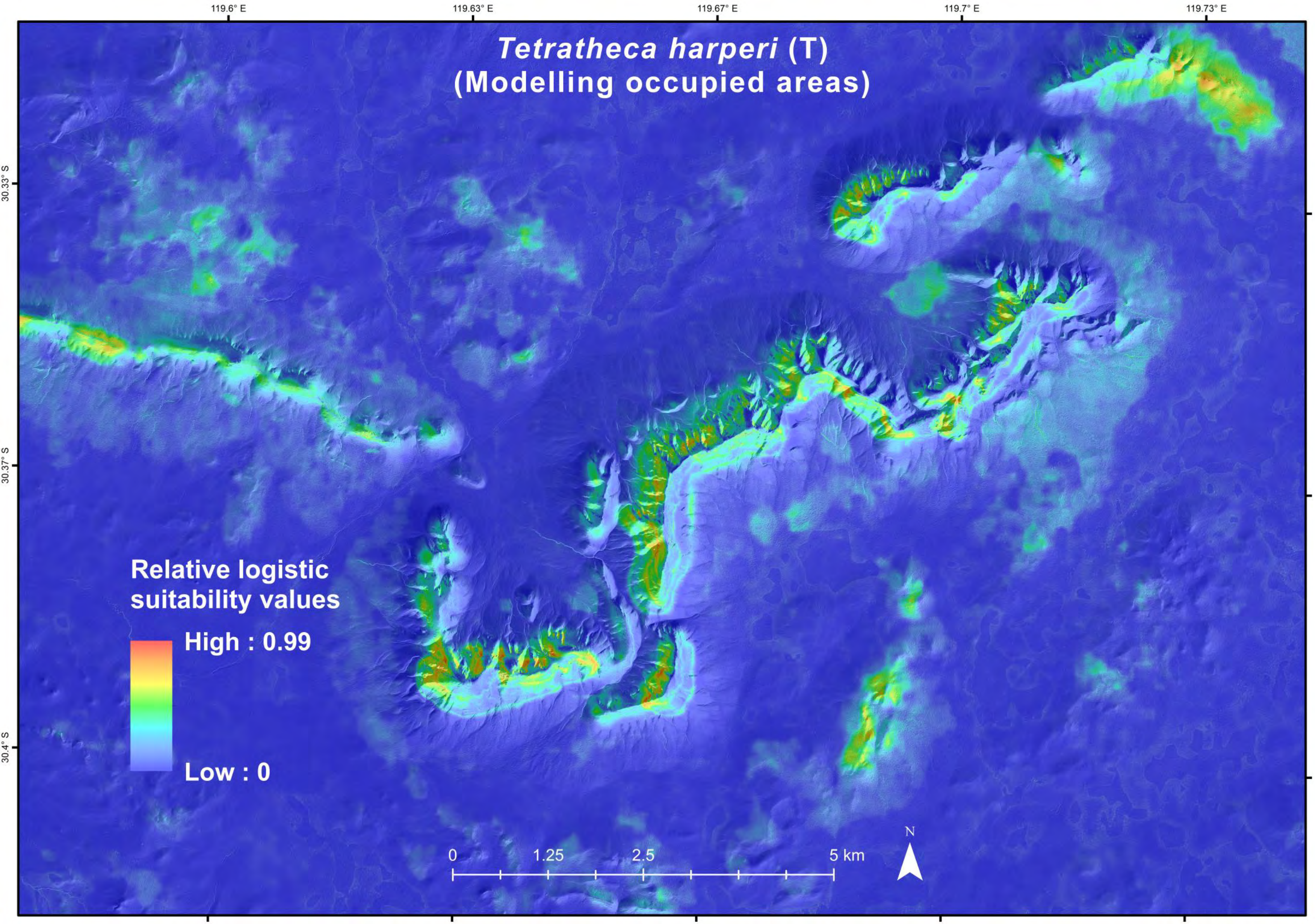

Figure S54. Predicted habitat suitability for *Tetratheca harperi* (restricted background sample selection).